Regioselective cycloaddition of potassium alkynyltrifluoroborates with 3-azetidinones and 3-oxetanone by nickel-catalysed C–C bond activation

Fathi Elwrfalli

Thesis submitted in accordance with the requirements of the University of Liverpool for the degree of

Doctor of Philosophy

UNIVERSITY OF LIVERPOOL

Department of Chemistry

June 2019

Abstract

Carbon–carbon (C–C) bond activation by nickel catalysts is an interesting strategy for simplifying organic synthesis. This thesis reveals that potassium alkynyltrifluoroborates undergo facile cycloaddition with 3-azetidinones and oxetanones to afford borylated dihydropyridinones and dihydropyranones, respectively, without the cleavage of the carbon–boron bond, in good yields and as a single regioisomer. Notably, the regioselectivity is independent of the alkyne substituent, which is in considerable contrast to a majority of the metal-catalysed cycloaddition reactions of alkynylboron derivatives. Instead, the regioselectivity is solely controlled by the trifluoroborate group. The results presented in this thesis are published in *Chem. Commun.* **2019**, *55*, 497–500.

Contents

Acknowledgements

I would like to acknowledge the contributions made to me by my primary supervisor, Doctor Christophe Aissa. Throughout my PhD, Dr. Aissa has been a consistently a great source of help guidance and enthusiasm for chemistry. Furthermore, Dr. Aissa gave countless hours of his time and has contributed greatly to my scientific development. Throughout my time in the Aissa group, all of my colleagues have been helpful to me. All have helped to keep my spirits high. Am thankful to all of the technical staff in the chemistry department of Liverpool. Finally, I am very grateful to my parents and my wife who have provided constant support during these 4 years. Could not have completed my PhD without them. Thank you always for encouraging me to do my best in life.

Abbreviations

δ	Chemical shift
°C	Degrees Celsius
Bn	Benzyl
br	Broad
Cl	Chemical ionisation
cod	Cyclooctadiene
d	Doublet
DMAc	N,N-Dimethylacetamide
DMSO	Dimethyl Sulfoxide
Equiv	Equivalent
ESI	Electrospray lonisation
EtOAc	Ethyl Acetate
Et_2O	Diethyl Ether
eV	Electronvolt
g	Gram
GC	Gas Chromatography
h	Hour
HOMO	Highest occupied molecular orbital
HMBC	Heteronuclear Multiple Bond Correlation
HRMS	High Resolution Mass Spectrometry

HSQC	Heteronuclear Single-Quantum Correlation
Hz	Hertz
IR	Infrared
Ipr	1,3-Bis(2,6-diisopropylphenyl)imidazol-2-ylidene
J	Coupling Constant
LUMO	Lowest unoccupied molecular orbital
m	Multiplet
M	Molar
m.p.	Melting point
mg	Milligram
MHz	Megahertz
min	Minute
ml	Millilitre
mmol	Millimole
MS	Mass spectrometry
NMR	Nuclear Magnetic Resonance
NOESY	Nuclear Overhauser effect spectroscopy
PE	Petroleum Ether (40/60)
Ph	Phenyl
PPh_3	Triphenylphosphine
ppm	Part per million
q	Quadruplet

rt	Room temperature
RCM	Ring-closing olefin metathesis
s	Singlet
t	Triplet
T	Temperature
THF	Tetrahydrofuran
TLC	Thin Layer Chromatography
TMS	Trimethylsilyl

Chapter 1: Nickel-catalysed cycloaddition of four-membered-ring ketones

The activation of four-membered rings by transition-metal catalysts occurs in two major modes: Oxidative addition of a single C–C bond to the metal and β-carbon elimination.[1] The ring strain for cyclobutane is 29.0 kcal/mol. As a result, cyclobutane derivatives occupy a privileged role in transition-metal-catalysed C–C σ-bond activation. Indeed, metallacyclopentane **2** may form as a result of the strain-driven oxidative addition of the C–C bond of generic cyclobutane **1** to a transition metal (Scheme 1).[2,3] This metallacycle can be used as a reactive intermediate in different reaction pathways to close catalytic cycles, which is described in this chapter. The other predominant mode for the cleavage of the C–C bond is the redox-neutral β-carbon elimination, wherein the cleavage of a C–C σ-bond occurs with the concomitant generation of a π-bond. However, according to thermodynamic considerations, such a process is not likely, except when it is driven by the release of ring strain, as in the case of cyclobutane derivatives, i.e. in the opening of intermediate **3** to afford **4** (Scheme 1).[3]

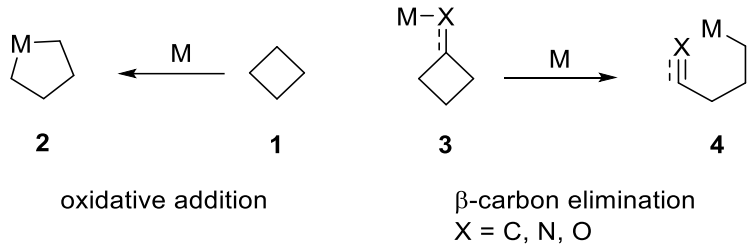

Scheme 1. Transition-metal-catalysed carbon–carbon bond activation of four-membered rings.

1. [4+2] Cycloaddition of cyclobutanones and alkynes

Murakami and co-workers reported the first nickel-catalysed cycloaddition of cyclobutanones with alkynes to afford a six-membered-ring ketone.[4] In their study, 3-methyl-3-phenylcyclobutanone and 4-octyne were heated in the presence of a nickel catalyst prepared in situ from bis(1,5-cyclooctadiene)nickel(0) (10 mol%), affording α,β-unsaturated ketone **6** in 95% yield (Scheme 2). However, by using an unsymmetrical alkyne, e.g. 1-phenyl-1-propyne, desired product **7** was obtained in a regioselective manner (92:8). Furthermore, by using electron-rich and electron-poor aryl substituents on the alkyne, the yield of the products decreased, as illustrated with **8** and **9**, respectively. The authors (Murukami and co-workers) reported that terminal alkynes do not undergo this reaction. Although 20 mol% of the nickel catalyst was required for the reaction of 3,3-diethylcyclobutanone to afford **10**, the yield was less than that of **7** or **11**. Cyclobutanones bearing substituents at the 2-position, e.g. 2-phenylcyclobutanone, failed to undergo this reaction, most likely due to steric reasons.[4] The oxidative cyclisation of the carbonyl group in cyclobutanone and the triple bond of the alkyne in nickel(0) complex **12** was proposed to lead to the formation of oxanickelacyclopentene **13**. The four-membered ring would then be cleaved by β-carbon elimination, leading to the ring expansion to afford seven-membered nickelacycle **14**. Finally, reductive elimination would afford the observed products and regenerate the catalyst (Scheme 3). The oxidative cyclisation that would afford **13** is in agreement with experimental and theoretical studies.

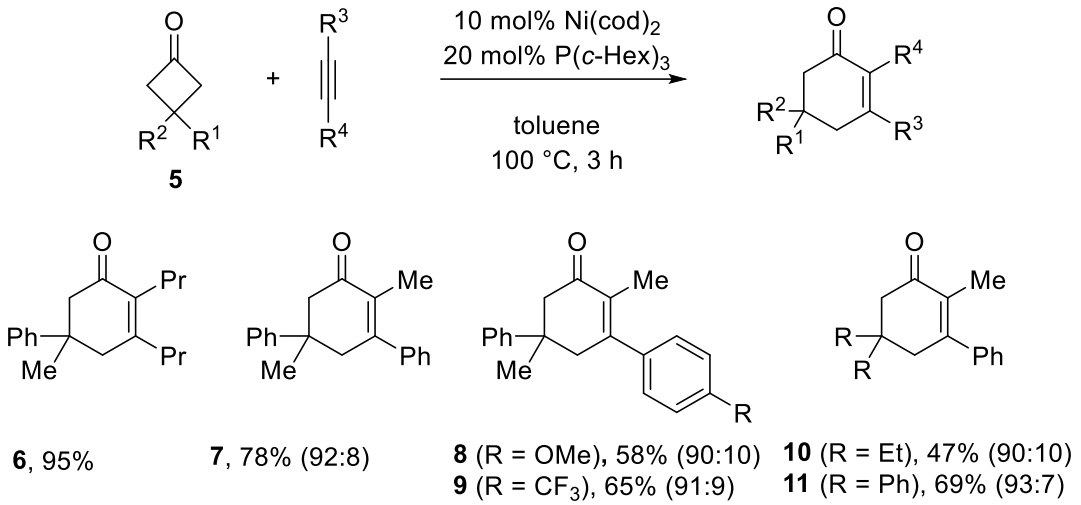

Scheme 2. Nickel-catalysed [4+2] cycloaddition of alkynes with cyclobutanones.

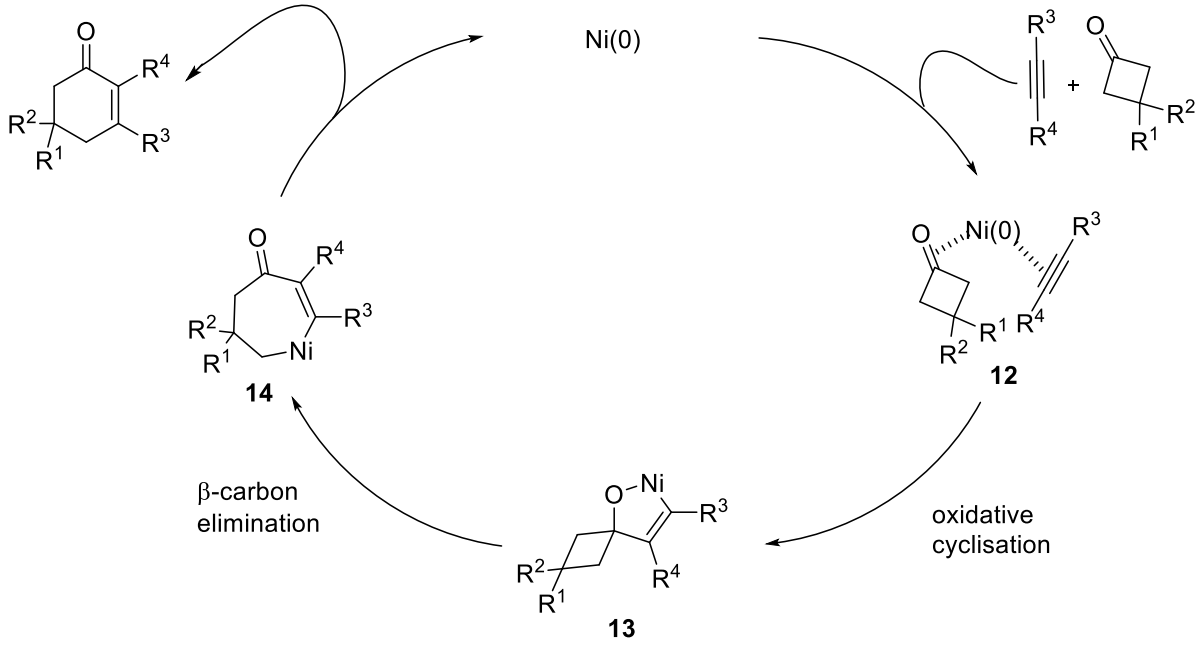

Scheme 3. Proposed mechanism for the nickel-catalysed [4+2] cycloaddition of alkynes with cyclobutanones (ligands are omitted for clarity).

Indeed, Ogoshi and co-workers reported the formation of nickel complex **16** by the reaction of 5-hexenal (**15**) with $Ni(cod)_2$ and PCy_3 (Scheme 4). NMR spectra revealed that C=C and C=O bonds coordinate to Ni(0) via the η^2 mode. The solution of **16** was heated at 80 °C, leading to

the oxidative cyclisation to afford nickelacycle complex **17**. The molecular structure of **17** was confirmed by X-ray diffraction analysis.[5] The same behaviour was observed for the intermolecular oxidative cyclisation of benzaldehyde with 2-butyne to afford dimeric complex **18** (Scheme 5).[6]

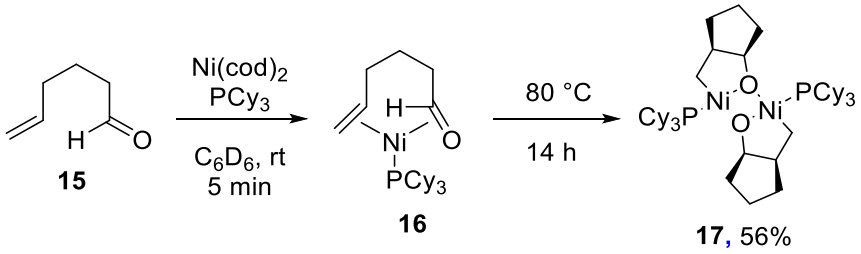

Scheme 4. Isolated nickel(0) complexes that undergo oxidative cyclisation.

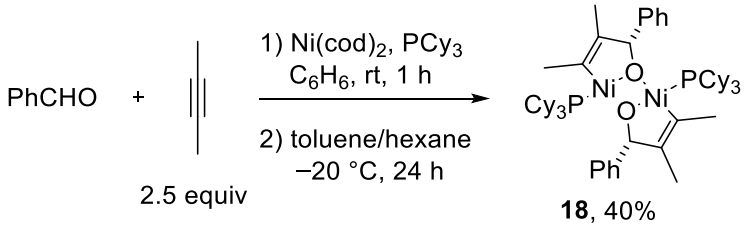

Scheme 5. Oxidative cyclisation of benzaldehyde with 2-butyne in the presence of Ni(0).

These stoichiometric studies confirmed the proposed mechanism previously reported for the nickel-catalysed reductive coupling of alkynes and aldehydes that was developed by Montgomery and Jamison[7] for the formation of allylic alcohols (Scheme 6). Notably, the regioselectivity observed for unsymmetrical alkynes in these reactions is the same as that observed in case of the [4+2] cycloaddition of alkynes and cyclobutanones reported by Murakami.[4]

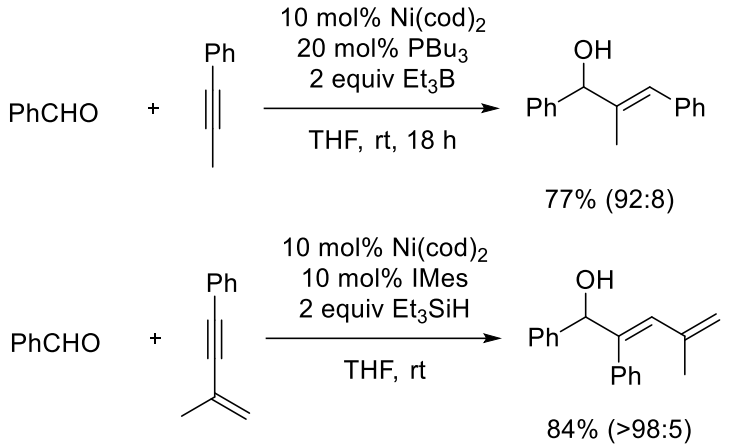

Scheme 6. Examples of the nickel-catalysed reductive coupling of aldehydes with alkynes.

Thus, it is not surprising that the regioselectivity of the nickel-catalysed reductive coupling of unsymmetrical alkynes and aldehydes was rationalised on the basis of steric hindrance in a theoretical study reported by Houk and co-workers (Scheme 7).[8] This study revealed that the oxidative addition of simple alkynes with aldehydes occurs via a planar five-membered cyclic transition state, where the metal acts as a Lewis acid and promotes the oxidative cyclisation via coordination with the aldehyde oxygen. In the transition state, the alkyne is significantly bent to enable simultaneous overlap with the metal and aldehyde carbon. Among the two possible transition states TS_1 and TS_2, the former is the most favoured due to the decreased steric hindrance between the alkyne and aldehyde substituents. Accordingly, it would be reasonable to assume a similar reason to explain the regioselectivity of the [4+2] cycloaddition reported by Murakami and co-workers, with TS_3 leading to the major regioisomer, whereas TS_4 would afford the minor regioisomer.

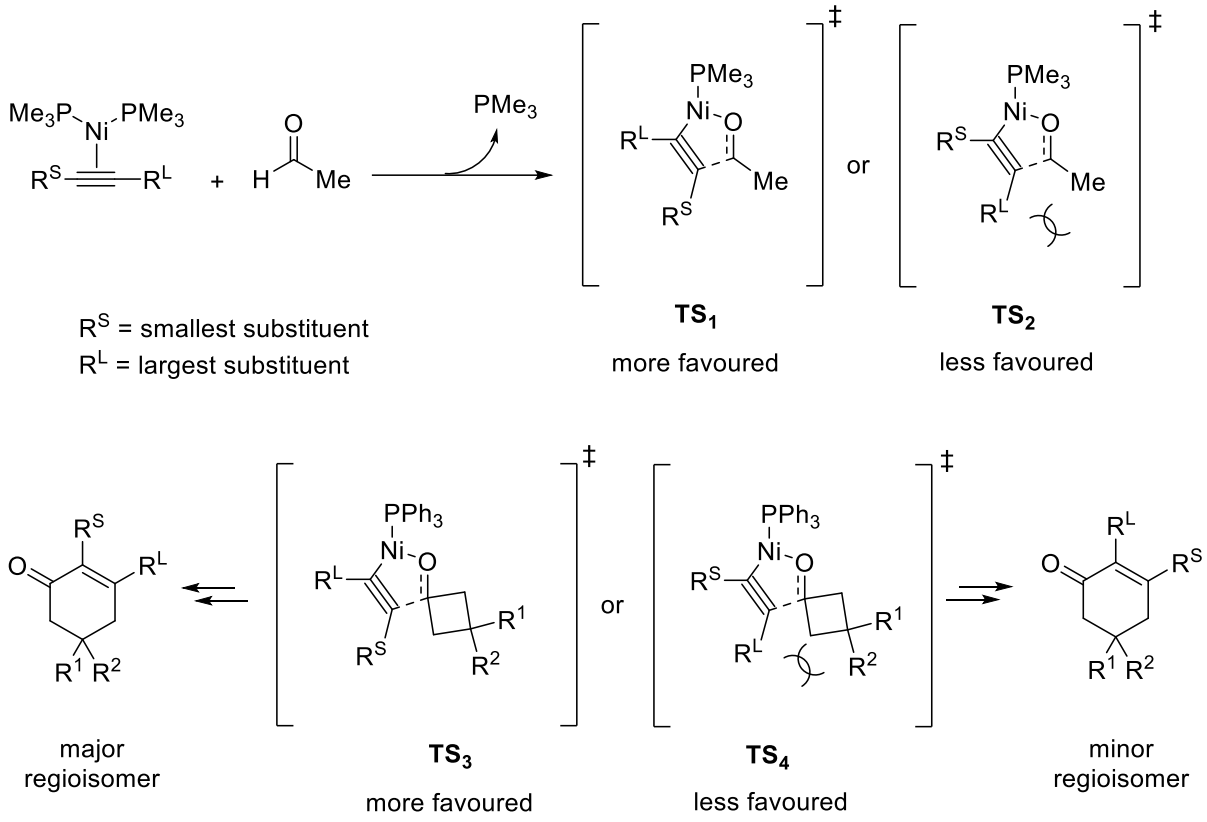

Scheme 7. Similar rationale for the regioselectivity of the [4+2] cycloaddition reported by Murakami and for the nickel-catalysed reductive coupling of alkynes with aldehydes.

2. [4+2+2] Cycloaddition of cyclobutanones and 1,n-diynes

In 2006, Murakami and co-workers reported the nickel-catalysed intermolecular [4+2+2] annulation reaction between cyclobutanones as the four-carbon unit and diynes, affording bicyclic eight-membered-ring ketones (Scheme 8).[9] For instance, desired product **22** is obtained in a good yield from the reaction of symmetrical 1,6-diyne **19** either under the same conditions used for the [4+2] cycloaddition of simple alkynes (conditions A) or even at room temperature (conditions C). However, by using unsymmetrical **20** instead, two regioisomers

22 and **23**, respectively, are obtained, although this issue is resolved under conditions C at the expense of the product yield.

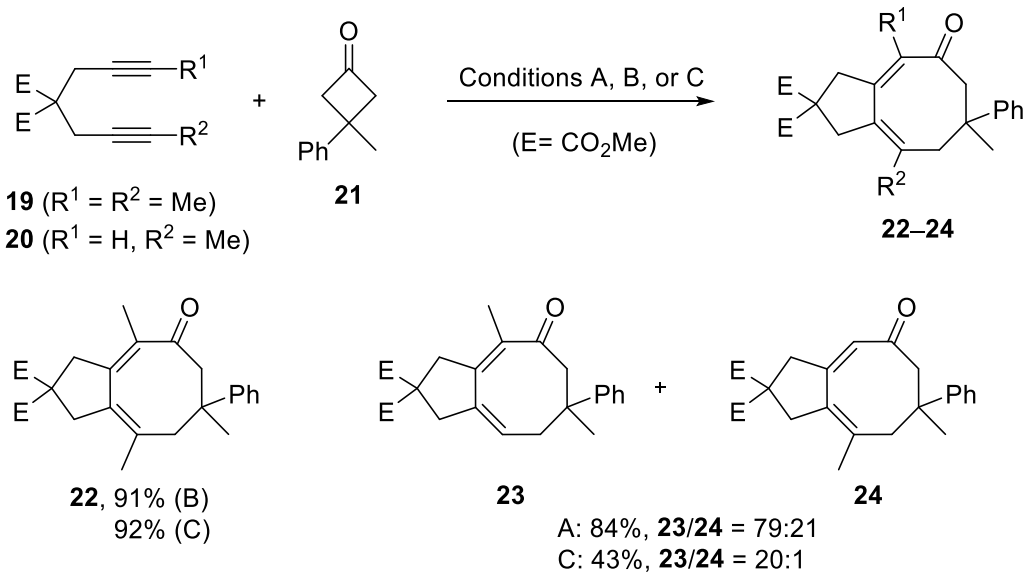

Scheme 8. Nickel-catalysed [4+2+2] annulation of cyclobutanones with 1,6-diynes.

Moreover, the reactions of unsymmetrical 2-substituted cyclobutanones **25** with **19** afford cycloadduct **27**, where only the least-hindered bond of the cyclobutanones undergoes cleavage (Scheme 9). The authors proposed that this regioselectivity can be explained by the β-carbon elimination of postulated intermediate **26**. Thus, the substituent R can sterically prevent the migration of the methyne carbon (C2), and hence favour the migration of the methylene carbon (C4).

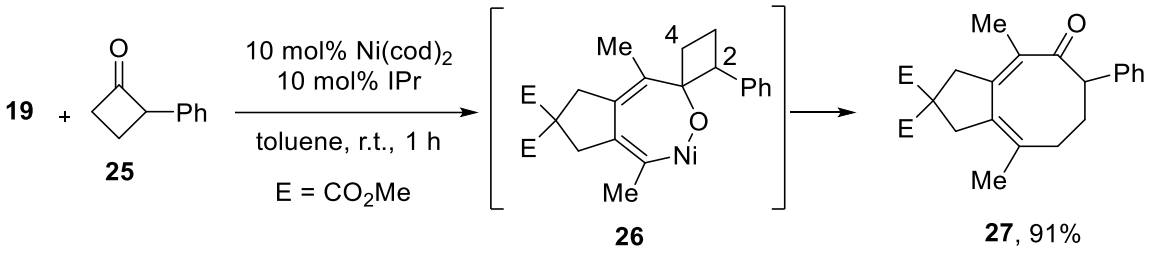

Scheme 9. [4+2+2] Cycloaddition of unsymmetrical 2-substituted cyclobutanone **25**.

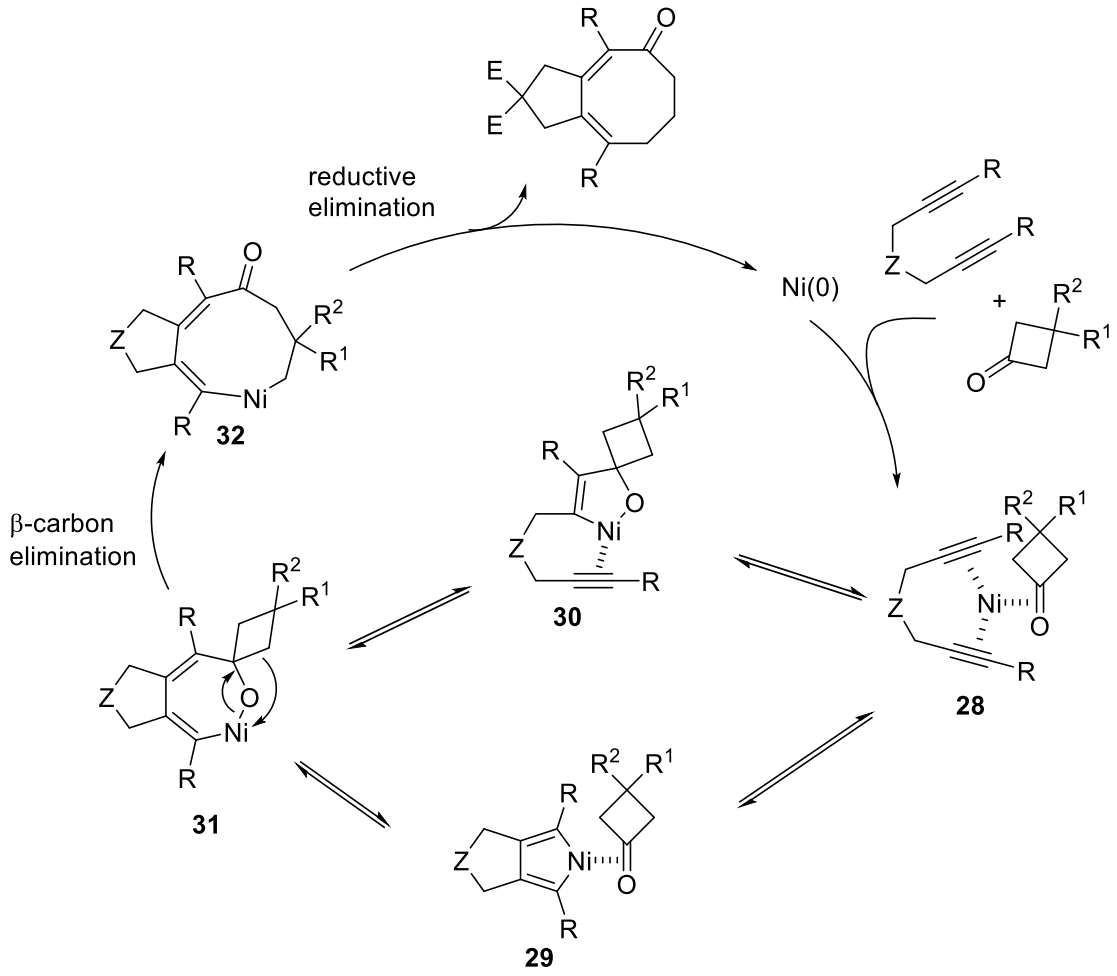

Scheme 10. Proposed mechanism for the nickel-catalysed intermolecular [4+2+2] cycloaddition of 1,6-diynes with cyclobutanones.

As has been previously proposed for the [4+2] cycloaddition of simple alkynes and cyclobutanones, β-carbon elimination is thought to be the key step for the cleavage of the C–

C bond. However, two possible intermediates can result from **28**. The oxidative cyclisation of the two alkyne moieties with nickel(0) would lead to the formation of **29**. However, the oxidative cyclisation of the carbonyl group and one of the alkyne moieties might afford **30**. Both these moieties can afford intermediate **31** by the insertion of either the remaining alkyne or the carbonyl group into a Ni–C bond. As has been argued previously, the β-carbon elimination of **31** would lead to nine-membered nickelacycle **32**, and the reductive elimination of this intermediate would afford the observed products (Scheme 10).[9] Notably, the formation of cyclohexenones, which might be formed by the β-carbon elimination of **30** with alkyne **25** with either ligand, is not observed in this reaction.

3. [4+2] Cycloaddition of cyclobutenones and alkynes

Huffman and co-workers reported the nickel-catalysed cycloaddition of substituted cyclobutenones with alkynes to afford phenols,[10] which represented the first metal-catalysed cycloaddition of these four-membered rings. The cycloaddition of 3-substituted and 3,4-disubstituted cyclobutenones with unsymmetrical alkynes was smoothly carried out to provide corresponding phenols **33–38** in good yields, albeit with poor regioselectivity (Scheme 11). Moreover, 2,3-disubstituted cyclobutenones did not undergo this reaction.

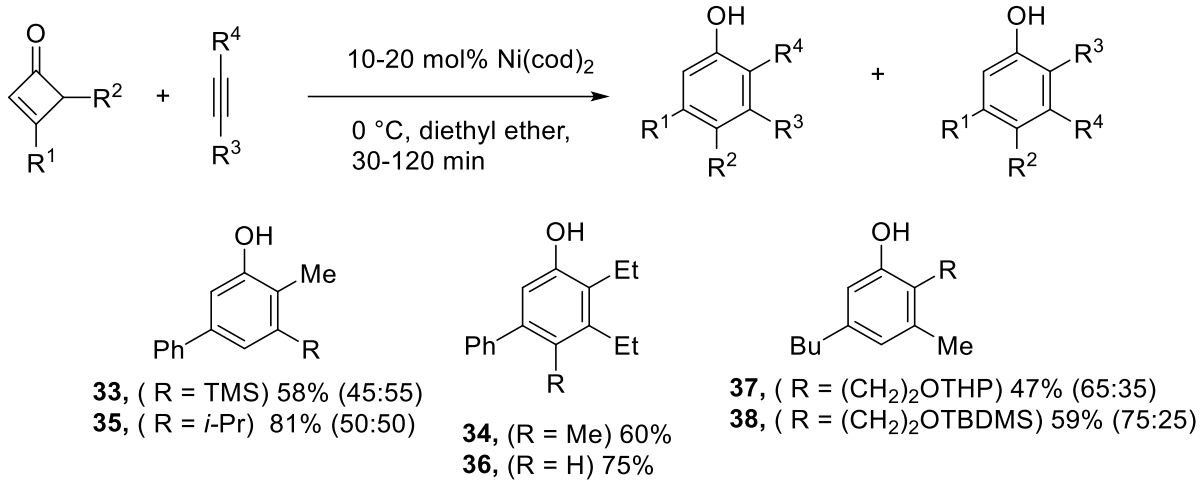

Scheme 11. Nickel-catalysed cycloaddition of cyclobutenone with alkynes.

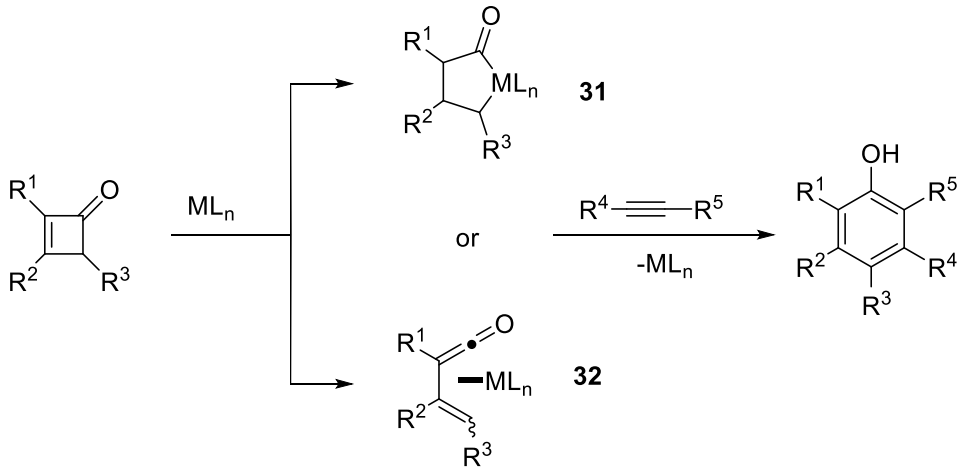

Scheme 12. Metal-catalysed cycloaddition of substituted cyclobutenones with alkynes *via* metallacycle **31** or η^4-vinylketene **32** metallic intermediate.

In principle, either the Csp^2–Csp^2 or Csp^2–Csp^3 single carbon–carbon bond of these cyclobutenones can be cleaved in this reaction. However, all of the products are obtained only by the apparent cleavage of the latter. This result might be explained by five-membered metallacycle **31** or η^4-vinylketene **32** metallic intermediate. Metallacycles such as **31** are formed *via* the insertion of $ClRh(PPh_3)_3$ into cyclobutenones. However, they did not react with

alkynes to afford phenols. η^4-Vinylketene complexes such as **32** are formed from (η^5-indenyl)Co(PPh_3)$_2$, and these intermediates react with alkynes to form phenols, but only in stoichiometric reactions.[11]

4. Cycloaddition of benzocyclobutenones

Hernandez and co-workers reported the nickel-catalysed [4+2] cycloaddition of benzocyclobutenones with diphenylacetylene to afford products *via* the cleavage of the proximal Csp^2–Csp^2 bond (Scheme 13).[12] In all cases, products **39–42** are obtained as a single regioisomer in good yields. The structure of **41** is confirmed by X-ray crystallography. On the other hand, by using dialkylacetylenes, terminal alkynes, or alkynes bearing aryl and alkyl groups on both ends, benzocyclobutenones are recovered, and the desired product is not obtained.

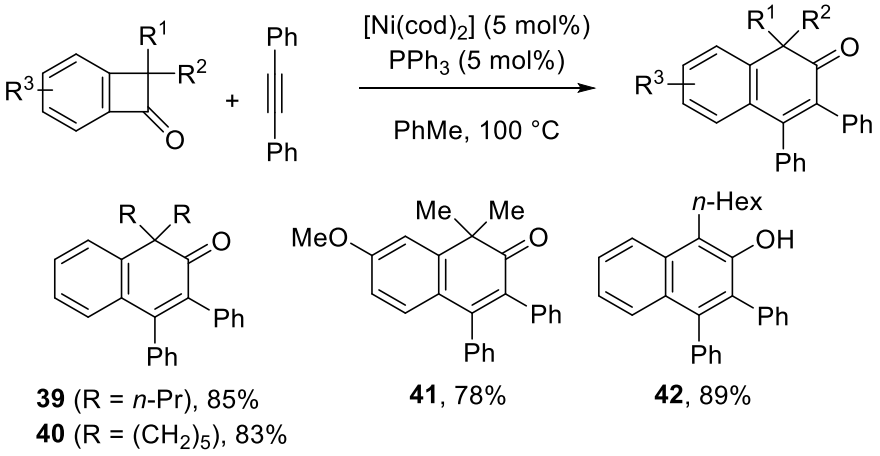

Scheme 13. Nickel-catalysed [4+2] cycloaddition of benzocyclobutenones with diphenylacetylene.

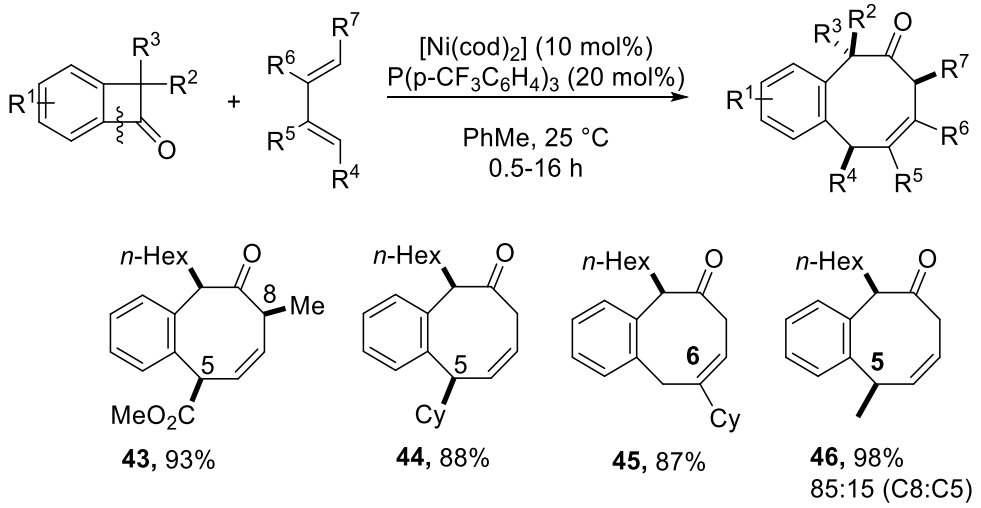

Scheme 14. Ni-catalysed intermolecular [4+4] cycloaddition of benzocyclobutenones with 1,3-dienes.

Similarly, the nickel-catalysed [4+4] cycloaddition of benzocyclobutenones with 1,3-diene affords benzo-fused eight-membered rings (Scheme 14). The dienes with a substituent at positions 1 and 4 typically afford only one regioisomer, as illustrated with **43**. Similarly, dienes bearing only one substituent at position 2 also afford only one diastereomer, as illustrated with **45**. On the other hand, terminal dienes afford only one regioisomer, as illustrated with **44**, or a mixture of the two possible regioisomers, as illustrated with **46**. In addition, notably, other olefins either in benzocyclobutenone or in 1,3-diene are tolerated in the reaction.

5. [4+2] Cycloaddition of azetidinones and oxetanones

The nickel-catalysed [4+2] cycloaddition of commercially available *N*-Boc-3-azetidinone with unsymmetrical alkynes affords two regioisomers, which are separated by flash chromatography (Scheme 15).[13] Products **47**–**52** having an alkyl group (R^1) α to the carbonyl are the major regioisomers.[13-15] Notably, **48** is obtained as a single regioisomer due to the

presence of a large alkyl group (R^2 = *t*-Bu). The cycloaddition with trimethylsilyl-substituted alkyne affords regioisomer **49**, in which case the silyl group is at a position α to the carbonyl group.[13] The use of tributylstannyl-methyl alkyne as the substrate affords stannyl piperidine **50** regioselectively, with the methyl group at a position α to the carbonyl group. However, the use of tributylstannyl-phenyl alkyne affords **51** instead, with the complete reversal of regioselectivity. In addition, Aïssa and co-workers investigated the regioselectivity of the insertion of unsymmetrical alkynes into the C–C bond of oxetan-3-one. The cycloaddition with trimethylsilyl-substituted alkyne affords pyranone **52** with good regioselectivity, which is similar to that observed with the azetidinone (Scheme 15).[13]

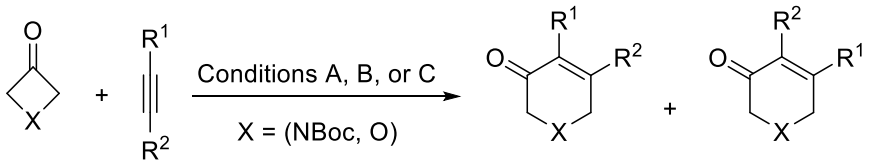

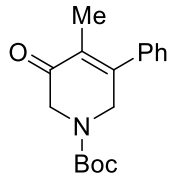
47, 92% (87:13), (A)

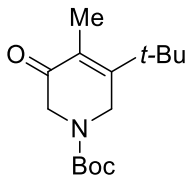
48, 87% (100:0), (A)

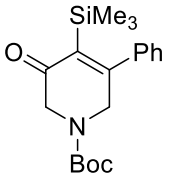
49, 91% (97:3), (A)

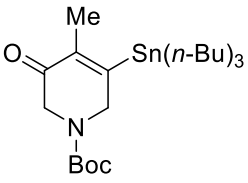
50, 89% (95:5), (B)

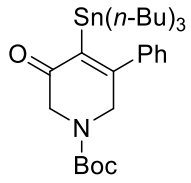
51, 83% (95:5), (C)

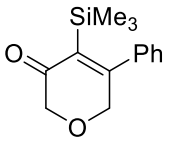
52, 99% (96:4), (A)

Conditions A: 10 mol% $Ni(cod)_2$, 30 mol% PPh_3, Dioxene, 90 °C, 17 h
Conditions B: 5 mol% $Ni(cod)_2$, 10 mol% PPh_3, Toluene, 60 °C, 17 h, alkyne (1.5 equiv)
Conditions C: 5 mol% $Ni(cod)_2$, 10 mol% PPh_3, Toluene, 100 °C, 17 h, alkyne (3 equiv and slow addition)

Scheme 15. Regioselective nickel-catalysed cycloaddition of *N*-Boc-3-azetidinone and 3-oxetanone with unsymmetrical alkynes.

Furthermore, the regioselectivity of the ring cleavage of α-substituted azetidinone **53** was examined, and products were obtained in a good yield, indicative of the sole cleavage of the less-substituted bond of **53** (Scheme 16).[13] The insertion of alkynylstannanes exclusively affords 2-stannylpiperidinones **54–56**. In contrast to the examples **50** and **51** reported by Louie (Scheme 15), the stannyl group is always found at a position α to the carbonyl. To explain this result, Murakami proposed that the moderate electronegativity of tin renders the carbon attached to it more negatively charged, and hence more prone to form a bond with the positively charged carbonyl carbon atom of the azetidinone.

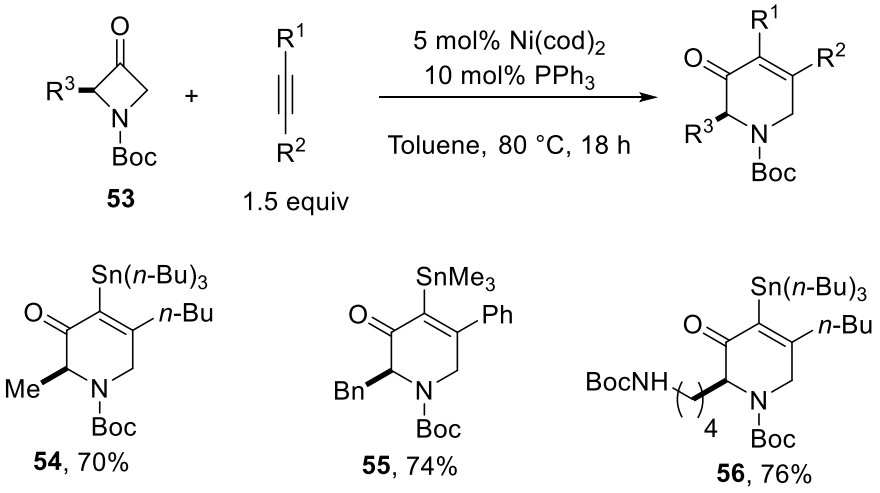

Scheme 16. Regioselectivity of the ring opening of α-substituted azetidinone.

The authors of these first studies on azetidinones and oxetanones[13-15] proposed a mechanism similar to that proposed by Murakami for the cycloaddition of alkynes with cyclobutanones.[4] Thus, the oxidative cyclisation intermediate **A** would undergo β-carbon elimination to afford a metallacycle **B** (Scheme 17).

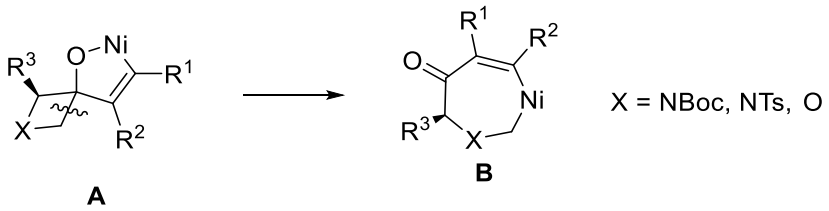

Scheme 17. Proposed mechanism for the nickel-catalysed [4+2] cycloaddition of azetidin-3-one and oxetanones with alkyne.

However, Li and co-workers employed density functional theory (DFT) to examine the nickel-catalysed cycloaddition of 3-azetidinones with alkynes and reported that the proposed cleavage of the C–C bond from **A** to **B** demands an inaccessibly high barrier of 46.5 kcal/mol.[16] Instead, the authors proposed a mechanism based on the oxidative addition of 1-Boc-3-azetidinone to the Ni(0) centre, followed by the insertion of an alkyne into the Ni–C(sp^2) or Ni–C(sp^3) bond, depending on the alkyne substrate. Thus, an electrophilic alkyne can insert into the Ni–C(sp^3) bond, whereas a nucleophilic alkyne inserts into the Ni–C(sp^2) bond. With respect to the insertion of **57** and **58**, four transition states TS_1–TS_4, respectively, are possible (Scheme 19). The lowest barrier of 21.8 kcal/mol is achieved by TS_3, where the alkyne behaves as nucleophile and inserts into the Ni–C(sp^2) bond with the minimisation of steric hindrance. Notably, TS_2 would lead to the same regioisomer, but the insertion of the alkyne into the Ni–C(sp^3) bond is clearly less favoured with a barrier of 27.2 kcal/mol. In the case of the TMS substituent, the lowest barrier for TS_7 is 25.6 kcal/mol, where the alkyne behaves as electrophile and preferentially inserts into the Ni–C(sp^3) bond.

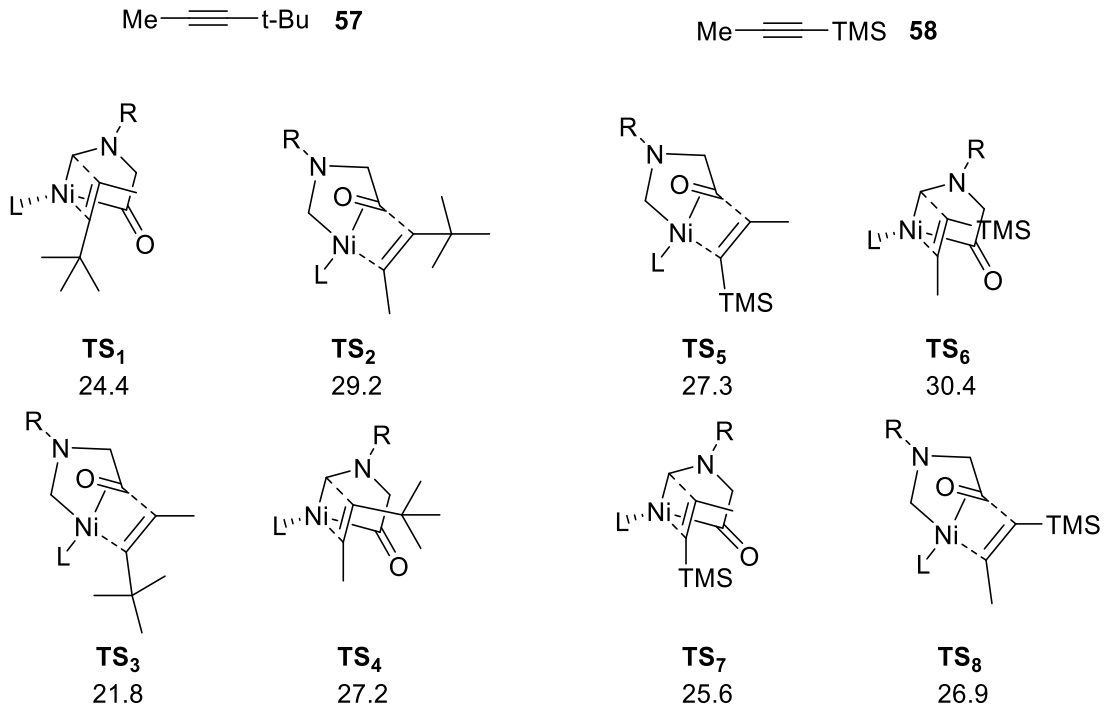

Scheme 19. Transition states illustrating the insertion of the alkyne into the relevant C–Ni bond for *t-Bu*-substituted and TMS-substituted alkynes.

Louie and co-workers reported the nickel-catalysed cycloaddition of 3-oxetanone (**59**) with diphenylacetylene using $NiCl_2(PPh_3)_2$ or $NiBr_2(PPh_3)_2$ with zinc powder in acetonitrile. However, the regioselectivity of the insertion of unsymmetrical alkynes into the C–C bond of 3-oxetanone was not investigated,[17] and Aïssa and co-workers reported an interesting effect of the 2-thiophenyl group on the regioselectivity of the insertion using $NiBr_2(PPh_3)_2$ and zinc powder in THF (Scheme 20).[18]

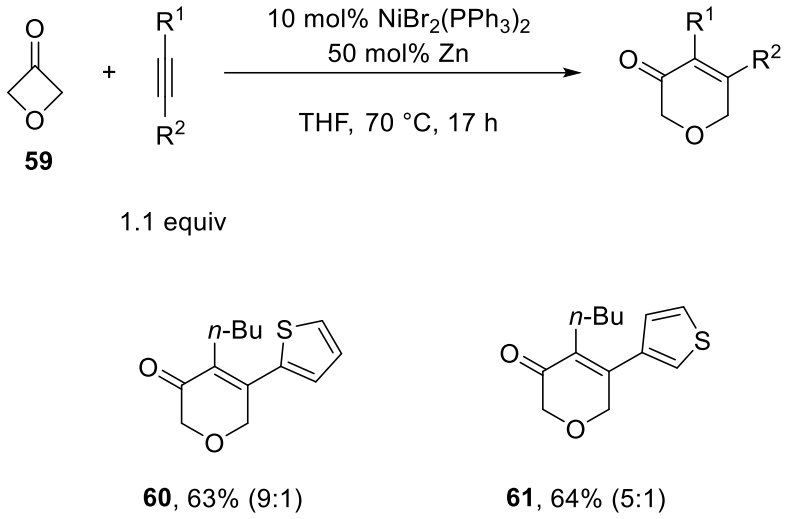

Scheme 20. Regioselective insertion of unsymmetrical alkynes into the C–C bond of oxetan-3-one.

The regioselectivity observed for the insertion of 2-(hex-1-yn-1-yl)thiophene **62** into the C–C bond of 3-oxetanone is considerably better than that observed for the insertion of 3-(hex-1-yn-1-yl)thiophene (**63**) (Scheme 21).[18] This result can be explained by the η^1-coordination of the sulfur atom either in the oxidative cyclisation transition state **I** towards the intermediate **II** (pathway a) or in the transition state **IV** from intermediates **III** to **V** (pathway b). Both pathways can converge towards intermediate **V**, liberating the catalyst and the major regioisomer **60** after reductive elimination.[13,18] Such η^1-coordination is not possible for alkyne **63**.

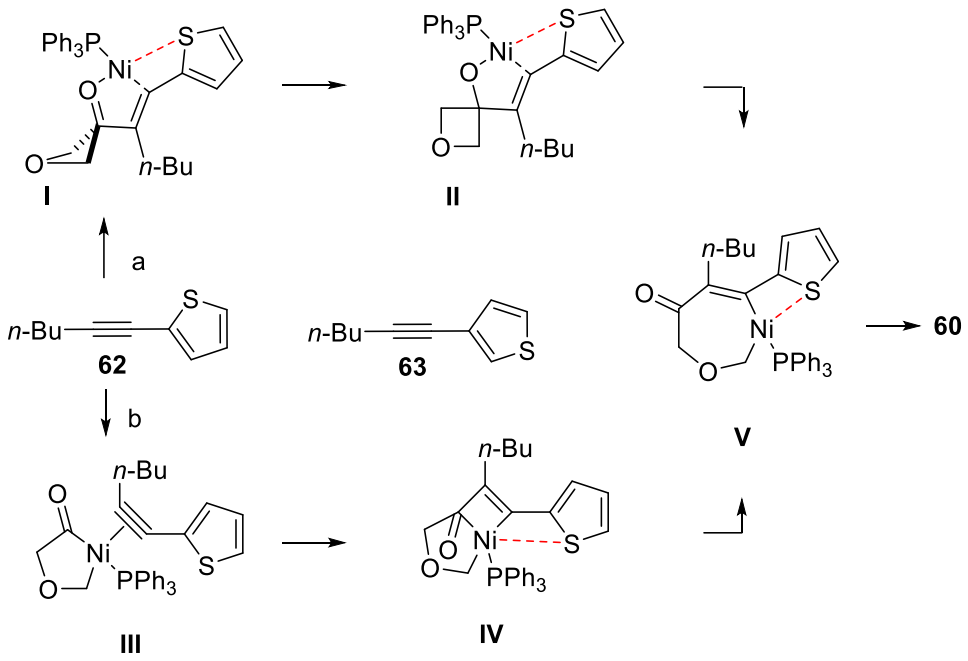

Scheme 21. Possible rationale for explaining the enhanced regioselectivity of the insertion of 2-(hex-1-yn-1-yl)thiophene during the formation of **60**.

Alkenes are another directing group that strongly affect the regioselectivity of the [4+2] cycloaddition of alkynes with azetidinones. Thus, the reaction of *N*-Ts-3-azetidinone with internal alkynes bearing two alkyl substituents that are not electronically or sterically often affords poor regioselectivity (Scheme 22).[19] Initial attempts of varying the ligand to improve the regioselectivity are not successful, leading to the decrease in the yield of desired product **64**.[13,14] Instead, the selection of the substituents on 1,3-enynes **65** and **66** and subsequent hydrogenation and aromatisation leads to complementary access to each of the two regioisomers of 3-hydroxy-4,5-alkyl-substituted pyridines **67** and **68**, respectively (Scheme 23).

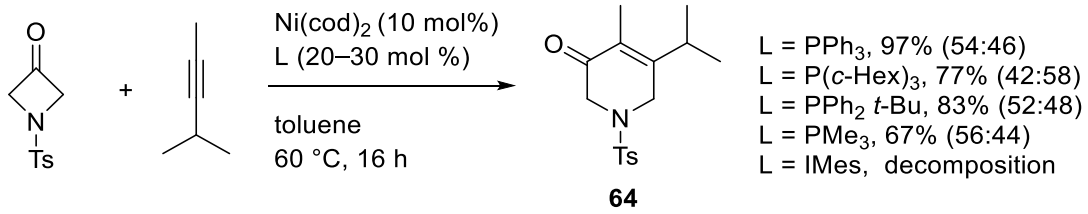

Scheme 22. Poor regioselectivity of the nickel-catalysed [4+2] cycloaddition of *N*-Ts-3-azetidinone with 4-methyl-pent-2-yne.

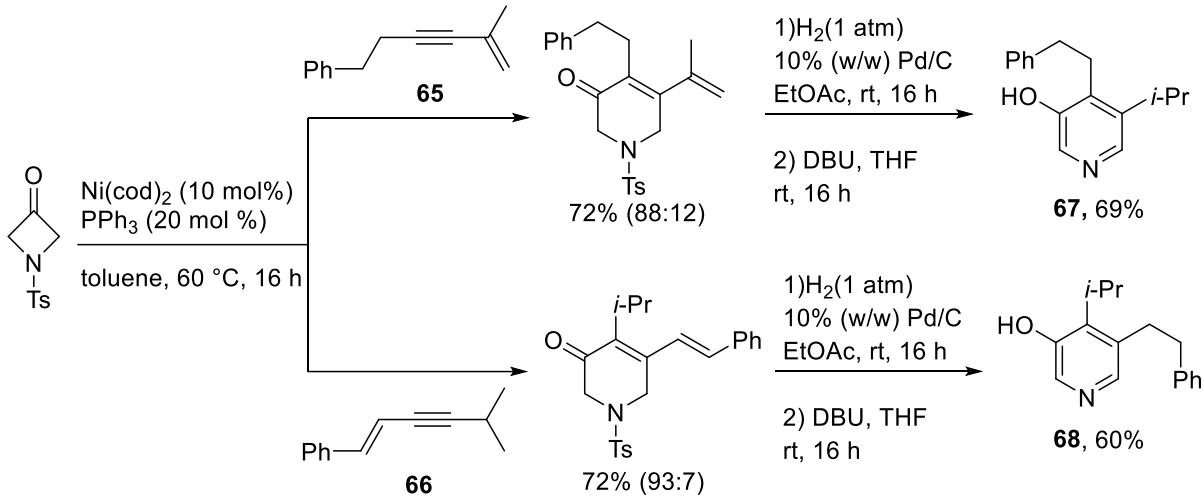

Scheme 23. Regioselective synthesis of 3-hydroxy-4,5-alkyl-substituted pyridines using 1,3-enynes as alkyne surrogates.

6. Other cycloaddition reactions of azetidinones and oxetanones

6.1.[4+2+2] Cycloaddition with 1,6-diynes

Kumar and co-workers reported the [4+2+2] nickel-catalysed cycloaddition of 1,6-diynes with 3-azetidinone **69** (Scheme 24).[20] For example, this reaction affords **70**, in a similar manner to the [4+2+2] cycloaddition of 1,6-diynes with cyclobutanones that was reported by Murakami and discussed previously in Section 2 of this chapter.[9]

However, the authors also investigated the reaction of unsymmetrical diynes and found the reaction to afford only one regioisomer, as illustrated in the case of **71** and **72** (Scheme 24).

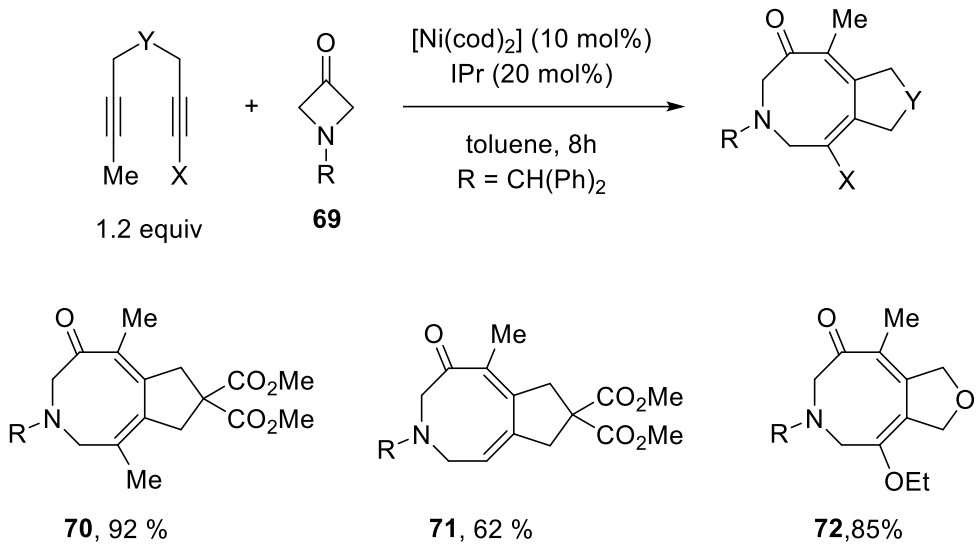

Scheme 24. Nickel-catalysed [4+2+2] cycloaddition of 3-azetidinone with unsymmetrical 1,6-diyne.

According to the same mechanism proposed by Murakami for cyclobutanones and based on oxidative cyclisation of the 1,6-enyne with the carbonyl group of the azetidinone, it is understandable that intermediate **73** would be favoured over **74** by the minimisation of steric interactions between the methyl group on the 1,6-enyne and the ligand on nickel (Scheme 25). In the case of an ethoxy-substituted diyne, the authors proposed that regioselectivity is governed by the electronic nature of the alkyne. Accordingly, the oxidative coupling of the methyl-group-bearing alkyne to afford **75** would be more favoured than the coupling of the alkyne with perturbed electronics to afford **76**. The isolation of hetereocycles **73** and **74** from 1,7-diynes supports this explanation.

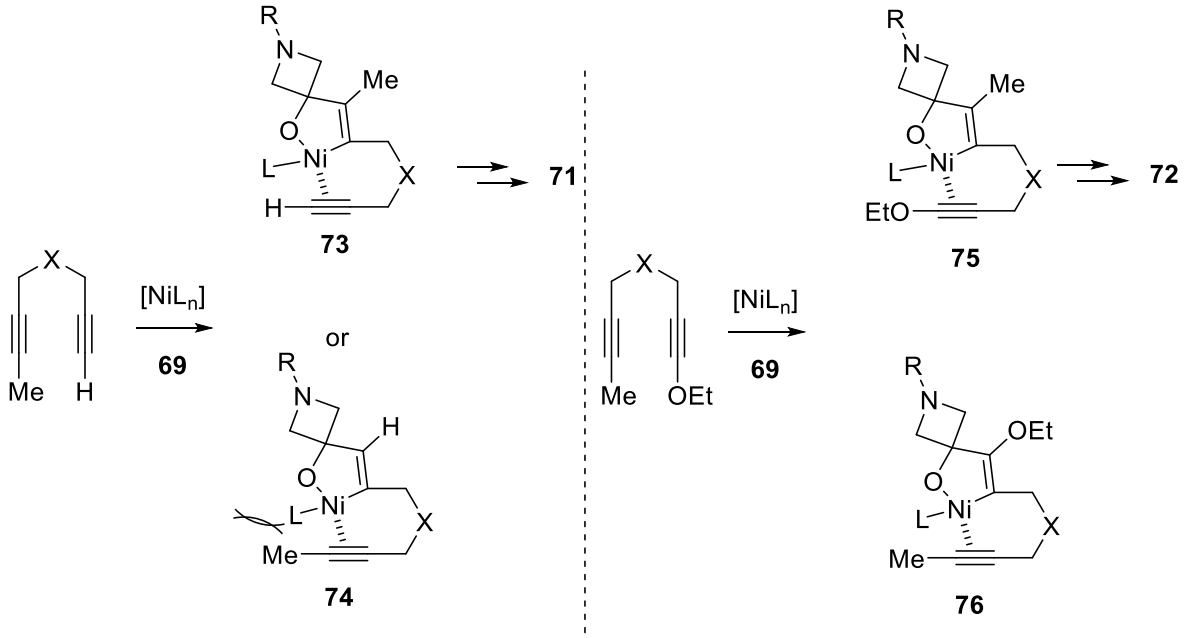

Scheme 25. Possible mechanism for the nickel-catalysed [4+2+2] cycloaddition of azetidinones with 1,n-diynes.

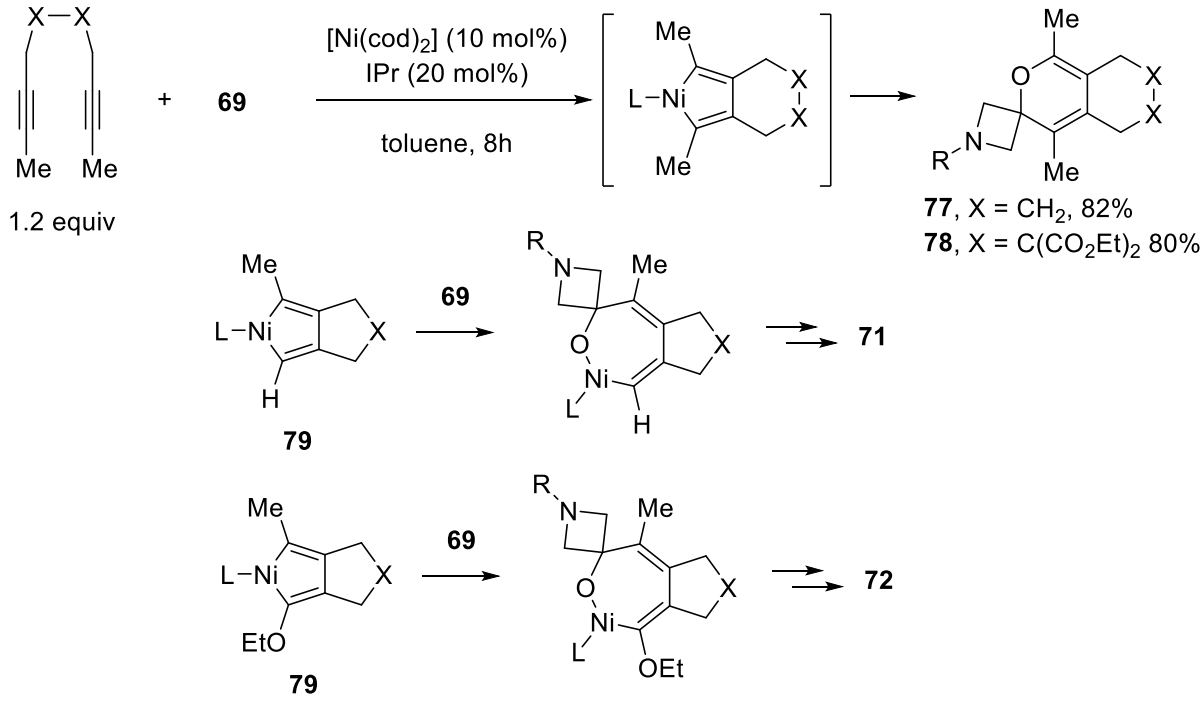

Scheme 26. Formation of cycloadducts without C–C cleavage and its consequence for the possible mechanism of the [4+2+2] cycloaddition of 1,6-diynes with 3-azetidinones.

An alternative explanation would be that the oxidative cyclisation of 1,6-diynes occurs before the migratory insertion of the carbonyl group. Louie and co-workers reported that 1,7-diyne affords products **77** and **78** without the C–C cleavage of the azetidine (Scheme 26). Therefore, the regioselectivity observed for **71** and **72** can result from the preferred migratory insertion of the azetidinone into one of the two C–Ni bonds of intermediates **79** and **80**.

6.2. [4+4] Cycloaddition with 1,3-dienes

In agreement with the [4+2] cycloaddition of 1,3-dienes with benzocyclobutenones reported by Martin,[12] Louie and co-workers reported the nickel-catalysed cycloaddition of azetidinones and oxetanones with 1,3-dienes (Scheme 27).[21]

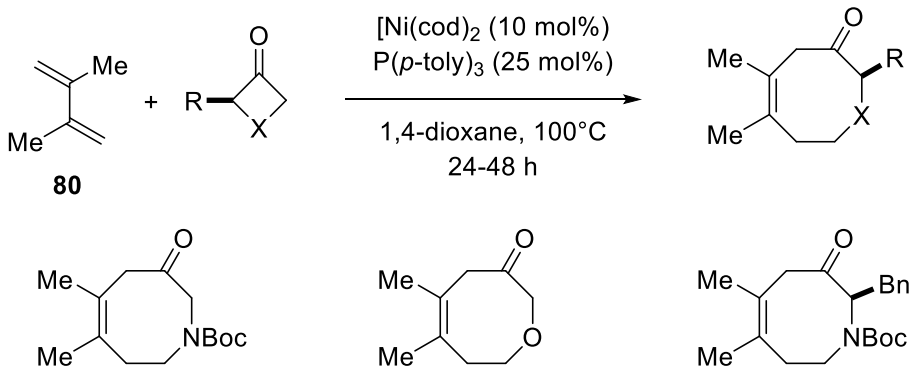

Scheme 27. Nickel-catalysed cycloaddition of azetidinone and oxetanone with 1,3-dienes.

The reactions of symmetrical 1,3-diene **80** with Boc-protected azetidinone and oxetanone afford **81** and **82**, respectively. Moreover, the cycloaddition of 2-benzyl-3-azetidinone with diene **76** affords desired product **83** in a high yield as a single regioisomer, but the

enantiomeric purity of the stereocentre is compromised during the reaction. However, in contrast to the results reported by Martin for benzocyclobutenones,[12] the use of terminal 1,3-diene **84** affords substituted [4+2] cycloaddition product piperidinone **85** in a moderate yield rather than the expected [4+2+2] product (Scheme 28).

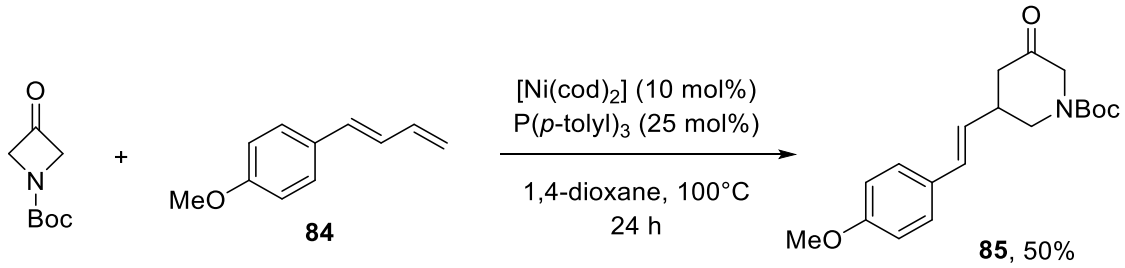

Scheme 28. Nickel-catalysed cycloaddition of *N*-Boc-3-azetidinone with unsymmetrical diene **80**.

One clear limitation is the tolerance of functional groups on the alkyne. Notably, attempts to use each of alkynylboron derivatives **86**–**88** in the nickel-catalysed [4+2] cycloaddition of azetidinones completely fail, and either alkynylboronic acids or the corresponding esters lead to the partial or complete decomposition of those alkynes without the formation of the desired product (Scheme 29).[17]

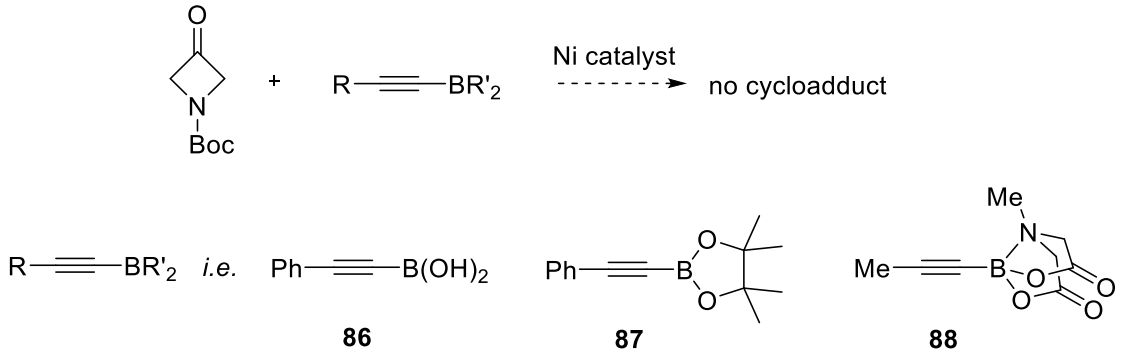

Scheme 29. Alkynylboron derivatives that failed to undergo the Ni-catalysed [4+2] cycloaddition with *N*-Boc-azetidinone.

7. Conclusion

In conclusion, remarkable progress is made on the development of atom-economical cycloaddition between unsaturated substrates, particularly alkynes, and four-membered ring ketones, with the concomitant C–C cleavage in the presence of nickel catalysts. The cycloaddition of alkynylboron derivatives is associated with multiple challenges, as will be discussed in the next chapter. However, overcoming these challenges would be extremely beneficial in view of the central role of organoboron compounds in modern organic synthesis.[22]

Chapter 2: Ni-catalysed cycloaddition of alkynyltrifluoroborates with azetidinones and oxetanones

1. Introduction

The main challenge associated with the cycloaddition of alkynylboron derivatives is the frequently observed poor regioselectivity,[23-35] as shown below in the brief overview of the literature.

2. Cycloaddition of alkynylboron compounds

2.1. Cycloaddition of alkynylboronates without metal catalysts

Those afforded by the cycloaddition reactions that are only promoted by thermal energy, which is discussed in the following

2.1.1. Cycloaddition of alkynylboronates with tetrazines

Helm and co-workers reported that the [4+2] cycloaddition of alkynylboronic esters **89** with symmetrical and unsymmetrical tetrazines **90** occurs at high temperature, affording corresponding pyridazine boronic esters **91–92** (Scheme 30).[24] In this reaction, the cycloaddition between alkynylboronic esters and unsymmetrical tetrazines affords a single regioisomer, as exemplified with **93**. Kinetic and computational (B3LYP/6-31G*) studies of this reaction suggested that the electronic behaviour of alkylboranes depends on the heteroatoms attached to the boron.[36]

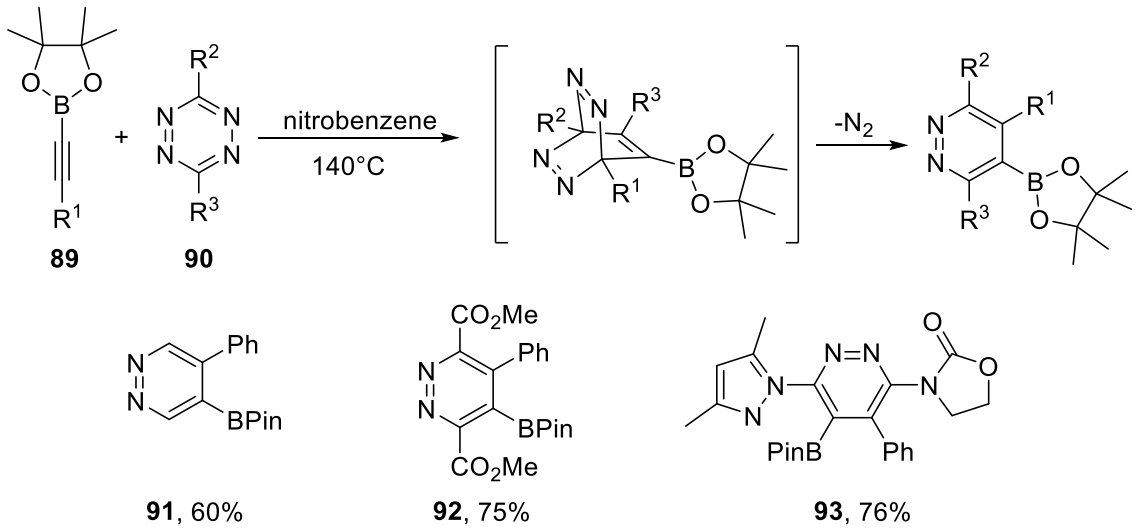

Scheme 30. [4+2] Cycloaddition of alkynylboronic esters with symmetrical and unsymmetrical tetrazines.

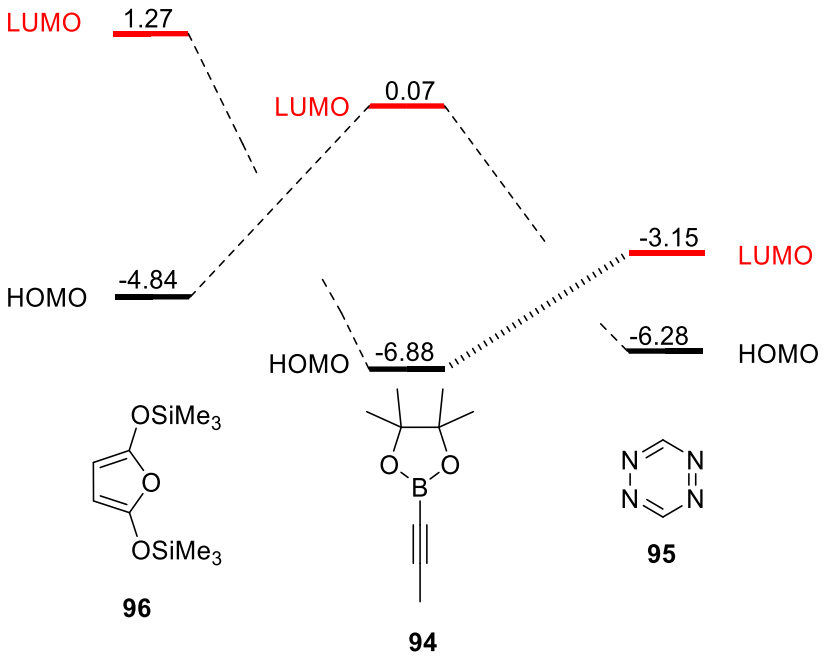

Scheme 31. HOMO and LUMO energies (in eV) for reactions between **96**+**94** and **94**+**95** calculated at the B3LYP/6-31G* level. Optimal HOMO–LUMO interactions for alkyne are denoted by bold dotted lines.

In contrast to expectations and in comparison with reactions of alkynylboranes and dichloroalkynylboranes, alkynylboronates appear to behave as relatively electron-rich dienophiles (Scheme 31). The preferred HOMO–LUMO interaction in the reaction between boronate **94** and tetrazine **95** is between the HOMO of the boronate (–6.88 eV) and the LUMO of the tetrazine (–3.15 eV). This is in agreement with an inverse-electron-demand Diels–Alder reaction, with an energy difference of 3.73 eV, whereas the gap energy between the HOMO of the tetrazine and LUMO of the boronate is 6.35 eV. Similarly, the gap between the HOMO of furan **96** and the LUMO of boronate **94** is 4.91 eV, which is extremely high for efficient orbital overlap. Hence, alkynylboronate reacts considerably faster with tetrazine **95** than with furan **96**.[36]

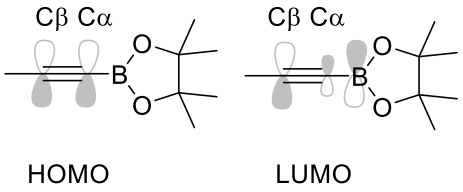

Scheme 32. HOMO and LUMO representations for **94**.

Scheme 32 shows the HOMO and LUMO orbitals of alkynylboronate **94**.[36] The HOMO is apparently centred on the triple bond, and the coefficient values at C_α and C_β are similar, while the coefficient at boron approaches zero. Hence, the boron atom does not participate in the transition state. In contrast, the LUMO of alkynylboronate **94** is apparently strongly polarized at C_α and C_β, and the coefficients on the boron atom and carbon atom C_β are large. In other words, the reactivity and electronic behaviour of alkylboronate through its HOMO are similar to the reactivity of acetylene.[36] As alkynylboronate esters react via their HOMO in

this reaction, and given that the coefficients at C_α and C_β are similar, it is likely that the regiochemistry of **93** is explained by steric interactions.

2.1.2. Cycloaddition of alkynylboronates with sydnones

In contrast to the excellent, predictable regioselectivity of the [4+2] cycloaddition of alkynylboronates with tetrazines, the [4+2] cycloaddition with sydnones occurs with variable regioselectivity (Scheme 33).[26]

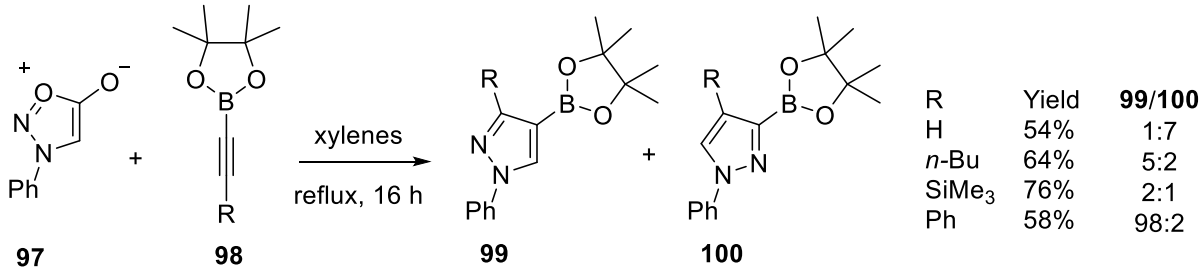

R	Yield	99/100
H	54%	1:7
n-Bu	64%	5:2
$SiMe_3$	76%	2:1
Ph	58%	98:2

Scheme 33. Regioselectivity of the [4+2] cycloaddition of alkynylboronates with sydnones.

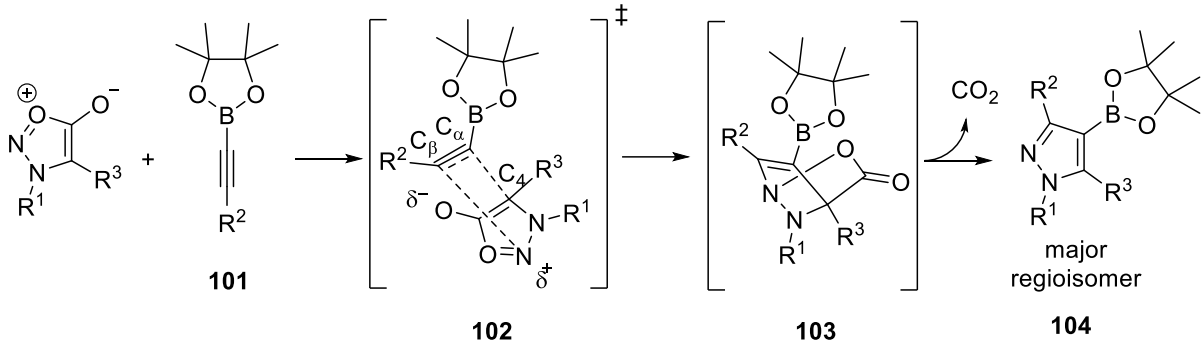

Scheme 34. Mechanism of the cycloaddition of alkynylboronates with sydnones.

The cycloaddition of acetyleneboronate **98** with 3-phenylsydnone **97** affords the corresponding pyrazole in a good yield and regioselectivity. However, switching R to *n*-Bu leads to the formation of pyrazoles with poor selectivity, with the inversion of regioselectivity.

Notably, the control of regioselectivity is explained in a theoretical study by the minimisation of the steric repulsion between R on the alkyne and the phenyl group on the sydnone.[37] The authors proposed that this possibly explain the reversal of regioselectivity between unsubstituted alkynylboronate (R = H) and more hindered derivatives (R = $SiMe_3$ or Ph).

Table 1. Cycloaddition of alkynylboronates with sydnones with more substituted sydnones

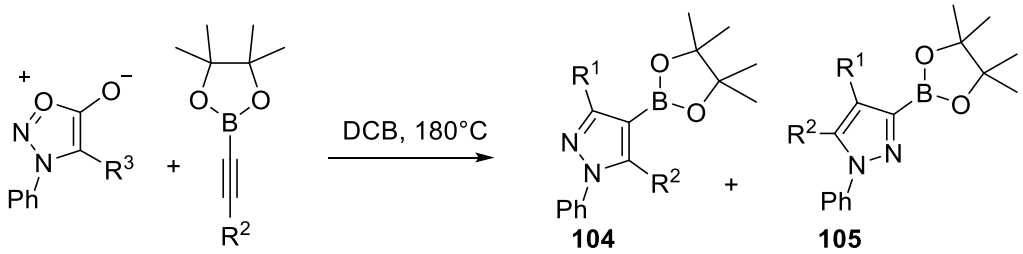

Entry	R^2	R^3	Yield	**104/105**	Entry	R^2	R^3	Yield	**104/105**
1	Ph	H	58%	>98:2	5	Mes	H	76%	2:1
2	Ph	Me	53%	>98:2	6	Mes	Me	56%	>98:2
3	Ph	*i*-Pr	38%	>98:2	7	Mes	*i*-Pr	43%	>98:2
4	Ph	Ph	59%	>98:2	8	Mes	Ph	73%	>98:2

As described in the previous section, the electron donation of oxygen atoms on the unoccupied orbital of the boron atom in **101** should exclude its participation in transition state **102** (Scheme 34). This transition state describes a concerted cycloaddition process where R^2 and R^3 are as remote as possible. This cycloaddition can be considered to be either [3+2] dipolar cycloaddition if one considers that the C^{-}–N–N^{+} fragment is the dipole or a [4+2] Diels Alder reaction if one considers that the C=C–O^{+}=N fragment is the diene. Notably, the bond-

forming distances between C_α (boronate) and C_4 (sydnone) are shorter by at least 2.1 Å than between C_β (boronate) and N (sydnone), indicating that a substituent R^3 on the sydnone exhibits considerable steric effects on the regioselectivity. Intermediate **103** is then converted to final product **104** after the loss of CO_2 (Scheme 34). On the one hand, the examples shown in Table 1 clearly reflect the effect of the substituent at C4 on the sydnone (R^3); on the other hand, in entries 6–8, in each case, only one regioisomer is observed, and compared to the phenyl or mesitylene group, the boronate fragment appears to be the more tolerated in terms of steric repulsion.[37]

2.1.3. Cycloaddition of alkynylboronates with nitrile oxides

Moore and co-workers reported the [3+2] cycloaddition of nitrile oxides with alkynylboronates to afford 3,4,5-trisubstituted isoxazoles and 3,5-disubstituted isoxazoles (Equations (1)–(4)).[38] Thus, the cycloaddition of alkynylboronate **106** with mesitylenecarbonitrile oxide **107** affords corresponding isoxazole boronic ester **108** in a good yield (Equation (1)). A single regioisomer is formed due to the steric repulsion between the butyl and mesityl groups, indicative of the moderate steric requirement of the pinacolboronate group. In the case of terminal alkynylboronate **109**, the steric repulsion is less important, and a mixture of regioisomers of **110** and **111** is obtained in a good yield (Equation (2)).

Alternatively, nitrile oxides can be formed in situ from hydroximic acid chlorides **112** and **113** in the presence of triethylamine in an ethereal solution or using K_3PO_4 in MeCN.[38,39] However, the mesityl group in **113** is bulkier than the phenyl group in **112**. Hence, the higher

regioselectivity in Equation (3) for products **114** and **115** as compared to that in Equation (4) for products **110** and **111** is surprising. Moreover, Grob and co-workers reported the [3+2] cycloaddition of ethynylboronic acid MIDA ester **116** with nitrile oxide derived from chlorooxime **112** to afford a single regiosiomer (Equation (5)).[40]

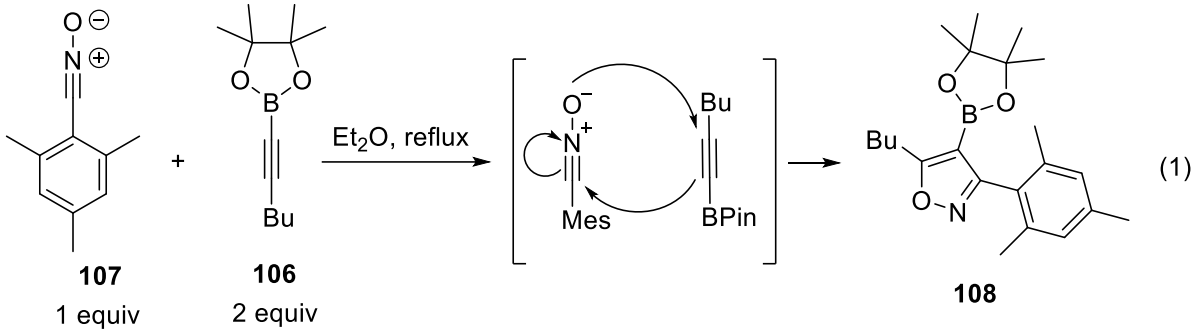

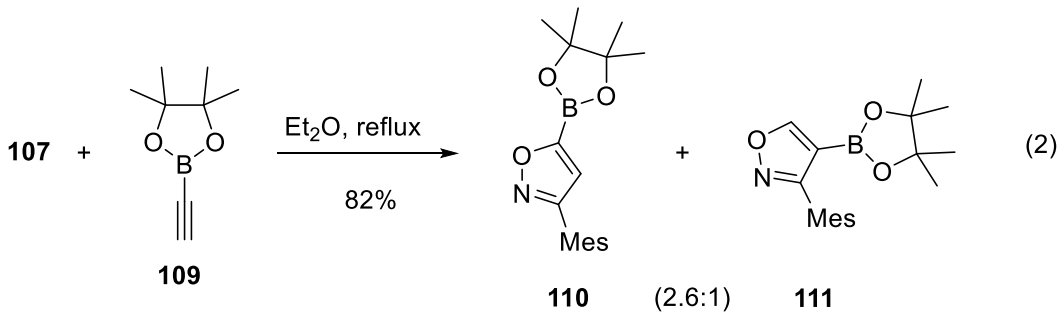

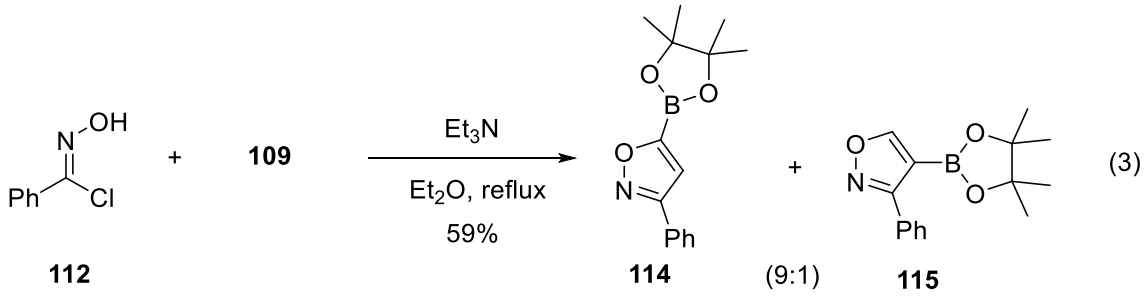

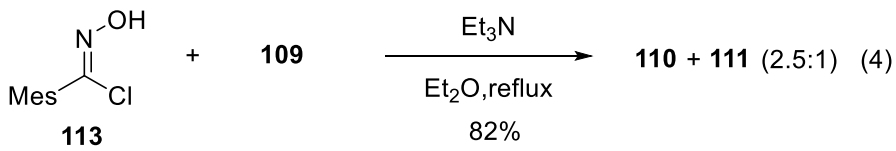

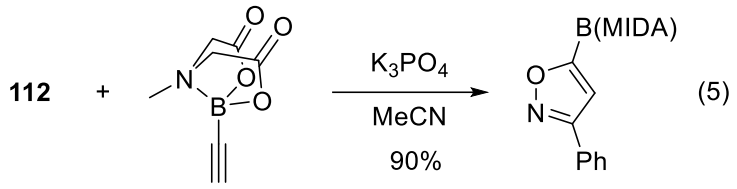

116
(MIDA boronate)

Clearly, steric hindrance alone cannot explain these results. In 2016, Lin and co-workers reported DFT studies on the regioselectivity of the 1,3-dipolar cycloaddition of nitrile oxides with terminal alkynylboronates.[41] The authors reported that the regioselectivity of the 1,3-dipolar cycloaddition of nitrile oxides with alkynylboronates is indeed not controlled only by steric hindrance. Instead, they proposed that the distortion energies mainly affect the ratio of 3,5- to 3,4-substituted isoxazole product. In other words, the electronic energies of activation are found to be mainly controlled by distortion energies required to achieve the transition states. Both electronic and steric effects affect regioselectivities.

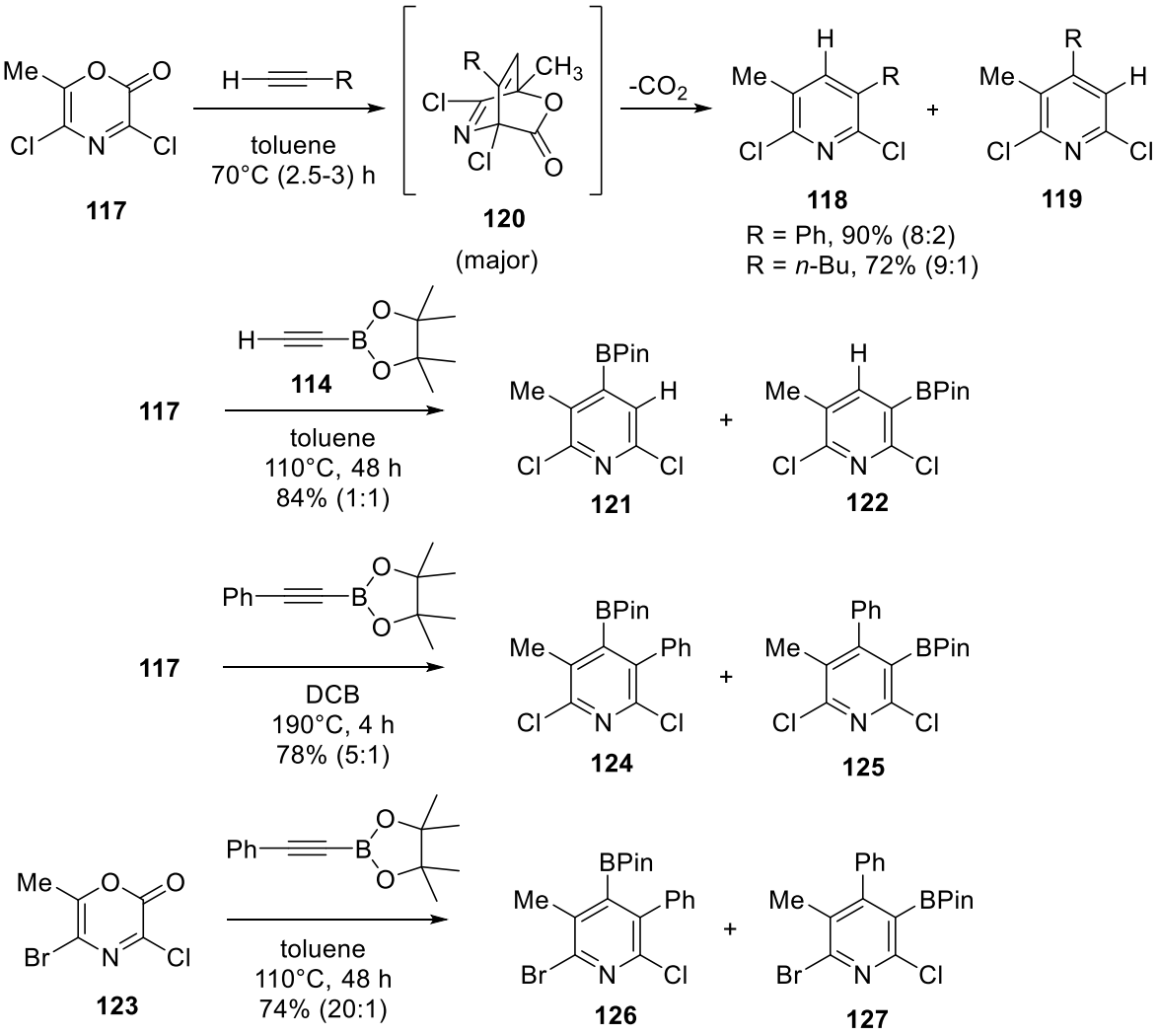

Scheme 35. Comparison of the [4+2] cycloaddition of alkynylboronates or other alkynes with 3,5-dihalo-2*H*-1,4-oxazin-2-ones.

2.1.4. Cycloaddition of alkynylboronates with 1,4-oxazin-2-ones

Notably, the regioselecitivity of the Diels–Alder reactions between 6-methyl-3,5-dichloro-2*H*-1,4-oxazin-2-one **117** and various alkynes was compared (Scheme 35).

The reaction of **117** with phenylacetylene or 1-hexyne exhibits considerably higher regioselectivity of **118** over **119** and in a considerably shorter reaction time[42] than the reaction of **117** with terminal alkynylboronate **114**, which affords an equimolar mixture of **121** and

122.[27] Overall, the regioselectivity of the reactions with alkynylboronates is apparently difficult to predict. Thus, the same alkynylboronate bearing a phenyl group on the triple bond can afford a 5:1 or 20:1 ratio of the regioisomer from **117** and 3-bromo,5-chloro-2*H*-1,4-oxazin-2-one (**123**).[27]

2.1.5. Cycloaddition of alkynylboronates with azides

Huang and co-workers reported the [3+2] direct cycloaddition of alkynylboronates with azides to afford triazole boronic esters.[28] When alkynylboronate **128** is used with benzyl azide **129**, the regioselectivity is poor, and products **130** and **131** are isolated as crude mixtures (Equation (6)).

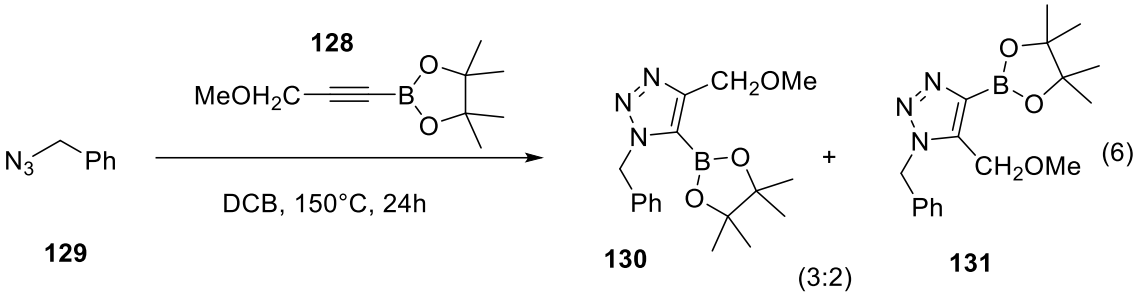

Furthermore, the cycloaddition of 1-ethoxynon-2-yne **132** with azide **129** also affords the corresponding triazole as a mixture of regiosiomers with poor selectivity (Equation (7)),[43] indicating that the regioselectivity of the reaction depicted in (equation (6)) is not governed by the pinacol boronate group on the alkyne.

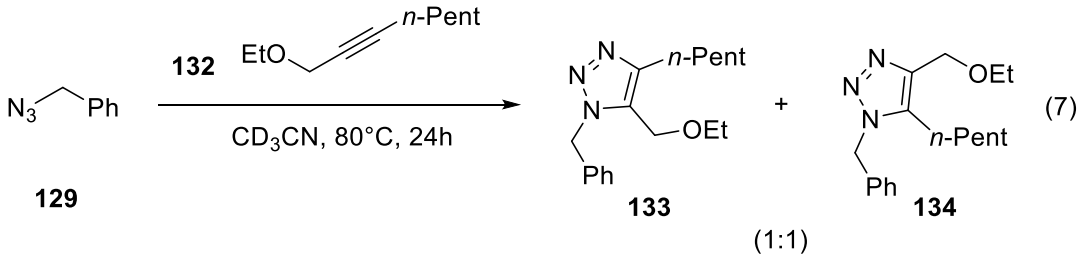

2.1.6. Cycloaddition of alkynyltrifluoroborates with 2-pyridylpyrones

One method to control the regioselectivity of the thermal cycloaddition of alkynylboron compounds is to utilize chelation by a directing group. In 2012, Kirkham and co-workers reported the efficiency of this strategy in the [4+2] cycloaddition of 2-pyrones **135** with alkynylpotassium trifluoroborates **136**.[29]

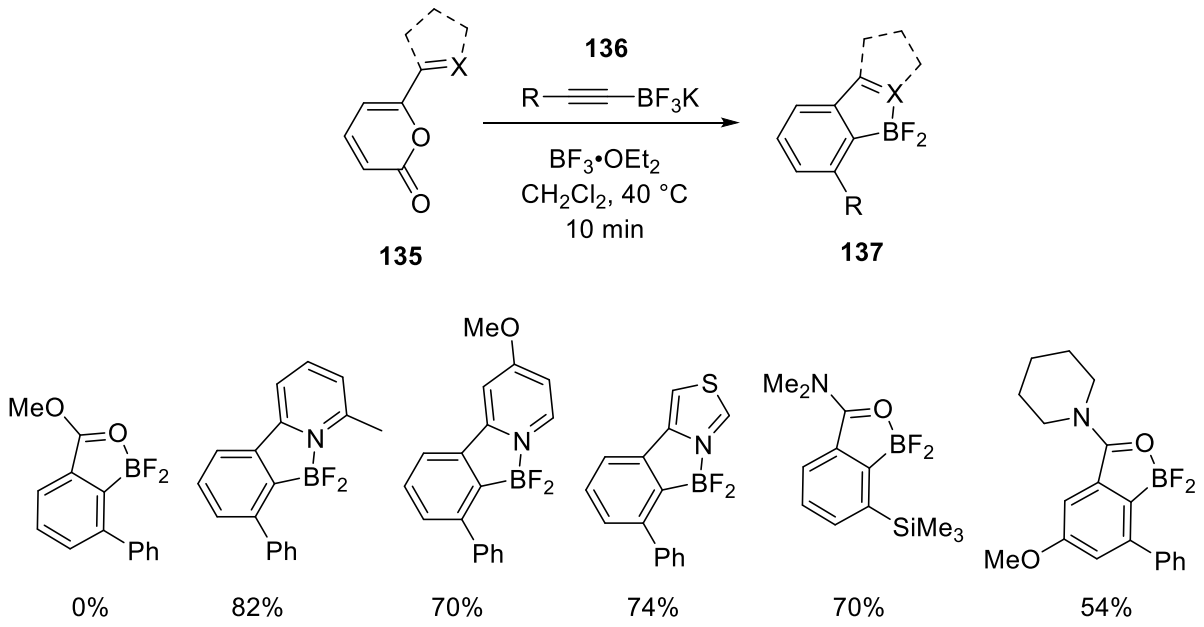

Scheme 36. Directed [4+2] cycloaddition of 2-pyrones with alkynylpotassium trifluoroborates.

The introduction of a Lewis acid was reported to dramatically accelerate the reaction and allow considerably milder conditions to be used. Besides pyridines, other directing groups are possible, and triazoles and amides are efficient, whereas an ester group is not efficient. The coordination of the directing group to boron is responsible for the regioselectivity.

2.2. Metal-catalysed cycloaddition of alkynylboron derivatives

The intermolecular metal-catalysed cycloaddition of alkynylboron reagents offers an access to motifs others than those afforded by the cycloaddition reactions that are only promoted by thermal energy, which is discussed in the previous section. However, the metal-catalysed intermolecular cycloaddition of alkynylboron reagents is extremely rare, and the reactions often lack regioselectivity.

2.2.1. [2+2+2] Cycloaddition

The cyclotrimerisation of **109** in the presence of 5 mol% of a cobalt catalyst leads to the formation of a 1.5:1 mixture of **138** and **139** (Scheme 37).[44] Moreover, all attempts for the cyclotrimerisation of potassium trifluoroborate **140** or tetrabutylammonium trifluoroborate **141** fail.

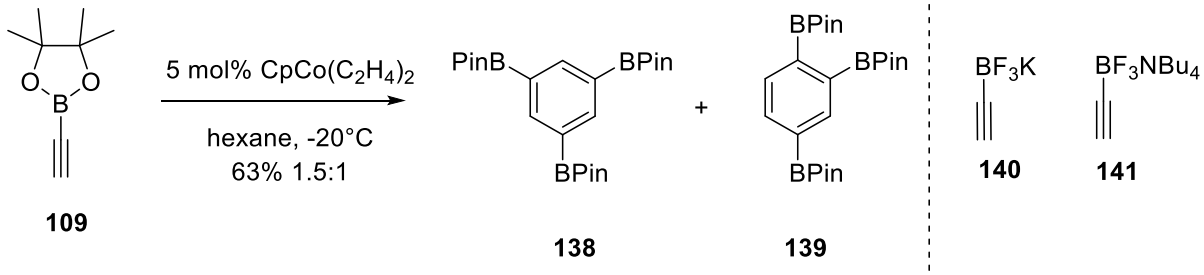

Scheme 37. Cyclotrimerisation of terminal alkynylboronate **114**.

According to the proposed mechanism of this cyclotrimerisation, two alkynes displace two ethylene ligands on the metal, and oxidative cyclisation would afford complex **142**. The complexation of a third terminal alkynyl boronate to afford either **143** or **144**, followed by alkyne insertion to afford **145** or **146**, before the reductive elimination of these seven-membered metallacycles would finally afford **138** or **139,** respectively (Scheme 38). The steric

differentiation between **143** and **144** is apparently not extremely significant since an almost equimolar mixture of products is obtained. This is in good agreement with the thermal cycloaddition of alkynylpinacolboronates reviewed at the beginning of this chapter, where pinacolboronate often serves as the less sterically hindered substituents of internal alkynes.

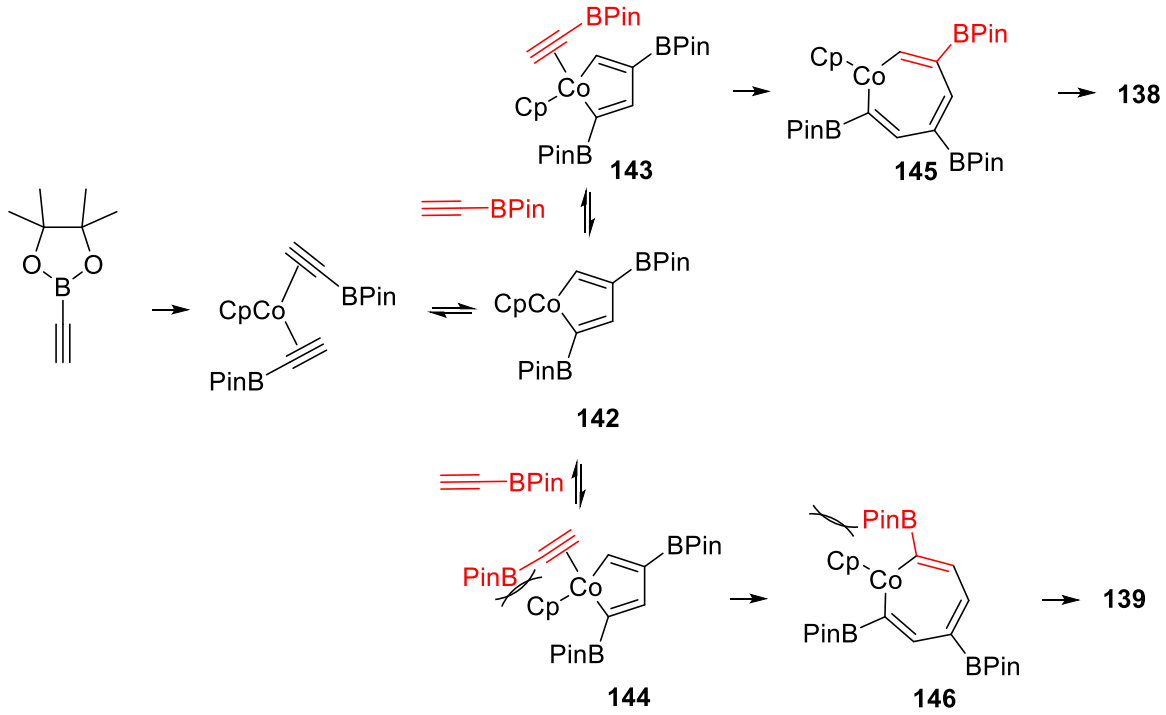

Scheme 38. Proposed mechanism for the cyclotrimerisation of terminal alkynylboronate **109**.

Similar mechanisms can explain the ruthenium- and iridium-catalysed reactions shown in Scheme 39. In 2005, Yamamoto and co-workers reported the [2+2+2] ruthenium-catalysed cycloaddition of alkynylboronate **114** with unsymmetrical diyne **149**, affording a mixture of regioisomers **150** and **151** in 73% yield and in a 71:29 ratio (Scheme 39).[45] The steric effect of the methyl group could explain this slight preference for **150**. The regioselectivity of the iridium-catalysed [2+2+2] cycloaddition is not investigated, and only symmetrical diynes are used, as exemplified by the reaction of **109** with **148**.[46]

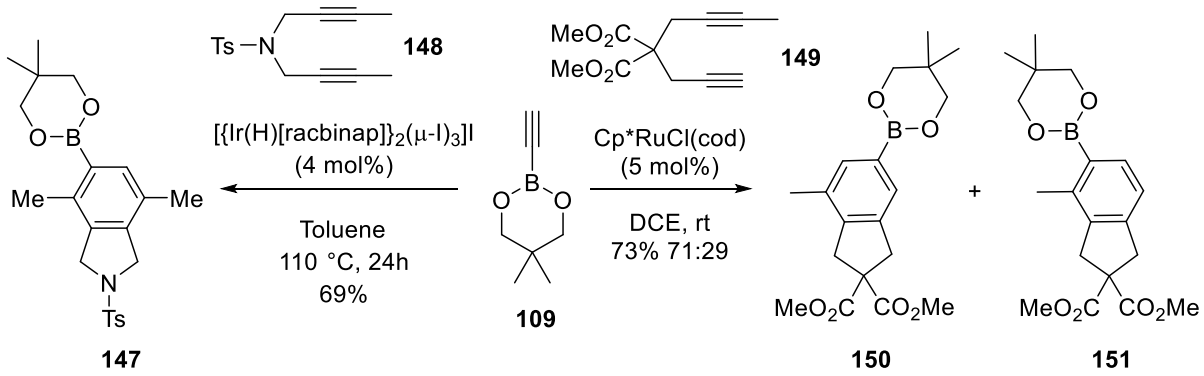

Scheme 39. [2+2+2] Cycloaddition of alkynylboronate with diynes catalysed by ruthenium and iridium complexes.

The same ruthenium catalyst as described for the preparation of **150** can be used in another design where the boronate ester is generated in situ to form a diyne (Scheme 40).[32,33] This design enables the better control of the regioselectivity of this intermolecular [2+2+2] between three unsymmetrical alkynes **153**, **154** and **155**. However, due to their facile hydrolysis, crude arylboronate **156** is used in the Suzuki cross-coupling reaction to afford **152**.

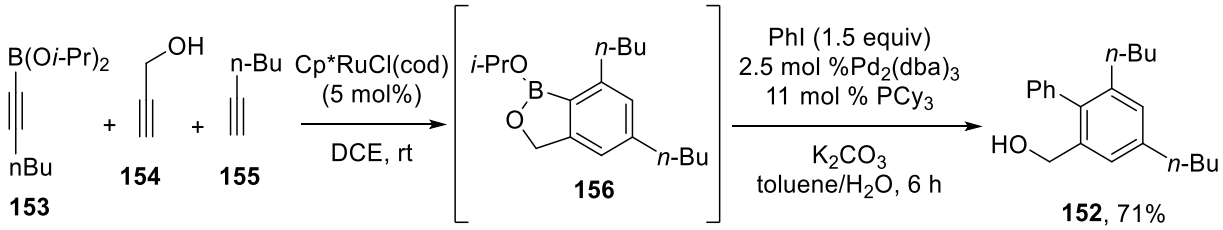

Scheme 40. Regioselective Ru(II)-catalysed [2+2+2] intermolecular cyclotrimerisation between three unsymmetrical alkynes.

Scheme 41 shows the proposed mechanism to explain the regioselectivity. Initially, alkynylboronate **153** and propargyl alcohol **154** are in equilibrium with diyne **157**. The replacement of cyclooctadiene (cod) on the metal would afford **158** and **169** by oxidative cyclisation. Owing to the steric repulsion between the ligand on ruthenium (Cp* and Cl) and

the n-butyl substituent on the coordinated alkyne, the reaction preferentially forms complex **160** over **161** via [2+2] coupling. The cleavage of the Ru–C bond followed by reductive elimination leads to desired product **152**.

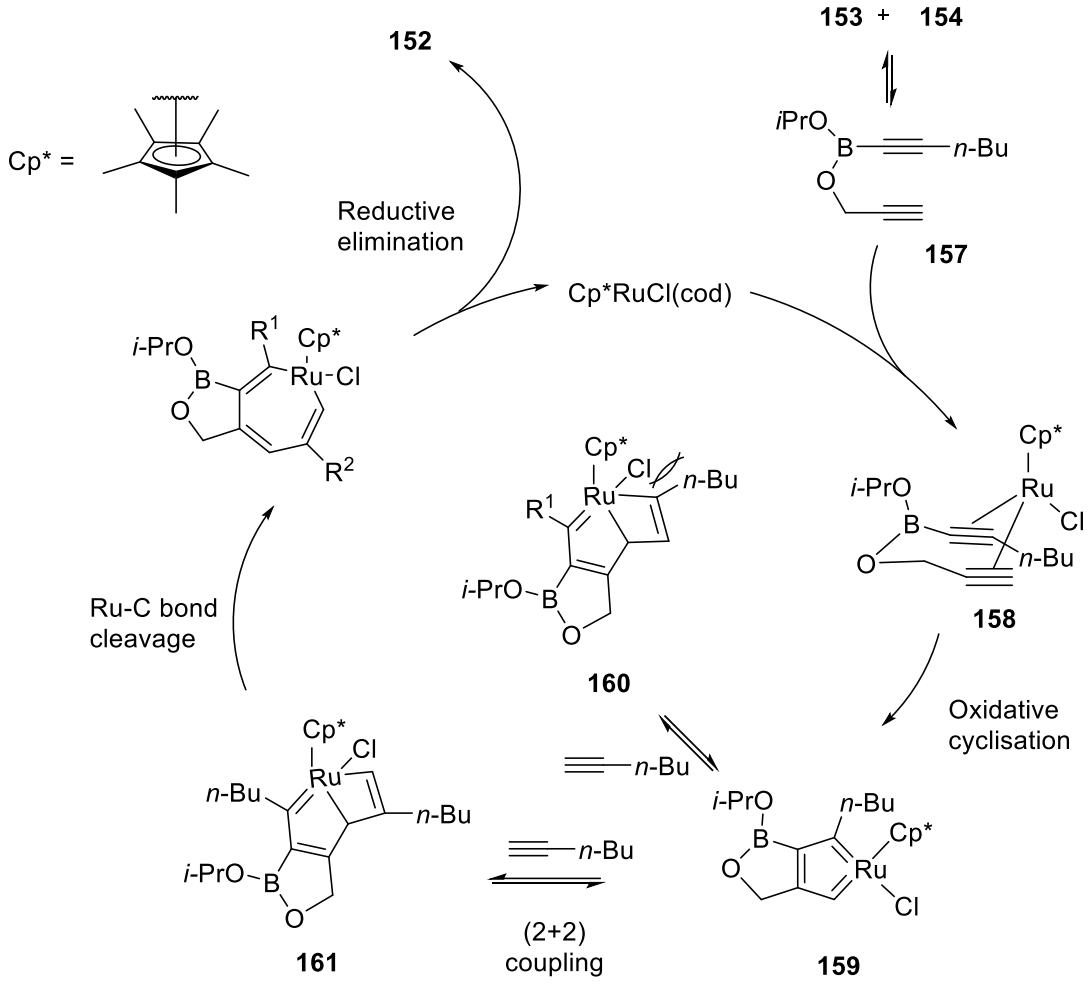

Scheme 41. Proposed mechanism to explain the regioselectivity of Ru(II)-catalysed [2+2+2] intermolecular cyclotrimerisation between three unsymmetrical alkynes.

2.2.2. Other cycloaddition reactions

Hilt and co-workers reported the cobalt(I)-catalysed Diels–Alder reactions of alkynylboronic esters **87** with isoprene **162**. The reaction is carried out under mild conditions to afford **163**

in a good yield, and with only traces of the other regioisomer (Scheme 42).[31] Notably, the reaction of isoprene with phenylacetylene under the same conditions affords the same regioselectivity of product **164**, indicating that the regioselectivity of the reaction is not governed by the boronate group on the alkyne.[47]

However, the use of a trimethylsilyl group on the alkyne to replace the boronate group leads to the reversal of the regioselectivity and affords a mixture of isomers in a good yield, favouring the formation of the *para*-substituted product.[47]

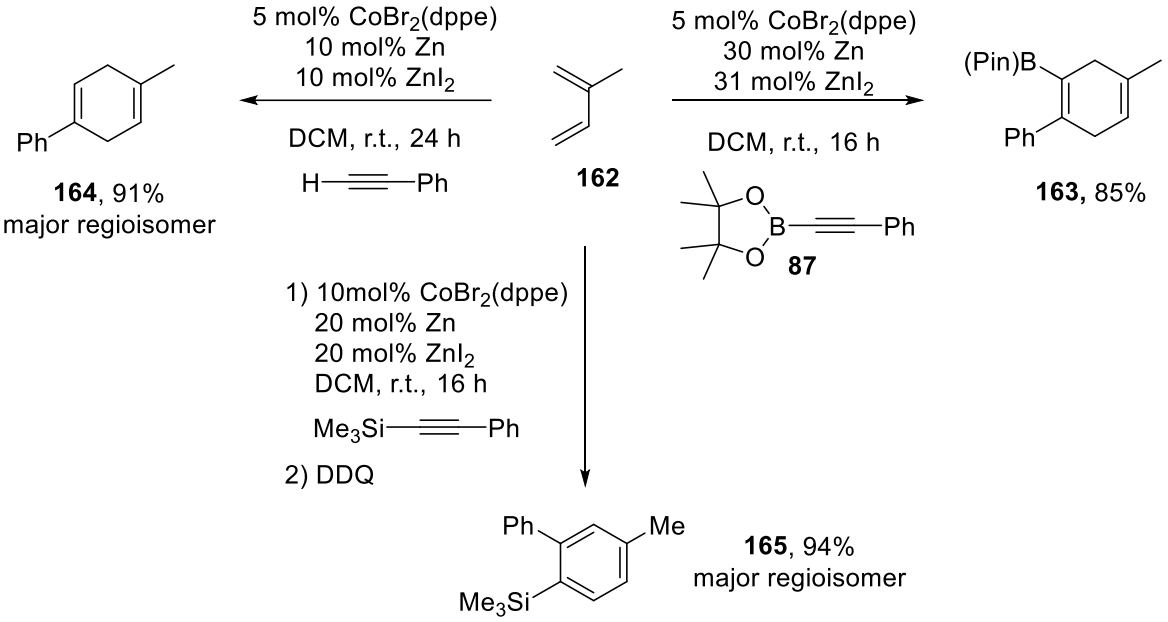

Scheme 42. Co-catalysed [4+2] cycloaddition of alkynylboronate with isoprene.

Moreover, Jung and co-workers reported the cycloaddition of potassium trifluoroborate **140** with azide **129** in a good yield (Scheme 43).[48] A single regioisomer is obtained. The same product could be obtained by the *in situ* formation of an alkyl azide from an alkyl halide and sodium azide.[49] Again, the regioselectivity, although outstanding, is not specific to the boron substituent on the alkyne. Instead, it is typical of the Cu-catalysed [3+2] cycloaddition of

azides with terminal alkynes, always affording 1,4-disubstituted triazoles.[50] A similar [3+2] cycloaddition was described by Grob and co-workers with other boron derivatives.[40]

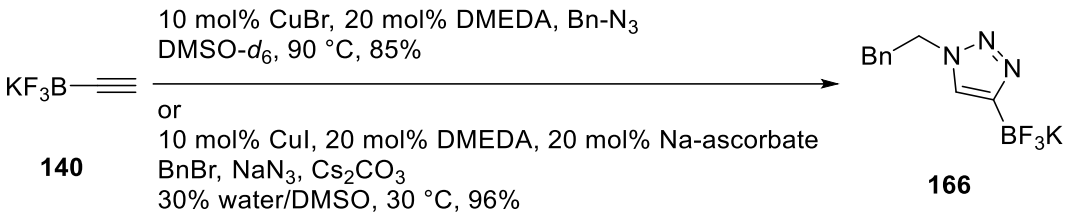

Scheme 43. Cycloaddition of acetylene potassium trifluoroborate with alkyl azides.

2.2.3. Nickel-catalysed [4+2] cycloaddition with cyclobutenones

Auvinet and co-workers reported the [4+2] nickel-catalysed cycloaddition of alkynylboronates **167** with cyclobutenones **168** to afford mixtures of phenols **169** and **170** (Scheme 44).[51] Notably, the regioselectivity considerably varies depending on the nature of alkyne substituent R^3, and it is often modest. Thus, when the R^3 group is a trimethylsilyl group, the regioselectivity is excellent, as demonstrated with compounds **171**, **174** and **175**. However, when it is a phenyl group, almost equimolar mixtures are obtained, as demonstrated with **172**, **173** and **176**. Then, when R is an alkyl group, the regioselectivity is restored, as demonstrated with **177** and **178**. The reaction mechanism is probably the same as that of the [4+2] cycloaddition of cyclobutenones with other alkynes, as discussed in Section 3 of Chapter 1.[11]

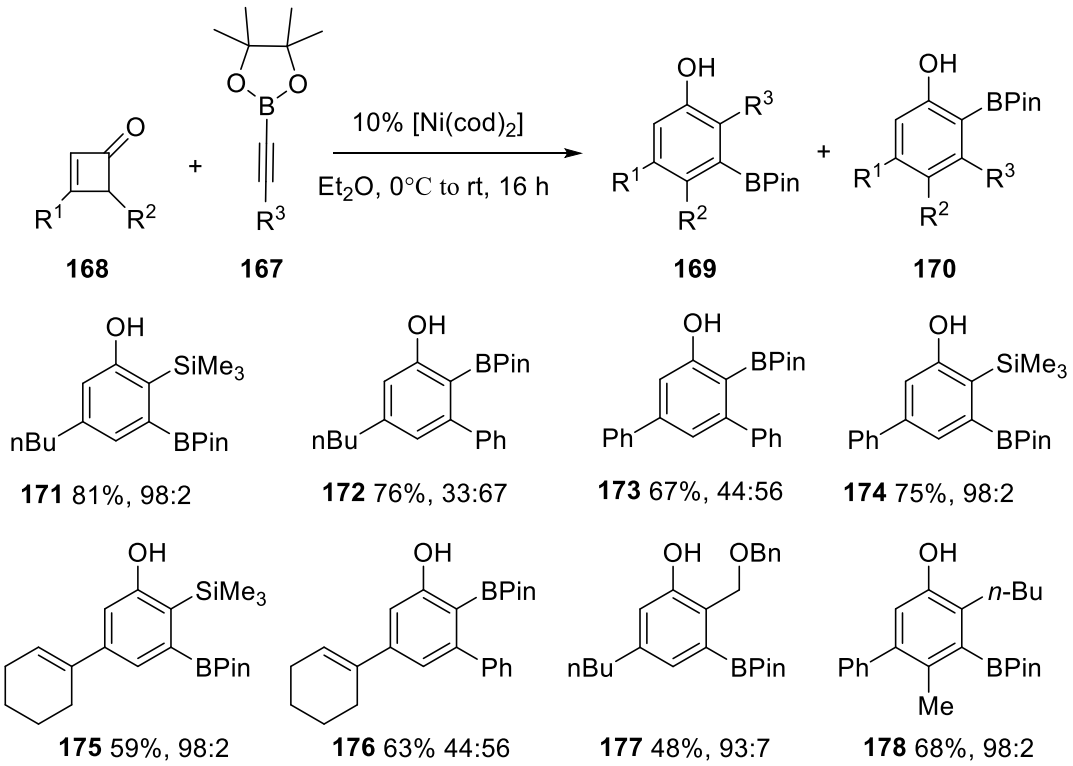

Scheme 44. Nickel-catalysed [4+2] cycloaddition of alkynylboronates **167** with cyclobutenones **168**.

2.3. Aim and hypothesis

As mentioned in the previous section, only rare examples of metal-catalysed reactions of alkynylboron were reported. Moreover nickel-catalysed reactions of alkynylboron derivatives with azetidinone or oxetanone reportedly failed,[17] whereas the only other nickel-catalysed [4+2] reactions of alkynylboron compounds with four-membered-ring ketones, namely cyclobutenones, showed issues of regioselectivity.[48]

Furthermore, although the nickel-catalysed cycloaddition of **179** and **180** affords the major product in a good amount after the separation of the regioisomers by flash chromatography, the minor regioisomer cannot be prepared in a good yield (Scheme 45).[13]

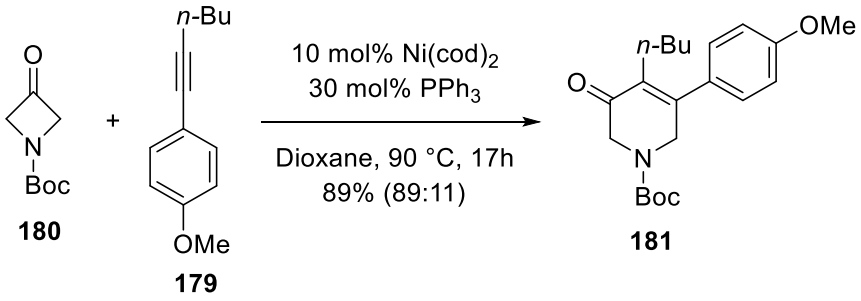

Scheme 45. Cycloaddition of *N*-Boc-3-azetidinone with an unsymmetrical alkyne.

Compared to other organometallic compounds, organoboranes, particularly boronic acids and boronic esters, are considered to exhibit low toxicity. However, several of these compounds are not stable under atmospheric conditions due to the vacant orbital on boron, making these compounds sensitive to oxygen and water, consequently leading to their decomposition. Notably, potassium alkynyltrifluoroborates exhibit stability and no sensitivity to air and water, and a majority of the products can be stored for a long time at room temperature without decomposition.

Hence, developing the nickel-catalysed [4+2] cycloaddition of 3-azetidinones with potassium alkynyltrifluoroborates would represent a powerful tool for the formation of functionalisable cycloadducts *via* the Suzuki–Miyaura cross coupling,[52-54] as well as enable access to regioisomers that could not be prepared in the initial study.

2.4. Results and discussion

2.4.1 Preparation of precursors

Includes all precursors used in the preparation of final compounds

2.4.1.1 Preparation of alkynyltrifluoroborates

Potassium alkynyltrifluoroborates **182–189** used in the nickel-catalysed [4+2] cycloaddition were prepared by the deprotonation of the corresponding terminal alkynes with *n*-BuLi in dry THF, followed by the addition of trimethyl borate and treatment of the alkynylboronate thus obtained with KHF_2.[55] Alkynyltrifluoroborates were obtained in yields ranging from 35% to 86% (Table 2). The products were characterised by ^{1}H and ^{19}F NMR spectroscopy. The products were isolated by their dissolution in a minimum amount of hot acetone, followed by precipitation by the addition of Et_2O. All of the obtained potassium alkynyltrifluoroborates were stable under atmospheric conditions and stored under air in the freezer for 2 years without decomposition.

Table 2. Preparation of alkynyltrifluoroborates

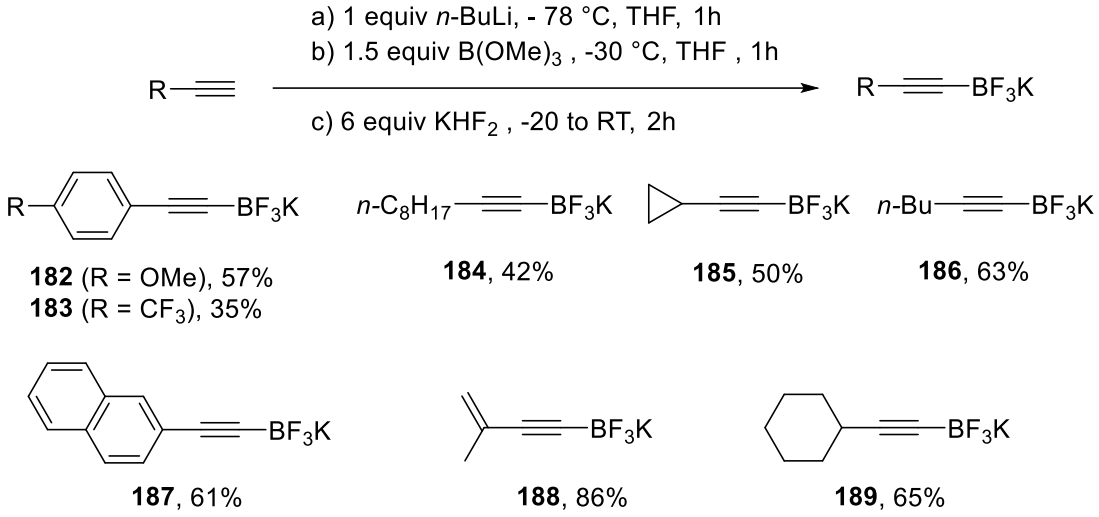

The above conditions are optimal for preparing alkynyltrifluoroborates. However, before the conditions were established, the Sonogashira reaction between **190** and **140** was attempted.[56] The reaction was carried out in DMSO as the solvent and in the presence of piperidine. Unfortunately, the desired product was not obtained (Scheme 46).

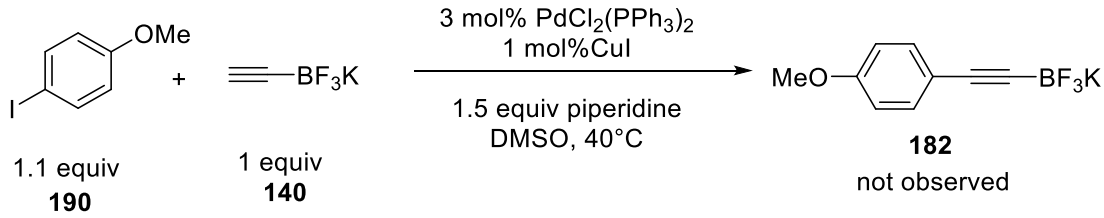

Scheme 46: Preparation of alkynyltrifluoroborates by the Sonogashira reaction.

2.4.1.2. Preparation of *N*-protected 3-azetidinones

2.4.1.2.1. Preparation of 1-Ts-3-azetidinone

Azetidinone was prepared in a two-step procedure starting from 3-hydroxy azetidine hydrochloride **191** (Scheme 47). Alcohol **192** was obtained by mono-protection with 1

equivalent of tosyl chloride in methanol and 3 equivalents of triethylamine. Next, Swern oxidation[57] afforded azetidinone **193** in 75% yield.[19]

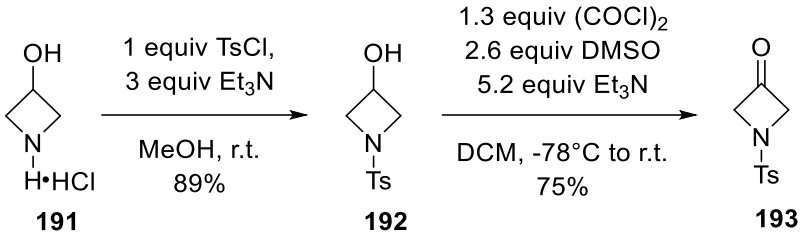

Scheme 47. Preparation of 1 -Ts-3-azetidinone.

2.4.1.2.2. Preparation of 1-Boc-3-azetidinone

1-Boc-3-azetidinone **180** was prepared from **191**, mono-protection with 1 equivalent of di-*tert*-butyl dicarbonate in methanol, and 3 equivalents of triethylamine to afford 1-Boc-3-hydroxyazetidine **194**.[58] 1-Boc-3-azetidinone was obtained by standard Swern oxidation[57] in 63% yield (Scheme 48).

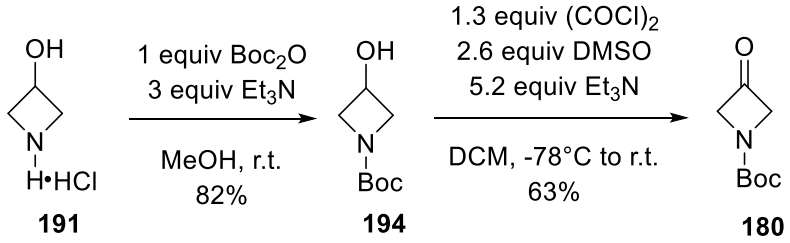

Scheme 48. Preparation of 1-Boc-3-azetidinone.

2.4.2. Optimisation of the Ni-catalysed cycloaddition of alkynyltrifluoroborates with 3-azetidinones

Based on the procedure reported by Kelvin Ho and co-workers,[13] the [4+2] cycloaddition of potassium alkynyltrifluoroborate **136** with 1-Boc-3-azetidinone (**180**) was performed under

nitrogen in the presence of 10 mol% $Ni(cod)_2$ and 30 mol% PPh_3. Potassium alkynyltrifluoroborate was not soluble in toluene, but it was slightly soluble in 75% toluene with 25% DMF. Hence, a homogeneous reaction is performed at 60°C using an optimum ratio of 65% toluene and 35% DMF, affording corresponding products **195–200** in yields ranging from 33% to 59% *as a single regioisomer* with full conversion (Table 3).

Table 3. Cycloaddition of potassium alkynyltrifluoroborates with 1-Boc-3-azetidinone in 65% toluene and 35% DMF

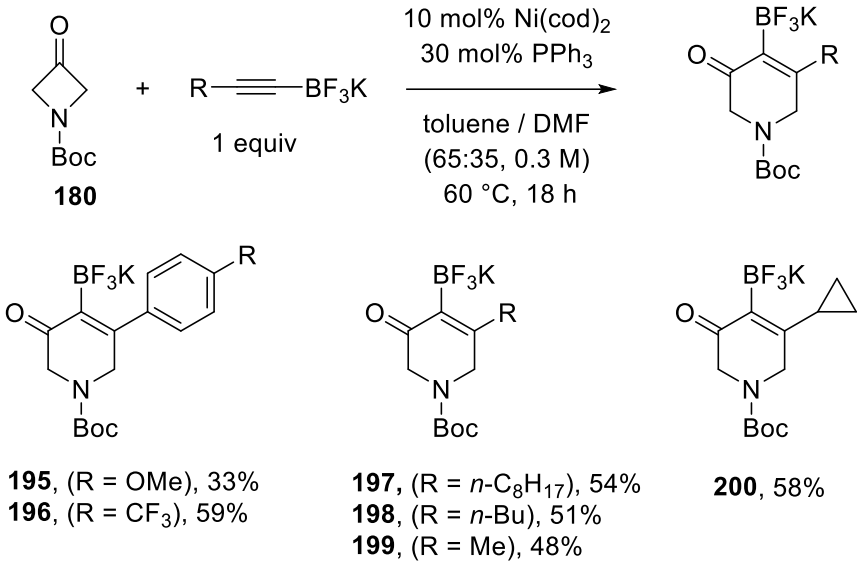

In an effort to improve the product yield, the effect of the solvent was examined. When the reaction was performed in toluene, product **199** was not observed. However, the use of dioxane led to an increase of the product yield to 59% (Scheme 49), albeit with a slight decrease in the conversion. Indeed, traces of potassium alkynyltrifluoroborate **201** were observed in the crude reaction mixture.

To address this issue, the optimal loading of **180** was investigated (Scheme 50). The use of 1.4 equivalents instead of 1 equivalent of **180** led to the full conversion with a slight increase in yield of **199**. Hence, traces of **201** are not observed in the crude reaction mixture, and the product is isolated in greater purity.

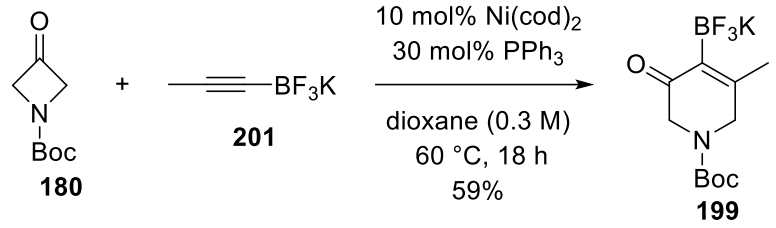

Scheme 49. Effect of the solvent dioxane on the nickel-catalysed [4+2] cycloaddition of **180** with **201**.

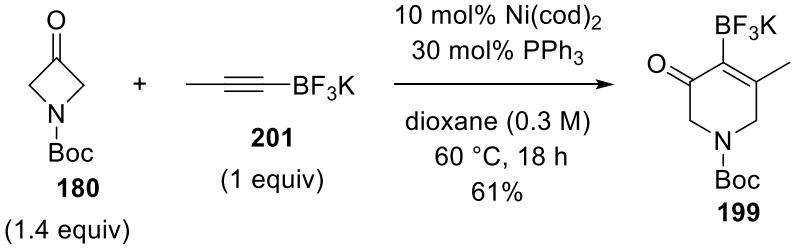

Scheme 50. Effect of the stoichiometry of the nickel-catalysed [4+2] cycloaddition of **180** with **201**.

Next, the ratio of nickel to PPh_3 was investigated (Table 4). When the reaction was performed with 30 mol% (entries 2, 4, 6 and 8 in Table 4), the desired products were obtained in good yield and with excellent conversion. However, the use of 20 mol% of PPh_3 (entries 1, 3, 5 and 7) led to the decrease of the product yield with incomplete conversion. Attempts to use $NiBr_2(PPh_3)_2$/Zn as an alternative to $Ni(cod)_2$ were not successful, and the starting material

was recovered. The optimum conditions were selected as 30 mol% PPh_3 and 10 mol% $Ni(cod)_2$ in dioxane at 60–90 °C. The azetidinone and alkynyltrifluoroborate were sequentially added after the formation of the active catalyst.

Table 4. Effect of the Ni/phosphine ratio on the product yield.

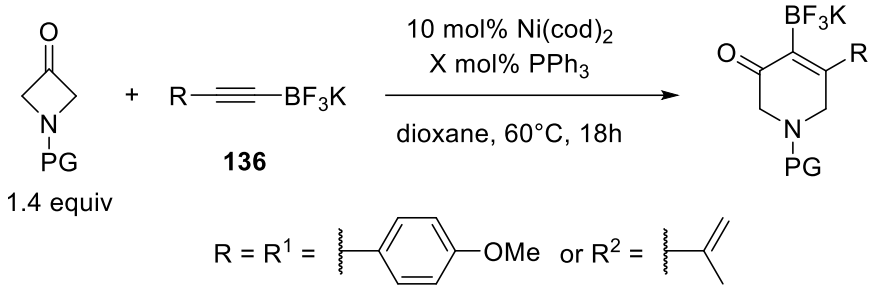

Entry	PG	PPh_3	R	Conversion	Yield
1	Boc	20 mol%	R^1	91%	67%
2	Boc	30 mol%	R^1	100%	80%
3	Boc	20 mol%	R^2	90%	70%
4	Boc	30 mol%	R^2	<98%	89%
5	Ts	20 mol%	R^1	94%	77%
6	Ts	30 mol%	R^1	100%	98%
7	Ts	20 mol%	R^2	91%	73%
8	Ts	30 mol%	R^2	<97%	92%

2.4.3. Scope of the Ni-catalysed cycloaddition of alkynyltrifluoroborates

2.4.3.1. 1-Boc-3-azetidinone

After the optimal reaction conditions were determined, the scope of the reaction with **180** was investigated (Table 5). After the smooth insertion of **136**, the desired products were obtained in good yields and as only one regioisomer. Owing to their high polarity, these products could not be separated by flash chromatography. Hence, another approach to isolate these products is selected. The use of acetone with diethyl ether to precipitate the product revealed good results. However, traces of dioxane were observed in the NMR spectra even after several attempts to remove dioxane in vacuo or by rotary evaporation at 70 °C. Hence, the optimised system for the isolation of the desired products is room temperature, with the addition of acetonitrile and the removal of all volatiles in vacuo. The resulting brown residue was dissolved in acetone, and diethyl ether was added to induce precipitation. The resulting solid was filtered through a sintered funnel, followed by trituration with diethyl ether at room temperature to afford the desired products as a white solid. Notably, neither the size nor the electronic properties of the alkyne substituent in potassium alkynyltrifluoroborates did not affect the reactivity and regioselectivity of the reaction, which is in contrast to that observed for the nickel-catalysed [4+2] cycloaddition of alkynylboronates with cyclobutenones.[51]

Table 5. Insertion of alkynyltrifluoroborates into 1-Boc-3-azetidinone

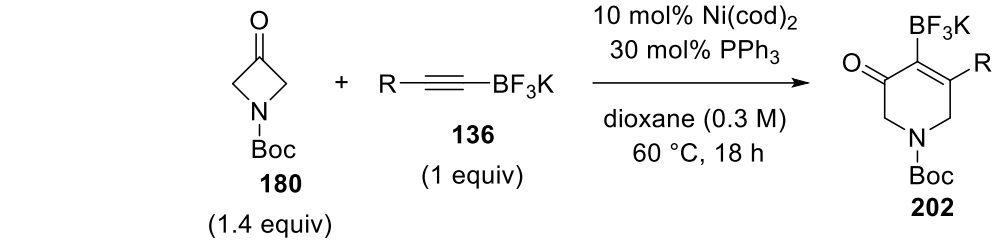

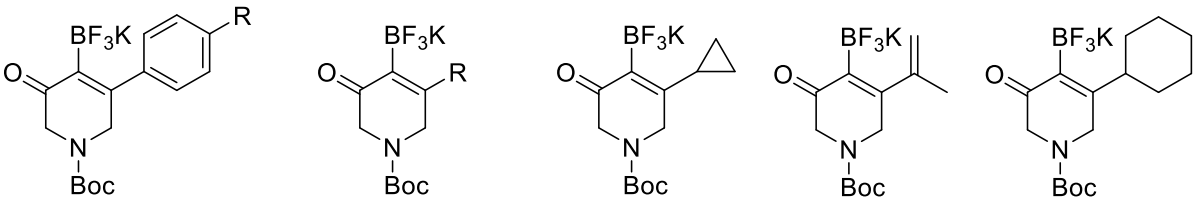

195, (R = OMe), 80%
196, (R = CF_3), 56%

197, (R = *n*-C_8H_{17}), 68%
198, (R = *n*-Bu), 70%
199, (R = Me), 61%

200, 56%

203, 89%

204, 62%

The products were characterised by ^{1}H, ^{19}F, ^{11}B and ^{13}C NMR spectroscopy, IR spectroscopy and mass spectrometry. The regioisomers were determined by NOESY, HMBC and HSQC. Thus, the NOESY spectrum of **203** revealed the correlation of the methylene proton H-2a and vinyl proton H-5a (Figure 1). The structure of **203** was unambiguously confirmed by X-ray crystallography. In the crystal, the sp^2-hybridised oxygen atom of the carbamoyl protective group established the shortest contact (2.635 Å) with the potassium ion (Figure 2a), whereas each potassium ion was in contact with six fluorine atoms of three other molecules of **203** at distances ranging from 2.756 Å to 3.001 Å (Fig. 2b).

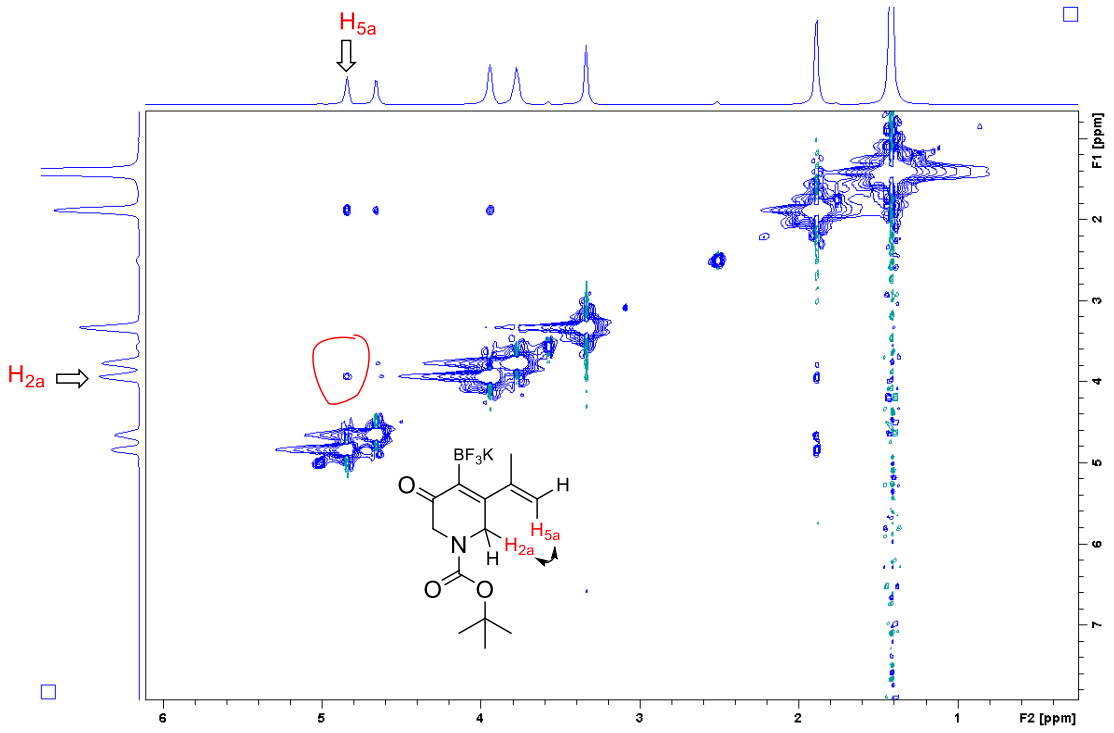

Figure 1. NOESY spectrum for the compound **203**

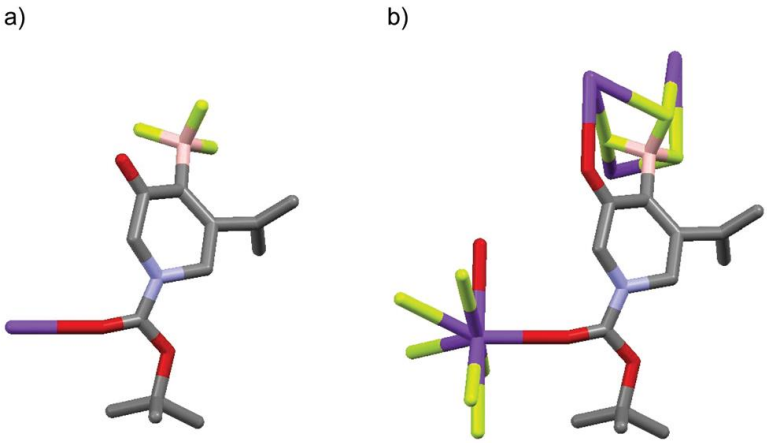

Figure 2. Single crystal structure of **203** (hydrogen atoms are omitted for clarity); (a) asymmetric unit showing the shortest contact with the potassium ion, (b) structure showing all O–K and F–K contacts.

Moreover, the *J* (^{11}B–^{19}F) values in the ^{11}B NMR spectra and *J* (^{19}F–^{11}B) in the ^{19}F NMR spectra are shown in Figure 3 and Figure 4, respectively. These coupling constants giving each peak of a quartet confirmed the presence of the BF_3 group. Actually, the solvent exhibited a strong effect on the ^{11}B and ^{19}F chemical shifts, and coupling constants were observed (Figure 5). Using MeCN-d_3 instead of DMSO-d_6 led to increase in the chemical shift, and the coupling constants in ^{11}B and ^{19}F spectra became visible. In addition, in MeCN-d_3, the acquisition parameters had to be changed to 40°C and 4-s delay with 1024 scans to show the spectra more clearly.

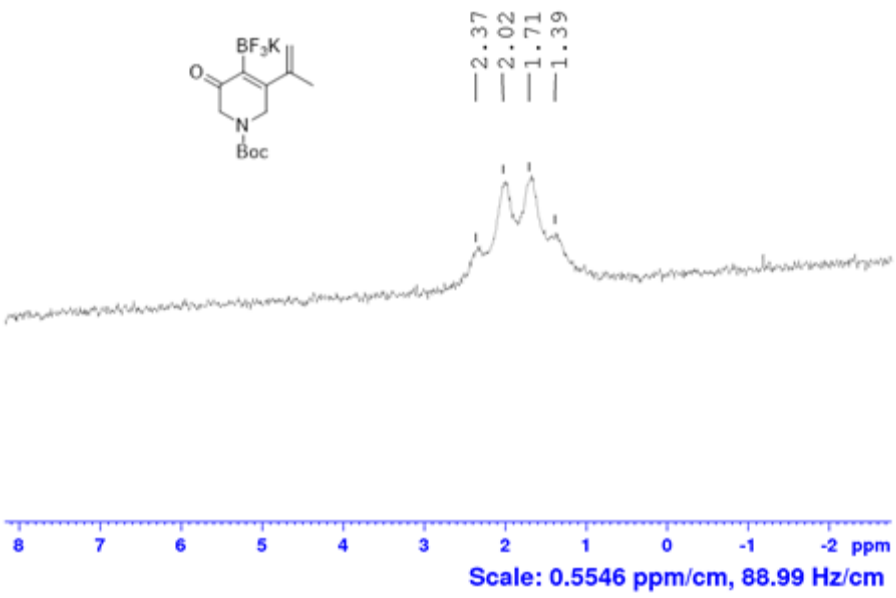

Figure 3. *J* (^{11}B–^{19}F) in the ^{11}B NMR spectra of **203**.

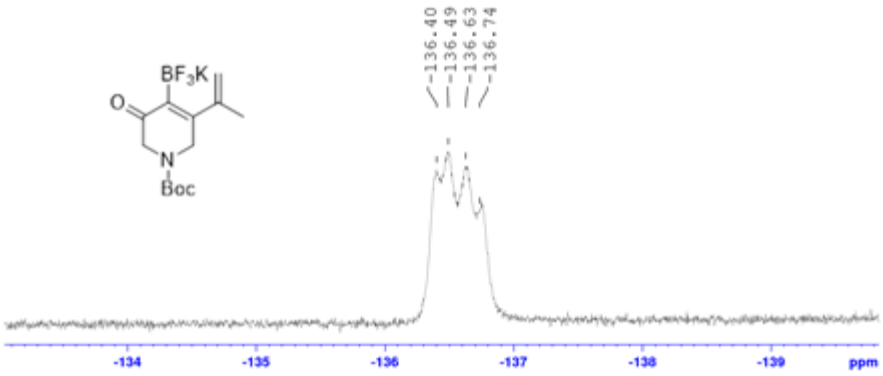

Figure 4. *J* (^{19}F–^{11}B) in the ^{19}F NMR spectra of **203**.

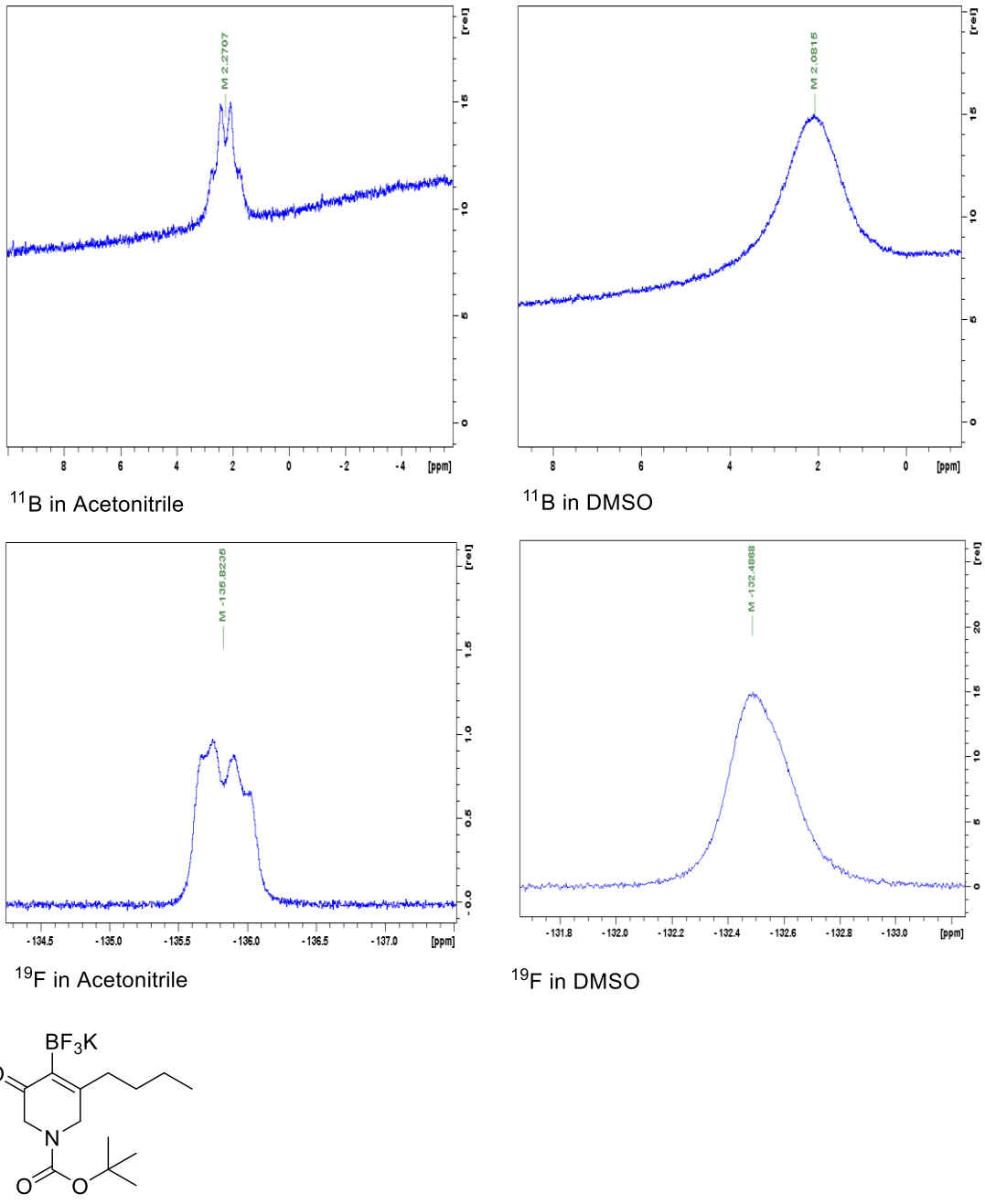

Figure 5. Effect of solvent on the ^{11}B and ^{19}F chemical shifts and coupling constants for **198**.

Although all of the products were purified in the same manner as described above, the results obtained from elemental analysis suggested that the purity varies between 95% and 98% for most compounds, as demonstrated with **196**, **198**, **200** and **203** (Table 6). The starting

alkynyltrifluoroborates used in the synthesis of these compounds exhibit different purities, and their purity affects that of the [4+2] adducts. However, the purities of these compounds were less than 90% when the conversion was not complete, as for example in the case of **199**, which emphasizes the necessity to reach full conversion to obtain products of reasonable purity.

Table 6. Elemental analysis data

Product	Calculated values			Experimental values			Purity	Purity of starting alkyne
	C	H	N	C	H	N		
196	45.66%	3.83%	3.13%	44.40%	3.66%	2.97%	95.90%	95.14%
198	46.81%	6.18%	3.90%	46.32%	6.10%	3.82%	98.53%	99.30%
199	41.66%	5.09%	4.42%	37.76%	4.52%	3.76%	88.17%	n.d.
200	45.50%	5.29%	4.08%	43.12%	5.23%	3.79%	95.51%	95.14%
203	45.50%	5.29%	4.08%	44.75%	5.20%	3.99%	98.15%	92.65%

Hence, although the presence of the trifluoroborate group was confirmed, 1,3,5-trifluorobenzene was used as an internal standard to identify the number of fluorine atoms bonded to the boron atom. In all cases, ^{19}F NMR spectra verified that three fluorine atoms are bonded to the boron atom. Indeed, the ratio of the number of hydrogen atoms in 1,3,5-trifluorobenzene to that in the product in ^{1}H NMR was equal to the ratio of the number of fluorine atoms in 1,3,5-trifluorobenzene to that in the product in ^{19}H NMR.

Owing to the quadrupolar relaxation mechanism of the ^{11}B nucleus, the resonances corresponding to the carbon bearing the boron atom were not observed in the ^{13}C NMR spectra (Figure 6).[59] Furthermore, the carbon atoms linked to the nitrogen atom were observed as two signals each, corresponding to the two rotamers of the product due to slow rotation at the carbamate resulting from the influence of the Boc group (Figure 6).[60,61]

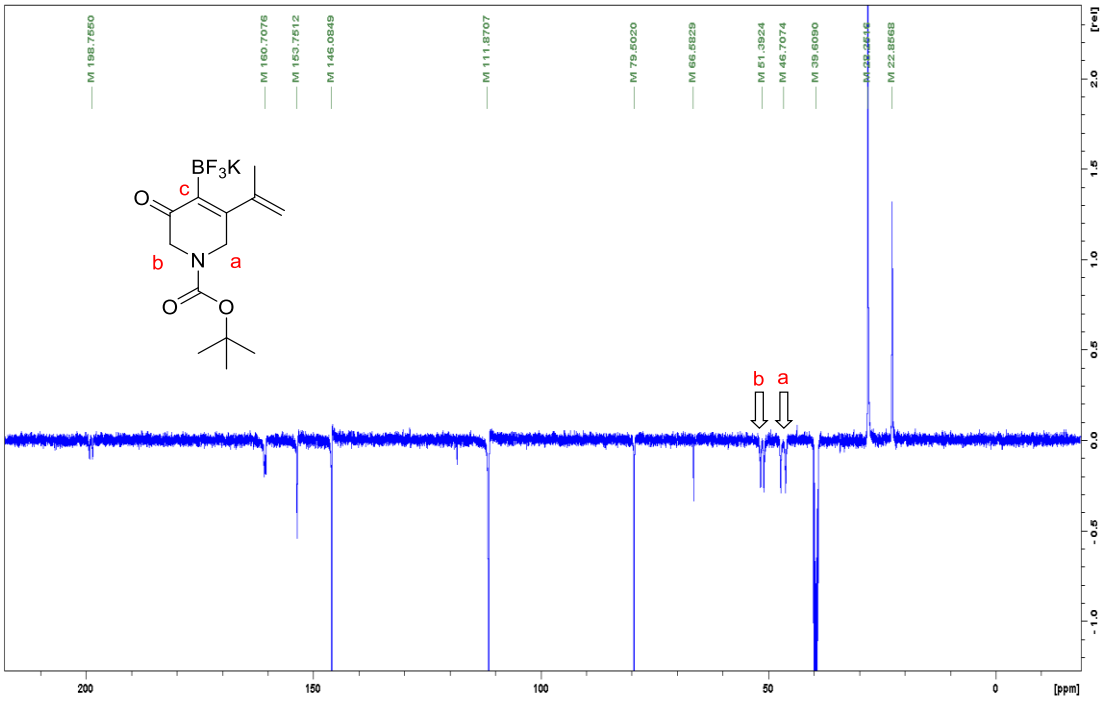

Figure 6. Effect of the Boc group on the carbon atoms linked to the nitrogen atom for **203**.

2.4.3.2. 1-Ts-3-azetidinone

The reaction conditions were identical to the use of 1-tosylazetidin-3-one **193** instead of 1-Boc-3-azetidinone **180**. However, 1-tosylazetidin-3-one **193** was dissolved in dioxane under nitrogen before it was added into the solution of $Ni(cod)_2$ and PPh_3 in dioxane, leading to the desired products with full conversion in a majority of cases. However, the insertion of alkyltrifluoroborate **189** into 1-tosylazetidin-3-one **193** required a higher temperature (90°C)

and proceeds with a lower conversion. Once again, all products were obtained as a single regioisomer (Scheme 51). Furthermore, the desired products were separated by precipitation using acetone with diethyl ether and using acetonitrile to remove the traces of dioxane in vacuo.

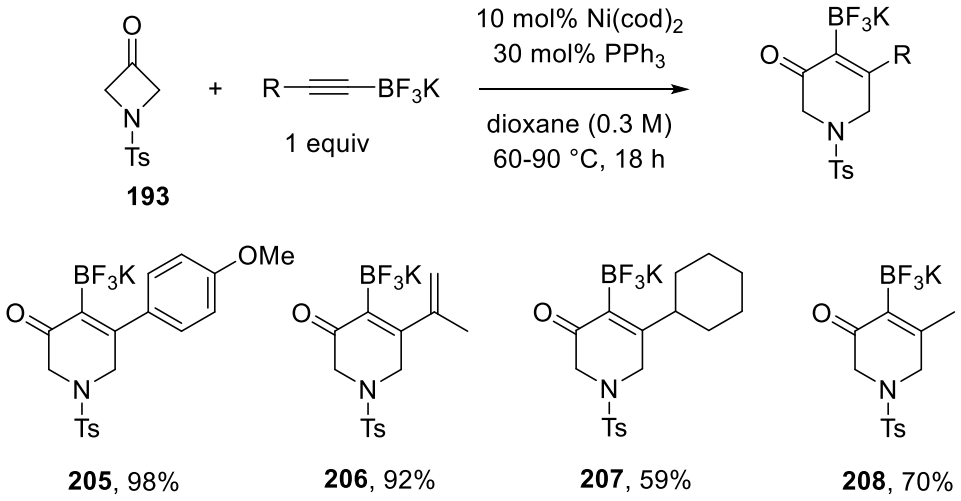

Scheme 51. Nickel-catalysed [4+2] cycloaddition of alkynyltrifluoroborates with 1-tosylazetidin-3-one.

In contrast to the *N*-Boc derivatives, the carbon atoms linked to the nitrogen atom were observed as a single peak (Figure 7). Again owing to the quadrupolar relaxation mechanism of the ^{11}B nucleus, the resonances corresponding to the carbon bearing the boron atom were not observed in the ^{13}C NMR spectra (Figure 7).[59] Once again, the use of MeCN-d_3 instead of DMSO-d_6 led to an increase of the chemical shifts and enabled the measurement of the coupling constants in ^{11}B and ^{19}F spectra.

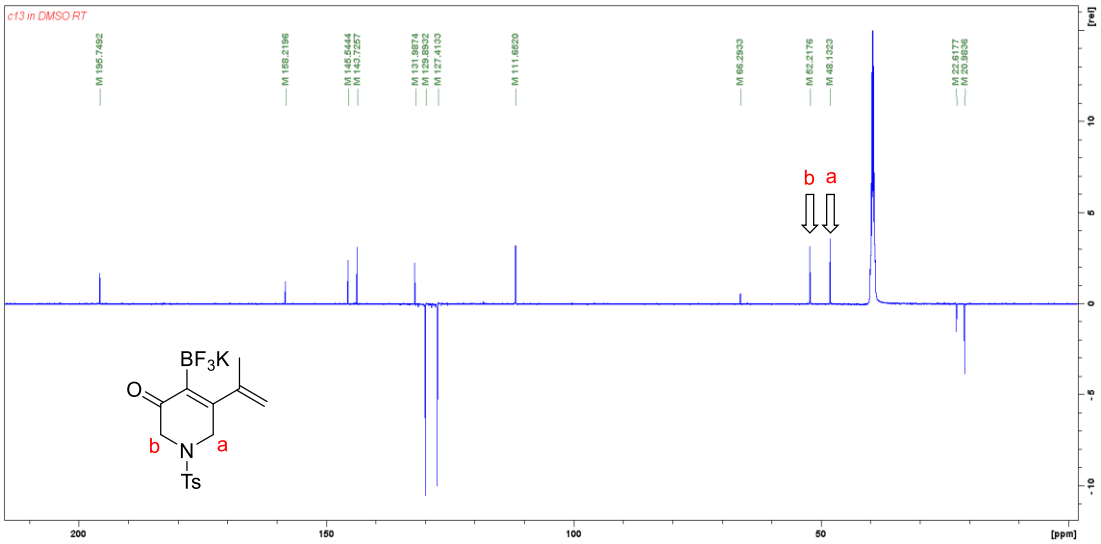

Figure 7. ^{13}C NMR spectrum of **206**.

Attempts to insert potassium propynyltrifluoroborate **201** into α-substituted 1-tosyl azetidin-3-one **209** were not successful under these conditions, and 95% of the starting material was recovered as determined by ^{1}H NMR (Scheme 36).

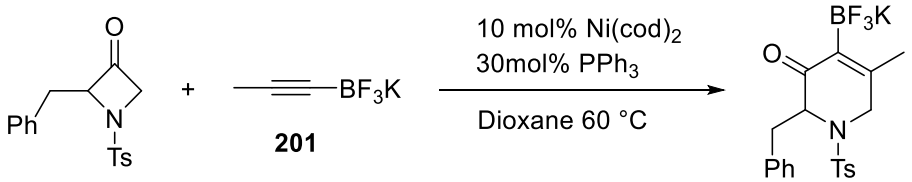

1.1 equiv
209

not observed
210

Scheme 52. Nickel-catalysed [4+2] cycloaddition of potassium propynyltrifluoroborate **201** with α-substituted 1-tosyl azetidin-3-one **209**.

2.4.3.3. 3-Oxetanone and 3-thietanone

The cycloaddition of potassium alkynyltrifluoroborate **136** with commercially available 3-oxetanone **59** was carried out under the same optimised conditions as those reported for the cycloaddition of 1-Boc-3-azetidinone **180** with 1-tosylazetidin-3-one **193** except that the

temperature was increased to 90 °C, leading to desired products with full conversion in a majority of cases. The corresponding products were obtained in a high yield with *only one isomer* (Scheme 53). However, the insertion of alkynyltrifluoroborate **182** afforded a lower yield compared with that of the same alkynyltrifluoroborate into 1-tosylazetidin-3-one **193** and 1-Boc-3-azetidinone **180**. The same optimised conditions as those reported for the reaction of 1-tosylazetidin-3-one **193** with 1-Boc-3-azetidinone **180** were utilised to isolate the products.

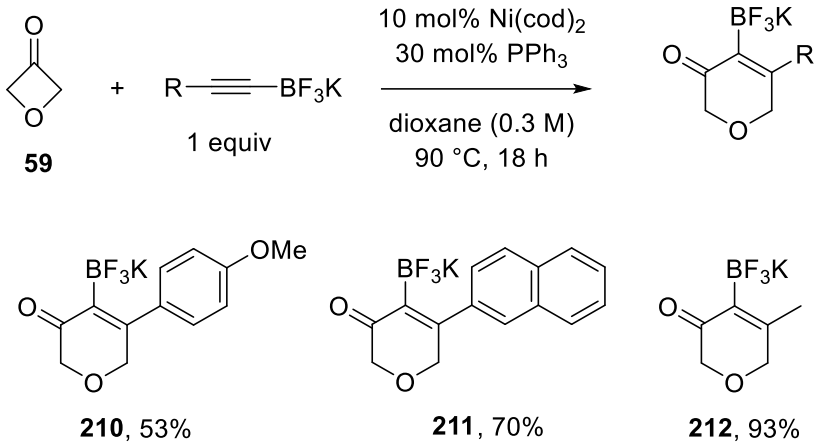

Scheme 53. Nickel-catalysed [4+2] cycloaddition of alkynyltrifluoroborates with 1-oxetan-3-one.

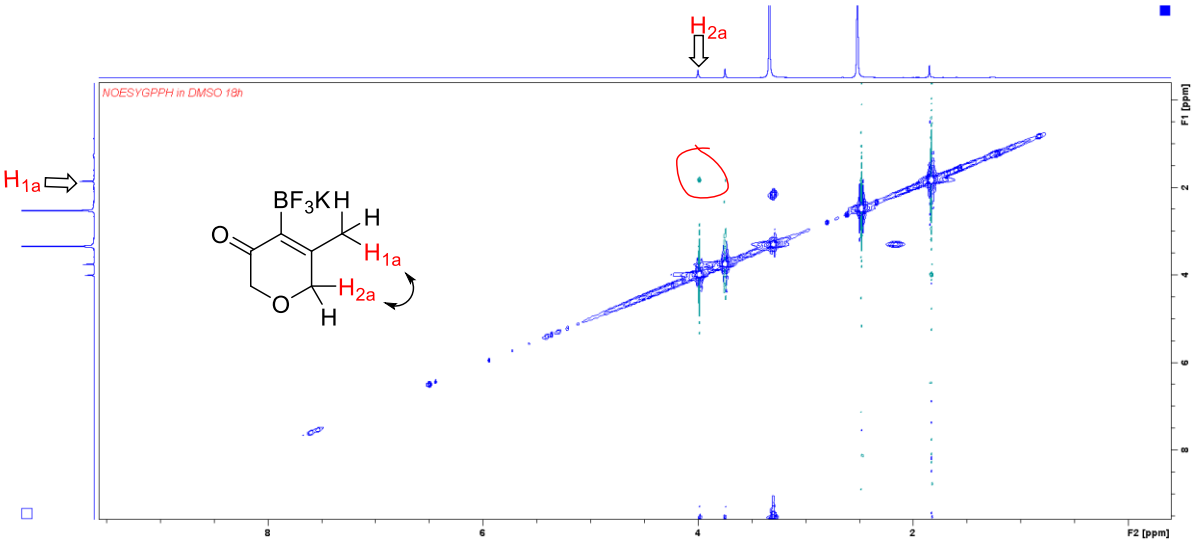

Figure 8: NOESY spectrum of **212**.

The NOESY spectrum of **212** showed the correlation of the methylene proton H-2a and the methyl proton H-1a (Figure 8), and the regiochemistry of the other compounds was determined analogously.

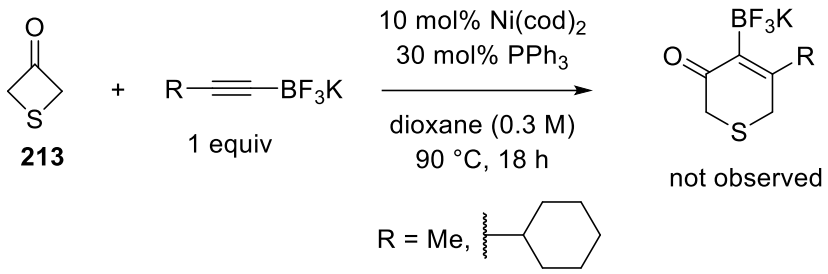

Scheme 54. Cycloaddition of potassium alkynyltrifluoroborate with thietan-3-one **213**.

Next, thietan-3-one was examined (Scheme 54). With potassium alkynyltrifluoroborate **201** and **189**, the corresponding products were not observed, and the starting material was recovered.

2.4.4. Mechanism of the Ni-catalysed cycloaddition of alkynyltrifluoroborates

In Sections 2.1 and 2.2 of this chapter, the regioselectivity of a majority of the metal-catalysed cycloaddition reactions of alkynyl boron compounds was found to often depend on the R^1 and R^2 substituents for most alkynes. However, the metal-catalysed cycloaddition of alkynyltrifluoroborates described in this thesis showed the opposite result, as the regioselectivity observed in these reactions was controlled by the trifluoroborate group. This group is a strong σ-donor substituent,[62] whereas its π-influence is weak. Three suggested mechanisms could explain the formation of the desired product as a single regioisomer in this

nickel-catalysed [4+2] cycloaddition; however, only the cases that lead to this specific regioisomer will be considered (Figure 9). Similar to the mechanism discussed in Chapter 1 and originally proposed for the nickel-catalysed [4+2] cycloaddition of simple alkynes and cyclobutanones,[4] the oxidative cyclisation of $^{2}\eta, ^{2}\eta$-alkyne–ketone–nickel complex **A** offers a route to a metallacycle **B** (path a), which is consistent with isolated complexes similar to **A**.[5,6,63,64] In addition, this speculation is also consistent with theoretical studies of the nickel-catalysed reductive coupling of alkynes with aldehydes.[8] These studies are based on the hypothesis that regioselectivity is far more controlled by steric effects than by electronic interactions. Thus, this hypothesis would assume that the potassium trifluoroborate group provides the largest steric clash with the phosphine on the metal; hence, it should be placed as remotely as possible, as depicted in **A**. However, as observed in Chapter 1, other theoretical studies do not support the proposed mechanism that involves the β-carbon elimination from **B** to **C** due to high-energy barriers for that elementary step.[16] Instead, the calculations support a mechanism that involves the oxidative addition of the strained azetidinone and oxetanone to afford intermediate **D**, followed by the migratory insertion of the alkyne into the Ni–C(sp^2) bond (path b), leading to **C**, or the Ni–C(sp^3) bond (path c), which then leads to **E**.

According to that observed from the formation of the same regioisomer for alkyne substituents **R**, which are extremely different sterically, a mechanism is proposed on the basis of the notion that regioselectivity is far more controlled by electronic interactions than by steric effects. Accordingly, notably, the trifluoroborate group is considered to behave as an inductive donor ($\sigma_I = -0.32$), while the π orbitals of the triple bond should not be affected by this group ($\sigma_R = -0.07$).[62] This donation should make the alkyne behave as a nucleophile and

would make path b more likely. The crystal structure of **203** (Figure 2) revealed that the potassium ion and the sp^2-hybridised oxygen atom of the ketone are in contact (2.700 Å), indicative of the possibility of a directing effect by coordination that may favour the formation of **C** via path b.[65,66] However, the coordination between the metal and one of the fluorine atoms of the trifluoroborate group, which appears in **E**, might favour path c.[67] Overall, paths b and c may contribute more than path a to the formation of the sole regioisomer observed in this reaction.

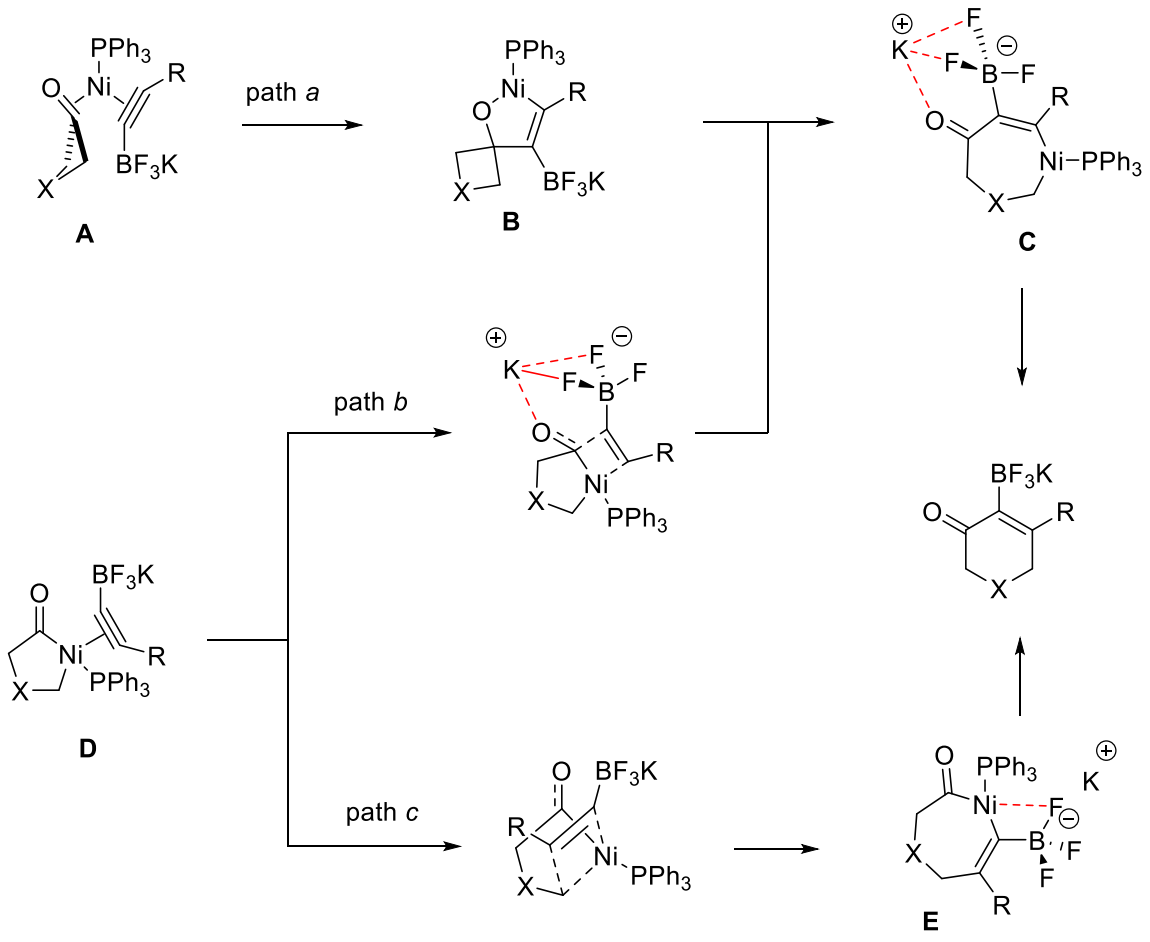

Figure 9: Plausible origin of the regioselectivity.

In 2013, Gutsulyak and co-workers reported the reaction of potassium phosphine–borate **214** with NiClPh $(PPh_3)_2$ to afford borate nickel complex **215** in a good isolated yield. In this paper,

an example of one Ni complex with an intramolecular F–Ni bond from a RBF_3 group (Scheme 55).[67] The ^{19}F NMR spectrum revealed that the chemical shift of BF_3 fluorines in borate nickel complex **215** is significantly upfield (δ = 177.3 ppm) in comparison with that of potassium phosphine–borate **214** (δ = 135.2 ppm), which is in agreement with the coordination of the BF_3 group to the nickel centre.[67]

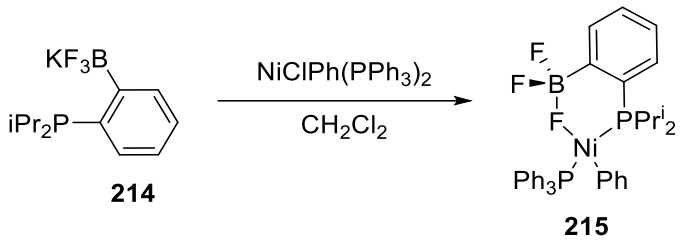

214 **215**

Scheme 55. Example of one Ni complex with an intramolecular F–Ni bond from a RBF_3 group.

2.4.5. Further functionalisation of the [4+2] cycloadducts

By utilising the conditions described by Martínez and co-workers,[68] the first attempt of Suzuki reaction of **198** with 4-bromoanisole in the presence of a palladium catalyst and potassium carbonate was carried out in a mixture of water and methanol or ethanol (Scheme 56).

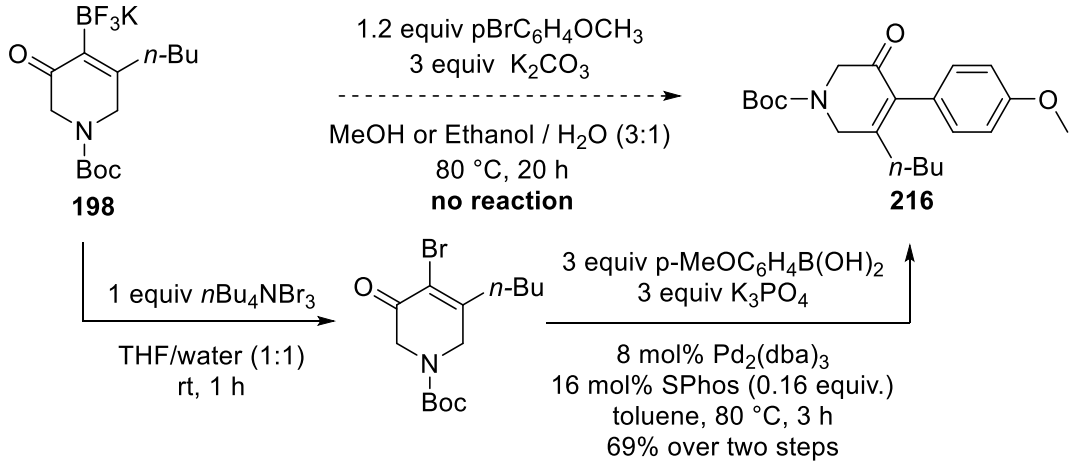

Scheme 56. Synthetic application (formation of **216**).

However, the desired product was not observed. Independently, Dr. Yannick Esvan reported the conversion of **198** into **216** in two steps. Indeed, the treatment of **198** with tetrabutylammonium tribromide[69] affords the corresponding vinyl bromide, which is used for the Suzuki–Miyaura cross-coupling reaction with para-methoxyphenylboronic acid to afford **216** in 69% yield in two steps (Scheme 56).

3. Conclusion

The intermolecular [4+2] cycloaddition of potassium alkynyltrifluoroborates triggered by the nickel-catalysed C–C bond activation of azetidinones and oxetanone is developed (Scheme 57). In contrast to previous attempts with alkynylboronic acids or their derivatives,[17] the reactions proceed without the undesired cleavage of the carbon–boron bond. Moreover, the reactions lead to the formation of a single regioisomer of dihydropyridinones and dihydropyranones, independent of the nature of the other alkyne substituent. This remarkable feature is in stark contrast to a majority of the metal-catalysed intermolecular cycloaddition reactions of alkynylboron derivatives reported thus far.[31,34,35,51,70,71] This study extends the scope of the metal-catalysed C–C bond activation[3,72-74] and of the chemistry of alkynylboron derivatives.[75,76] Finally, it offers new possibilities for the synthesis of organoboron compounds that are vital to modern organic synthesis.

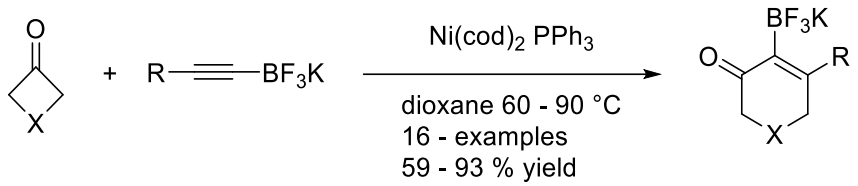

Scheme 57. Ni-catalysed cycloaddition of alkynyltrifluoroborate with 3-azetidinone and oxetanone.

Chapter 3: Experimental data

General. Otherwise noted, all reactions were carried out in flame-dried glassware under dry nitrogen atmosphere. The solvents were purified with the solvent purification system Pure Solv MD-6 (THF, Et_2O, CH_2Cl_2); toluene and dioxane were purchased from Acros (>99%, Extra Dry over Molecular Sieve, AcroSeal™). Oxetanone **59** was purchased from Fluorochem. Compounds **192-199** were prepared according to the literature.[2,56,77-79] Flash chromatography: Merck silica gel 60 (230-400 mesh). NMR: Spectra were recorded on a Bruker DRX 500 in the indicated solvent; chemical shifts (δ) are given in ppm. The solvent signals were used as references and the chemical shifts converted to the TMS scale (MeCN-d_3: δC = 118.2 ppm; δH = 1.96 ppm / DMSO-d_6: δC = 39.5 ppm; δH = 2.50 ppm;); apparent splitting patterns are designated using the following abbreviations: s (singlet), d (doublet), t (triplet), q (quartet), quint. (quintuplet), sept. (septuplet), m (multiplet), br (broad), and the appropriate combinations. In ^{19}F NMR, 1,3,5-trifluorobenzene was used as internal standard (δF = -110.6 ppm). Note that the rapid quadrupolar relaxation of ^{11}B prevented the observation of the quaternary carbon atom that bears the boron atom in ^{13}C NMR spectra. IR: PerkinElmer Spectrum 100 FT-IR spectrometer, wavenumbers in cm^{-1}. HRMS determined at the University of Liverpool on micromass LCT mass spectrometer (ES) and Trio-1000 or Agilent QTOF 7200 mass spectrometers (CI). Melting points: Griffin melting point apparatus (not corrected). All commercially available compounds were used as received.

Synthesis of 3-azetidinones

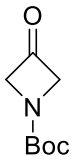

***N-tert*-Butyloxycarbonylazetidin-3-one (Boc-3-azetidinone) 180.**

Step 1. To a stirred cold (0 °C) solution of 3-hydroxyazetidine hydrochloride (10 g, 92 mmol) in methanol (92 mL) was added triethylamine (38 mL, 274 mmol) followed by Boc_2O (20 g, 91 mmol). The resultant solution was stirred at room temperature for 18 h. Volatiles were removed in vacuo and the residue was diluted with DCM (40 mL) and washed with water (30 mL) and brine (20 mL). The organics were dried over sodium sulphate filtered and concentrated to give 1-Boc-3-hydroxyazetidine **194**.

Step 2. A solution of oxalyl chloride (7 ml, 87 mmol) in dichloromethane (81 mL) was cooled to -78 °C. DMSO (11 mL, 174 mmol) was added at -78°C (internal temperature) over 15 mins.1-Boc-3-hydroxyazetidine (12 g, 67 mmol in 45 mL of dichloromethane) was added and stirred for 15 minutes, finally triethylamine (48 mL, 348 mmol) was added. The mixture was allowed to warm to room temperature and with stirring for 1 hours. The reaction mixture was diluted with 30 ml water and partitioned. The organic layer was washed twice with water then the combined aqueous solution was extracted once with dichloromethane. The combined organic layer was washed with brine, dried over sodium sulphate, filtered and concentrated to afford a yellow oil which was purified by silica gel column chromatography (20% ethyl acetate in petroleum ether) to afford Boc-3-azetidinone **180** as a white solid (7 g, 63%). ^{1}H NMR (500 MHz, $CDCl_3$): δ = 4.67 (s, 4H), 1.42 (s, 9H); ^{13}C NMR (125 MHz, $CDCl_3$): δ = 196.9, 156.2, 81.2,

71.2, 28.3; HRMS (ES+): calcd for $[M + Na]^+$: 194.0793; found:194.0791. This data is in agreement with the literature. [80]

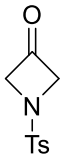

Tosyl-3-azetidinone 204. Triethylamine (20 mL, 141 mmol) was added dropwise at 0 °C to a suspension of with 3-hydroxyazetidine hydrochloride (5 g, 46 mmol) and suspended in methanol (46 mL). After stirring at r.t. for 30 minutes, tosyl chloride (9 g, 46 mmol) was added at 0°C portionwise. After stirring at r.t. overnight, all volatiles were evaporated and the residue was then partitioned between EtOAc and water. The aqueous layer was extracted 3 times with EtOAc. The combined organic layer was washed with water, brine and then dried over $MgSO_4$ before being filtered and concentrated. The *N*-tosyl-azetin-3-ol (white solid, 9.9 g, 93%) thus obtained was used without further purification. DMSO (8 mL, 112 mmol) was slowly added at -78 °C to a solution of oxalyl chloride (5 mL, 56 mmol) in CH_2Cl_2 (98 mL) under N_2. After stirring for 15 minutes at -78 °C, a solution of *N*-tosylazetin-3-ol (9 g, 43 mmol) in CH_2Cl_2 (53 mL) was added. The mixture was stirred for another 15 minutes at -78 °C, then triethylamine (31 mL, 180 mmol) was added. After stirring for 2 hours at r.t., the reaction mixture was quenched with saturated aqueous solution of NH_4Cl. The aqueous layer was extracted 3 times with diethyl ether. The combined organic layer was washed with water, brine and then dried over $MgSO_4$ before being filtered and concentrated. Purification by flash chromatography (PE/EtOAc = 2:1 to 1:1) on silica gel gave a yellow solid. The latter was washed with pentane then filtered to give **193** as white solid (7 g, 75%). ^1H NMR (500 MHz, $CDCl_3$): δ = 7.78 (d, *J* = 8.2 Hz, 2H), 7.40 (d, *J* = 8.2 Hz, 2H), 4.63 (s, 4H), 2.47 (s, 3H). HRMS

(ES+): calcd for $[M + Na]^+$:248.0357; found:248.0357 this data is in agreement with the literature.[19]

Synthesis of alkynylborates: general procedure

n-BuLi (2.5 M in hexane, 8 mmol, 1.0 equiv.) was added dropwise to a solution of alkynes 1-ethynyl-4-methoxybenzene (8 mmol, 1.0 equiv.) in 8 mL of dry THF at -78 °C under nitrogen atmosphere. After 60 min at this temperature, trimethyl borate (11 mmol, 1.5 equiv.) was added dropwise at -30 °C. The mixture was stirred at this temperature for 60 min and slowly allowed to warm to room temperature within another 60 min. A saturated 4.5 M aqueous solution of potassium hydrogen difluoride (KHF_2) (45 mmol, 6.0 equiv.) was added at -20 °C to the vigorously stirred solution. The resulting mixture was stirred for 60 min at -20 °C after which it was allowed to warm to room temperature for 60 min (white mixture). The solvent was removed under reduced pressure (rotavapor), and the resulting white solid was dried under high vacuum (to remove water). The solid was washed with acetone, and the acetone was decanted. Then, hot acetone was added to the solid, and the solid was filtered. The filter cake was washed with further hot acetone (four times), and Et_2O was added to the filtrate in order to precipitate the product. The solution was cooled to -20°C to aid precipitation. The solid was then filtered and washed with Et_2O (3 times) to afford the desired product. [2]

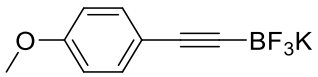

Trifluoro((4-methoxyphenyl)ethynyl)-λ⁴-borane, potassium salt (182). This compound was prepared from 4-ethynylanisole (1 mL, 8 mmol, 1.0 equiv.) according to the general procedure synthesis of alkynylborates. The product was collected as white solid in 609 mg, 57% yield. ^1H

NMR (500 MHz, DMSO-d_6): δ = 7.22 (d, 2H, *J*= 8.6 Hz), 6.84 (d, 2H, *J*= 8.7 Hz), 3.73 (s, 3H); ^{19}F NMR (376 MHz, DMSO-d_6): δ = -131.4; ^{11}B NMR (160 MHz, DMSO-d_6): δ = -1.14. this data is in agreement with the literature.[2]

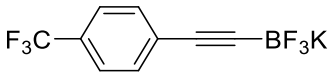

Trifluoro((4-(trifluoromethyl)phenyl)ethynyl)-λ^4-borane, potassium salt (183). This compound was prepared from 4-ethynyl-*α,α,α*-trifluorotoluene (0.5 mL, 4 mmol) according to the general procedure synthesis of alkynylborates. The product was collected as white solid in 355 mg, 35% yield. ^{1}H NMR (500 MHz, Acetone-d_6): δ = 7.59 (d, 2H, *J* = 8.0 Hz), 7.50 (d, 2H, *J* = 8.0 Hz); ^{19}F NMR (376 MHz, DMSO-d_6 + MeCN-d_3): δ = -135.3; ^{11}B NMR (160 MHz, DMSO-d_6 + Acetonitrile-d_6): δ = -1.39. This data is in agreement with the literature.[56]

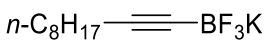

Dec-1-yn-1-yltrifluoro-λ^4-borane, potassium salt (184). This compound was prepared from dec-1-yne (0.5 mL 4 mmol) according to the general procedure synthesis of alkynylborates. The product was collected as white solid in 384 mg, 42% yield. ^{1}H NMR (500 MHz, DMSO-d_6): δ = 1.96 (m, 2H), 1.39–1.15 (m, 12 H) 0.85 (t, 3H, *J* = 6.8 Hz); ^{19}F NMR (376 MHz, DMSO-d_6): δ = -130.9; ^{11}B NMR (160 MHz, DMSO-d_6): δ = -1.52. This data is in agreement with the literature.[2]

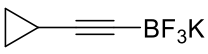

(Cyclopropylethynyl)trifluoro-λ^4-borane, potassium salt (185). This compound was prepared from cyclopropylacetylene (0.3 mL. 4 mmol) according to the general procedure synthesis of alkynylborates. The product was collected as white solid in 318 mg, 50% yield. ^{1}H NMR (500

MHz, DMSO-d_6): δ = 1.11-1.04 (m, 1H), 0.60 - 0.55 (m, 2H), 0.43-0.32 (m, 2H); ^{19}F NMR (376 MHz, DMSO-d_6): δ = -131.1; ^{11}B NMR (160 MHz, DMSO-d_6): δ = -2.02. This data is in agreement with the literature. [78]

Trifluoro(hex-1-yn-1-yl)-λ^4-borane, potassium salt (186). This compound was prepared from hex-1-yne (2 mL, 15mmol) according to the general procedure synthesis of alkynylborates. The product was collected as white solid in 2 g, 63% yield. ^{1}H NMR (500 MHz, DMSO-d_6): δ = 1.98 (m, 2H), 1.33 (m, 4H), 0.85 (m, 3H); ^{19}F NMR (376 MHz, DMSO-d_6): δ = -131.0; ^{11}B NMR (160 MHz, DMSO-d_6): δ = -1.30 This data is in agreement with the literature.[81]

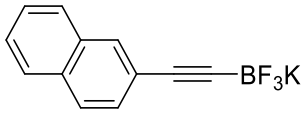

Trifluoro(naphthalen-2-ylethynyl)-λ^4-borane, potassium salt (187). This compound was prepared from 2-ethynylnaphthalene (1 g 6 mmol) according to the general procedure synthesis of alkynylborates. The product was collected as white solid in 930mg, 61% yield. ^{1}H NMR (500 MHz, DMSO-d_6): δ = 7.98-7.75 (m, 4H), 7.49 (m, 2H), 7.41 (d, 1H, *J* = 8.4 Hz); ^{19}F NMR (376 MHz, DMSO-d_6): δ = -131.5; ^{11}B NMR (160 MHz, DMSO-d_6): δ = -1.05. This data is in agreement with the literature.[2]

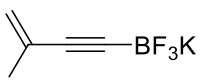

Trifluoro(3-methylbut-3-en-1-yn-1-yl)-λ^4-borane, potassium salt (188). This compound was prepared from 2-Methyl-1-buten-3-yne (1mL, 16 mmol) according to the general procedure

synthesis of alkynylborates. The product was collected as white solid in 2 g, 86% yield. ^{1}H NMR (500 MHz, acetone-d_6): δ = 4.99 (s (br), 1H), 4.97-4.95 (m, 1H), 1.77 (t, *J* = 1.2, 3H); ^{19}F NMR (376 MHz, acetone-d_6): δ = -135.4; ^{11}B NMR (160 MHz, acetone-d_6): δ = -1.8. This data is in agreement with the literature.[79]

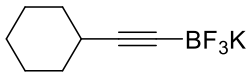

(Cyclohexylethynyl)trifluoro-λ^4-borane, potassium salt (189). This compound was prepared from cyclohexylacetylene (1mL, 11mmol) according to the general procedure synthesis of alkynylborates. The product was collected as white solid in 2 g, 65% yield. ^{1}H NMR (500 MHz, DMSO-d_6): δ = 2.14 (m, 1H), 1.78–1.54 (m, 4H), 1.46 (m, 1H), 1.34–1.09 (m, 5H); ^{19}F NMR (376 MHz, DMSO-d_6): δ = -130.8; ^{11}B NMR (160 MHz, DMSO-d_6): δ = -1.43. This data is in agreement with the literature.[2]

[4+2] Ni(cod)$_2$: Synthesis of compounds 195-212

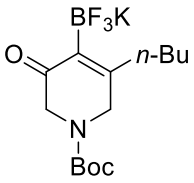

Tert-butyl 5-butyl-3-oxo-4-(trifluoro-λ^4-boraneyl)-3,6-dihydropyridine-1(2H)-carboxylate, potassium salt (198). Inside an argon-filled glovebox, a J-Young flame-dried Schlenk flask equipped with a small stirrer bar was charged with Ni(cod)$_2$ (48 mg, 0.2 mmol, 0.1 equiv) and PPh_3 (142 mg, 0.6 mmol, 0.3 equiv). Then, outside the glovebox and under N_2, dioxane (2 mL) was added. The mixture was stirred at room temperature for 10 minutes, then **180** (431 mg, 3 mmol, 1.4 equiv), potassium trifluoro(hex-1-yn-1-yl)borate **186** (339 mg, 2 mmol, 1equiv)

and dioxane (4 mL) were added in that order. The tube was sealed and the mixture was stirred at 60 °C for 18 h. At room temperature, MeCN (30 mL) was added and all volatiles were removed in vacuo. The resulting brown residue was dissolved in acetone (15 mL) and Et_2O (60 mL) was added to induce precipitation. The resulting solid was filtrated through a sintered funnel followed by trituration with Et_2O (3 x 15 mL) at room temperature to afford **198**as a white solid (457 mg, 70%); m.p.: 155–157 °C; 1H NMR (500 MHz, MeCN-d_3): δ 4.02 (s, 2H), 3.83 (s, 2H), 2.49-2.41 (m, 2H), 1.56-1.47 (m, 2H), 1.48 (s, 9H), 1.45-1.33 (m, 2H), 0.953 (t, *J* = 7.4 Hz); ^{13}C NMR (126 MHz, MeCN-d_3): δ 201.7 (br), 165.5, 155.2, 80.7, 52.4 (br), 47.9 (br), 34.6, 32.4, 28.7 (3C), 23.8, 14.4; ^{19}F NMR (376 MHz, MeCN-d_3): δ = -136.7 – -137.5 (m); ^{11}B NMR (160 MHz, MeCN-d3): δ = 2.29 (q, *J* = 50.5 Hz); elemental analysis (%) calcd for ($C_{14}H_{22}BF_3KNO_3$): C 46.81, H 6.18, N 3.9; found: C 46.32, H 6.10, N 3.82; IR (neat): $\tilde{\nu}$ = 2960, 2969, 2871, 1675, 1665, 1609, 1479, 1418, 1377, 1366, 1315, 1293, 1245, 1160, 1140, 1098, 1065, 1015, 984, 958, 898 cm^{-1}; HRMS (ES-): calcd for $[M – K]^-$: 320.1645; found: 320.1655

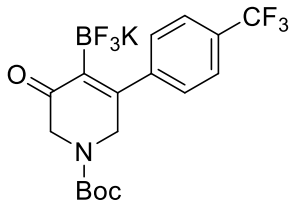

Tert-butyl 3-oxo-4-(trifluoro-λ^4-boraneyl)-5-(4-(trifluoromethyl)phenyl)-3,6-dihydropyridine-1(2H)-carboxylate, potassium salt (196). This compound was obtained from **180** (144 mg, 0.8 mmol) and potassium (((4-trifluoromethyl)phenyl)ethynyl)trifluoroborate **183** (166 mg, 1 mmol) by the procedure described for the preparation of **198**. White solid, 141 mg, 57%; m.p.: 152–155 °C; 1H NMR (500 MHz, MeCN-d_3): δ 7.67 (d, *J* = 8.1 Hz, 2H), 7.52 (d, *J* = 8.2 Hz, 2H), 4.23 (s, 2H), 4.00 (s, 2H), 1.49 (s, 9H); ^{13}C NMR (126 MHz, MeCNd_3): δ 201.8

(br), 159.5 (br), 155.3, 146.7, 129.9 (2C), 129.8 (q, *J* = 32.1 Hz), 125.7 (q, *J* = 271.1 Hz), 125.3 (q, *J* = 4.1 Hz, 2C), 81.1, 52.7 (br), 49.6 (br), 28.7 (3C); ^{19}F NMR (376 MHz, MeCN-d_3): δ = -64.2, -135.5 – -136.3 (m); ^{11}B NMR (160 MHz, MeCN-d_3): δ = 1.68 (q, *J* = 46.8 Hz); elemental analysis (%) calcd for ($C_{17}H_{17}BF_6KNO_3$): C 45.66, H 3.83, N 3.13; found: C 44.40, H 3.66, N 2.97; IR (neat): $\tilde{\nu}$ = 1701, 1665, 1604, 1419, 1368, 1325, 1303, 1247, 1223, 1180, 1135, 1114, 1105, 1066, 1015, 968 cm^{-1}; HRMS (ES-): calcd for [M - K]$^-$: 408.1211; found: 408.1196.

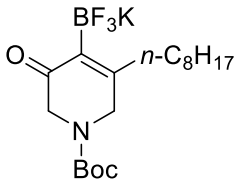

Tert-butyl 5-octyl-3-oxo-4-(trifluoro-λ^4-boraneyl)-3,6-dihydropyridine-1(2H)-carboxylate, potassium salt (197). This compound was obtained from **180** (72 mg, 0.4 mmol) and potassium dec-1- ynyltrifluoroborat **184** (73 mg, 0.3 mmol) by the procedure described for the preparation of **198**, white solid, 85 mg, 68%; ^{1}H NMR (500 MHz, DMSO-d_6): δ 3.87 (s, 2H), 3.67 (s, 2H), 2.32-2.23 (m, 2H), 1.45-1.37 (m, 2H), 1.31-1.19 (m, 10H), 0.86 (t, *J* = 6.9 Hz, 3H); ^{13}C NMR (126 MHz, DMSO-d_6): δ 198.7, 161.0, 153.6, 79.1, 51.4, 46.2, 33.5, 31.31, 29.48, 28.94, 28.65, 28.0, 22.1, 13.9; ^{19}F NMR (376 MHz, MeCN-d_3): δ = -133.1 – -133.7 (m); ^{11}B NMR (160 MHz, MeCN-d_3): δ = 2.26 (q, *J* = 54.22 Hz); HRMS (ES-): calcd for [M - K]$^-$: 376.2472; found: 376.2476; IR (neat): $\tilde{\nu}$ = 2957 (m), 2922 (m), 2854 (m), 1678 (s), 1658 (s), 1612 (m), 1410 (m), 1376 (m), 1306 (m), 1248 (s), 1159 (s)$^{-1}$cm.

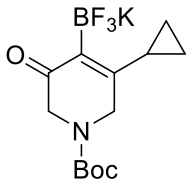

Tert-butyl 5-cyclopropyl-3-oxo-4-(trifluoro-λ^4-boraneyl)-3,6-dihydropyridine-1(2H)-carboxylate, potassium salt (200). This compound was obtained from **180** (288 mg, 2 mmol) and potassium (cyclopropylethynyl)trifluoroborate **185** (206 mg, 1 mmol) by the procedure described for the preparation of **198**, except that the precipitation was induced by a mixture of acetone and petroleum ether. White solid, 206 mg, 56%; m.p. > 105 °C (decomposition); ^{1}H NMR (500 MHz, DMSO-d_6): δ 3.70 (s, 2H), 3.46 (s, 2H), 2.62–2.50 (m, 1H), 1.39 (s, 9H), 0.79–0.64 (m, 4H); ^{13}C NMR (126 MHz, DMSO-d_6): δ 197.3 (br), 161.3 (br), 153.2, 79.2, 52.00 (br), 28.0 (3C), 14.4, 5.8 (the signal of one methylene of the heterocycle is overlapped with the NMR solvent); ^{19}F NMR (376 MHz, DMSO-d_6): δ = -133.6 – -134.4 (m); ^{11}B NMR (160 MHz, MeCN-d_3): δ = 2.49 (q, *J* = 52.2 Hz); elemental analysis (%) calcd for ($C_{15}H_{11}BF_3KO_3$): C 45.5, H 5.29, N 4.08; found: C 43.12, H 5.23, N 3.79; IR (neat): $\tilde{\nu}$ = 2974, 1691, 1641, 1612, 1582, 1418, 1378, 1365, 1310, 1249, 1168, 1127, 1083, 1028, 1003, 974, 900 cm^{-1}; HRMS (ES-): calcd for [M - K]$^-$: 303.1374; found: 303.1378.

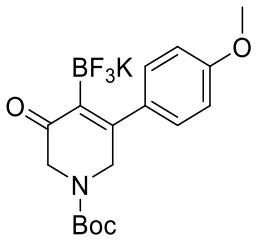

Tert-butyl 5-(4-methoxyphenyl)-3-oxo-4-(trifluoro-λ^4-boraneyl)-3,6-dihydropyridine-1(2H)-carboxylate, potassium salt (195). This compound was obtained from **180** (288 mg, 2 mmol) and potassium ((4-methoxyphenyl)ethynyl)trifluoroborate **182** (286 mg, 1 mmol) by the procedure described for the preparation of **198**, except that the precipitation was induced by amixture of acetone and petroleum ether. White solid, 395 mg, 80%; m.p.: 151–153 °C; 1H

NMR (500 MHz, MeCN-d_3): δ 7.36 (d, *J* = 8.8 Hz, 2H), 6.92 (d, *J* = 8.3 Hz, 2H), 4.24 (s, 2H), 3.96 (s, 2H), 3.83 (s, 3H), 1.50 (s, 9H); ^{13}C NMR (126 MHz, MeCN-d3): δ 202.6 (br), 161.5 (br), 160.9, 155.4, 134.3, 130.9 (2C), 113.9 (2C), 81.0, 56.0, 52.8 (br), 49.6 (br), 28.7 (3C); ^{19}F NMR (376 MHz, MeCN-d^3): δ = -135.5 – -136.4 (m); ^{11}B NMR (160 MHz, MeCN-d_3): δ = 3.09–0.90 (m); IR (neat): $\tilde{\nu}$ = 2977, 2836, 1694, 1643, 1606, 1509, 1434, 1415, 1363, 1305, 1285, 1243, 1162, 1130, 1087, 1030, 968, 907, 890 cm^{-1}; HRMS (ES): calcd for [M - K]$^-$: 369.1479; found: 369.1489.

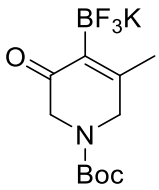

Tert-butyl 5-methyl-3-oxo-4-(trifluoro-λ^4-boraneyl)-3,6-dihydropyridine-1(2H)-carboxylate, potassium salt (199). This compound was obtained from **180** (163 mg, 1 mmol) and commercially available potassium propynyltrifluoroborate **201** (100 mg, 1 mmol) by the procedure described for the preparation of **198**, White solid, 131 mg, 61%; ^{1}H NMR (500 MHz, DMSO-d_6): δ 3.81 (s, 2H), 3.65 (s, 2H), 1.91 (s, 3H), 1.40 (s, 9H); ^{13}C NMR (126 MHz, DMSO-d_6): δ 197.2, 157.3, 153.3, 79.4, 51.0, 47.9, 28.0 (3C), 20.1; ^{19}F NMR (376 MHz, MeCN-d_3): δ = -135.1 – -135.8 (m); ^{11}B NMR (160 MHz, MeCN-d_3): δ = 2.86 – 1.59 (m); HRMS (ES): calcd for [M - K]$^-$: 278.0582; found: 278.0586; elemental analysis (%) calcd for ($C_{11}H_{16}BF_3KNO_3$): C 41.66, H 5.09, N 4.42; found: C 37.76, H 4.52, N 3.76; IR (neat): $\tilde{\nu}$ = 2975, 1690, 1653, 1479, 1449, 1388, 1400, 1372, 1360, 1305, 1249, 1187, 1120, 1089, 975, 901, 770, 861 cm^{-1}.

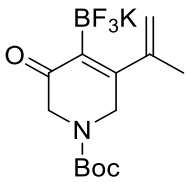

Tert-butyl 3-oxo-5-(prop-1-en-2-yl)-4-(trifluoro-λ⁴-boraneyl)-3,6-dihydropyridine-1(2H)-carboxylate (203). This compound was obtained from **180** (288 mg, 2 mmol) and potassium (3-methylbut-3-en-1-yn-1-yl)trifluoroborate **188** (206 mg, 1 mmol) by the procedure described for the preparation of **198**. White solid, 365 mg, 89%; m.p.: 168–170 °C; 1H NMR (500 MHz, DMSO-d_6): δ 4.83 (s, 1H), 4.66 (s, 1H), 3.94 (s, 2H), 3.77 (s, 2H) 1.89 (s, 3H), 1.41 (s, 9H); ^{13}C NMR (126 MHz, DMSO-d_6): δ 198.8 (br), 160.5, 153.4, 145.7, 139.2 (br), 111.3, 79.3, 51.2 (br), {46.9 (br) & 46.2 (br), two signals for one of the methylene of the heterocycle are visible, corresponding to two rotamers, 27.9 (3C), 22.5; ^{19}F NMR (376 MHz, MeCN-d_3): δ = -136.2 – -136.9 (m); ^{11}B NMR (160 MHz, MeCN-d_3): δ = 1.89 (q, *J* = 51.6 Hz); elemental analysis (%) calcd for ($C_{13}H_{18}BF_3KNO_3$): C 45.50, H 5.29, N 4.08; found: C 44.75, H 5.20, N 3.99 IR (neat): $\tilde{\nu}$ = 2976, 2911, 2819, 1702, 1658, 1604, 1476, 1431, 1415, 1366, 1311, 1265, 1239, 1161, 1139, 1087, 1022, 1006, 982, 950 cm^{-1}; HRMS (ES-): calcd for [M - K]$^-$: 303.1374; found: 303.1385.

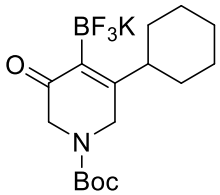

Tert-butyl 5-cyclohexyl-3-oxo-4-(trifluoro-λ⁴-boraneyl)-3,6-dihydropyridine-1(2H)-carboxylate, potassium salt (204). This compound was obtained from **180** (431 mg, 3 mmol) and potassium (cyclohexylethynyl)trifluoroborate **189** (385 mg, 2 mmol) by the procedure

described for the preparation of **198**. White solid, 430 mg, 62%; m.p.: 145–147 °C; 1H NMR (500 MHz, MeCN-d_3): δ 4.00 (s, 2H), 3.81 (s, 2H), 3.21-3.10 (m, 1H), 1.80–1.72 (m, 2H), 1.72–1.65 (m, 1H), 1.65–1.58 (m, 2H), 1.43 (s, 9H), 1.40-1.15 (m, 5H); ^{13}C NMR (126 MHz, MeCN-d3): δ 202.8 (br), 169.4, 155.2, 80.7, 53.0 (br), 44.1 (br), 43.6, 31.7, 28.7 (3C), 27.3, 27.0; ^{19}F NMR (376 MHz, MeCN-d_3): δ = -136.3 – -137.0 (m); ^{11}B NMR (160 MHz, MeCN-d_3): δ = 2.23 (q, *J* = 53.3 Hz); IR (neat): $\tilde{\nu}$ = 2978, 2928, 2850, 1686, 1656, 1594, 1424, 1391, 1376, 1367, 1303, 1285, 1250, 1162, 1141, 1120, 1078, 1013, 986, 962, 934, 898 cm^{-1}; HRMS (ES-): calcd for [M - K]$^-$: 345.1843; found: 345.1844.

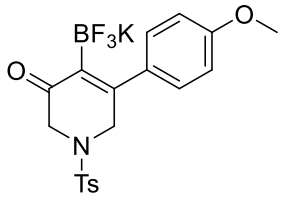

5-(4-Methoxyphenyl)-1-tosyl-4-(trifluoro-λ^4-boraneyl)-1,6-dihydropyridin-3(2H)-one, potassium salt (205). Inside an argon-filled glovebox, a Teflon-screw flame-dried Schlenk flask equipped with a small stirrer bar was charged with Ni(cod)$_2$ (16 mg, 0.1 mmol, 0.1 equiv) and PPh_3 (48 mg, 0.2 mmol, 0.3 equiv). Then, outside the glovebox and under N_2, dioxane (0.5 mL) was added. The mixture was stirred at room temperature for 10 minutes, then a solution of **193** (182 mg, 1 mmol, 1.4 equiv) in dioxane (0.5 mL) was added, followed by **182** (143 mg, 1 mmol, 1 equiv) and finally dioxane (1mL). The tube was sealed and the mixture was stirred at 60 °C for 18 h. At room temperature, MeCN (15 mL) was added and all volatiles were removed in vacuo. The resulting brown residue was dissolved in acetone (5 mL) and Et_2O (30 mL) was added to induce precipitation. The resulting solid was filtrated through a sintered funnel followed by trituration with Et_2O (2 x 15 mL) at room temperature to afford **205** as a cream-

coloured solid (275 mg, 98%); m.p.> 155 °C (decomposition); 1H NMR (500 MHz, DMSO-d_6): δ 7.67 (d, *J* = 8.6 Hz, 2H), 7.42 (d, *J* = 8.6 Hz, 2H), 7.22 (d, *J* = 8.6 Hz, 2H), 6.84 (d,*J* = 8.6 Hz, 2H), 3.76 (s, 3H), 3.76 (s, 2H), 3.43 (s, 2H), 2.38 (s, 3H); ^{13}C NMR (126 MHz, DMSO-d_6): δ 196.1, 159.0, 155.8, 143.8, 132.7, 132.1, 130.0 (2C), 129.6 (2C), 127.6 (2C), 112.6 (2C), 55.0, 52.5, 49.4, 21.0; ^{19}F NMR (376 MHz, MeCN-d_3): δ = -135.8 – -136.6 (m); ^{11}B NMR (160 MHz, DMSO-d_6): δ = 4.06 – -0.39 (m); IR (neat): $\tilde{\nu}$ = 1651, 1604, 1509, 1440, 1348, 1306, 1289, 1249, 1162, 1120, 1091, 1028, 962 cm-1; HRMS (ES+): calcd for $[M + K]^+$: 502.0276; found: 502.0266.

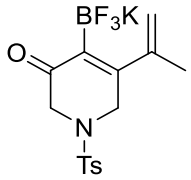

5-(Prop-1-en-2-yl)-1-tosyl-4-(trifluoro-λ^4-boraneyl)-1,6-dihydropyridin-3(2H)-one, potassium salt (206). This compound was obtained from **193** (189 mg, 0.84 mmol) and potassium ((4-methoxyphenyl)ethynyl)trifluoroborate **188** (103 mg, 0.6 mmol) by the procedure described for the preparation of **205**. Pale brown solid, 216 mg, 92%; m.p.: 112–115 °C; 1H NMR (500 MHz, DMSO-d_6): δ 7.66 (d, *J* = 8.1 Hz, 2H), 7.44 (d, *J* = 8.1 Hz, 2H), 4.80 (s, 1H), 4.59 (s, 1H), 3.56 (s, 2H), 3.37 (s, 2H), 2.39 (s, 3H), 1.83 (s, 3H); ^{13}C NMR (126 MHz, DMSO-d_6): δ 195.7, 158.2, 145.6, 143.8, 132.1, 129.9 (2C), 111.7 (2C), 52.2, 48.1, 22.6, 20.1; ^{19}F NMR (376 MHz, MeCN-d_3): δ = -137.6 – -138.4 (m); 11B NMR (160 MHz, MeCN-d_3): δ = 3.87 – -0.57 (m); IR (neat): $\tilde{\nu}$ = 2981, 2889, 1653, 1596, 1462, 1382, 1349, 1263, 1160, 1088, 955 cm^{-1}; HRMS (ES+): calcd for $[M + K]^+$: 436.0170; found: 436.0171.

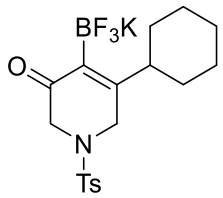

5-Cyclohexyl-1-tosyl-4-(trifluoro-λ⁴-boraneyl)-1,6-dihydropyridin-3(2H)-one, potassium salt (207). This compound was obtained from **193** (147 mg, 0.7 mmol) and potassium (cyclohexylethynyl)trifluoroborate **189** (100 mg, 0.5 mmol) by the procedure described for the preparation of **205**. Pale brown solid, 123 mg, 59%; ^{1}H NMR (500 MHz, MeCN-d3): δ 7.69 (d, *J* = 8.1 Hz, 2H), 7.44 (d, *J* = 8.1 Hz, 2H), 3.47 (s, 2H), 3.23 (s, 2H), 3.15-3.05 (m, 1H) 2.40 (s, 3H), 1.98-1.89 (m, 1H), 1.75-1.40 (m, 4H), 1.3-1.12 (m, 5H); ^{13}C NMR (126 MHz, DMSO-d_6): δ = 196.19, 163.24, 143.61, 132.19, 129.84, 127.5, 52.70, 44.32, 41.81, 29.84, 25.49, 20.86; ^{19}F NMR (376 MHz, MeCN-d_3): δ = -135.1 – -135.9 (m); ^{11}B NMR (160 MHz, MeCN-d_3): δ = 2.5 – 1.7 (m); HRMS (ES+): calcd for $[M + K]^+$: 478.0640; found: 478. 0642; IR (neat): $\tilde{\nu}$ = 2929, 2852 , 1648, 1595, 1448, 1349, 1303, 1139, 1160, 113, 994, 959, 931^{-1}cm.

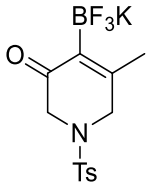

5-Methyl-1-tosyl-4-(trifluoro-λ⁴-boraneyl)-1,6-dihydropyridin-3(2H)-one, potassium salt (208). This compound was obtained from **193** (113 mg, 0.5 mmol) and commercially available potassium propynyltrifluoroborate **201** (70 mg, 0.4 mmol) by the procedure described for the preparation of **205**. Pale brown solid, 94 mg, 70%; ^{1}H NMR (500 MHz, MeCN-d3): δ 7.67 (d, *J* = 8.5 Hz, 2H), 7.41 (d, *J* = 8.0 Hz, 2H), 3.62 (s, 2H), 3.44 (s, 2H), 2.42 (s, 3H), 2.00 (s, 3H); ^{13}C NMR (126 MHz, DMSO-d_6): δ 194.6, 155.5, 143.5, 131.9, 129.6 (2C), 127.3 (2C), 51.9, 49.1,

20.7, 19.9; ^{19}F NMR (376 MHz, MeCN-d_3): δ = -136.5 – -137.4 (m); ^{11}B NMR (160 MHz, MeCN-d_3): δ = 2.92 – 1.22 (m); IR (neat): $\tilde{\nu}$ = 1658, 1603, 1437, 1342, 1303, 1187, 1161, 1141, 1122, 1096, 1035, 962, 919, 896, 835, 813 cm-1; HRMS (ES+): calcd for $[M + K]^+$: 410.0014; found: 410.0017.

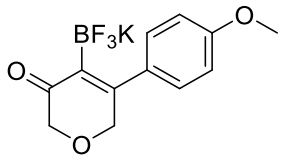

5-(4-Methoxyphenyl)-4-(trifluoro-λ^4-boraneyl)-2H-pyran-3(6H)-one, potassium salt (210). Inside an argon-filled glovebox, a Teflon-screw flame-dried Schlenk flask equipped with a small stirrer bar was charged with Ni(cod)$_2$ (16 mg, 0.1 mmol, 0.1 equiv) and PPh_3 (48 mg, 0.2 mmol, 0.3 equiv). Then, outside the glovebox and under N_2, dioxane (0.5 mL) was added. The mixture was stirred at room temperature for 10 minutes, then commercially available 1-oxetan-3-one **59** (54 µL , 0.8 mmol, 1.4 equiv), **182** (143 mg, 0.6 mmol, 1 equiv) and dioxane (1.5 mL) were added in that order. The tube was sealed and the mixture was stirred at 90 °C for 18 h. At room temperature, MeCN (15 mL) was added and all volatiles were removed in vacuo. The resulting brown residue was dissolved in acetone (5 mL) and Et_2O (30 mL) was added to induce precipitation. The resulting solid was filtrated through a sintered funnel followed by trituration with Et_2O (2 x 10 mL) at room temperature to afford **210** as a cream-coloured solid (93 mg, 55%); m.p.> 145 °C (decomposition); ^{1}H NMR (500 MHz, DMSO-d_6): δ 7.33 (d, J = 8.4 Hz, 2H), 6.83 (d, J = 8.4 Hz, 2H), 4.30 (s, 2H), 3.87 (s, 2H), 3.76 (s, 3H); ^{13}C NMR (126 MHz, DMSO-d_6): δ 199.4, 158.9, 158.6, 131.6, 129.7 (2C), 112.4 (2C), 71.5, 68.7, 54.9; ^{19}F NMR (376 MHz, MeCN-d_3): δ = -135.6 – -136.4 (m); ^{11}B NMR (160 MHz, MeCN-d_3): δ = 1.97 (q,

J = 51.1 Hz); elemental analysis (%) calcd for ($C_{12}H_{11}BF_3KO_3$): C 46.48, H 3.58; found: C 44.12, H 3.45; IR (neat): $\tilde{\nu}$ = 1642, 1602, 1589, 1564, 1506, 1470, 1435, 1416, 1387, 1313, 1287, 1249, 1223, 1178, 1134, 1118, 1104, 1050, 955, 944, 927, 888, 870, 826, 814 cm^{-1}; HRMS (ES-): calcd for $[M - K]^-$: 271.0753; found: 271.0754.

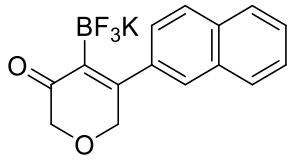

5-(Naphthalen-2-yl)-4-(trifluoro-λ⁴-boraneyl)-2H-pyran-3(6H)-one, potassium salt (211).This compound was obtained from **59** (35 µL, 0.5 mmol) and potassium ((2-naphthyl)ethynyl)trifluoroborate **187** (93 mg, 0.36 mmol) by the procedure described for the preparation of **210**. Pale yellow solid, 83 mg, 70%; ^{1}H NMR (500 MHz, DMSO-d_6): δ 7.92–7.84 (m, 3H), 7.83–7.76 (m, 1H), 7.55–7.44 (m, 3H), 4.44 (s, 2H), 3.97 (s, 2H); ^{13}C NMR (126 MHz, DMSO-d_6): δ 199.3, 158.9, 137.4, 132.4, 132.3, 127.9, 127.4, 127.1, 126.4, 126.0, 125.7, 125.6, 71.4, 68.9; ^{19}F NMR (376 MHz, MeCN-d_3): δ = -135.8 – -136.6 (m); ^{11}B NMR (160 MHz, MeCN-d_3): δ = 1.92 (q, *J* = 48.5 Hz); elemental analysis (%) calcd for ($C_{15}H_{11}BF_3KO_3$): C 54.57, H 3.36; found: C 52.83, H 3.3; IR (neat): $\tilde{\nu}$ = 1647, 1634, 1603, 1585, 1428, 1377, 1310, 1258, 1126, 1107, 107, 997, 943 cm^{-1}; HRMS (ES-): calcd for $[M - K]^-$: 291.0804; found: 291.0797.

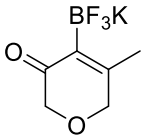

5-Methyl-4-(trifluoro-λ⁴-boraneyl)-2H-pyran-3(6H)-one, potassium salt (212). This compound was obtained from **59** (140 µL, 2.0 mmol) and commercially available potassium propynyltrifluoroborate **201** (213 mg, 1.5 mmol) by the procedure described for the

preparation of **210**. white solid, 243 mg, 93%; ^{1}H NMR (500 MHz, DMSO-d_6): δ 4.0 (s, 2H), 3.76 (s, 2H), 1.85 (s, 3H); ^{13}C NMR (126 MHz, DMSO-d_6): δ 199.21, 159.75, 71.90, 69.81, 18.72; ^{19}F NMR (376 MHz, MeCN-d_3): δ = -135.2 – -136.1 (m); ^{11}B NMR (160 MHz, MeCN-d_3): δ = 2.29 (q, *J* = 52.2 Hz)); HRMS (ES-): calcd for $[M - K]^-$: 179.0491; found: 179.0493.

X-Ray data for compound 203

Table 1 Crystal data and structure refinement for final.

Identification code	final
Empirical formula	$C_{13}H_{18}BF_3KNO_3$
Formula weight	343.19
Temperature/K	150
Crystal system	monoclinic
Space group	$P2_1/c$
a/Å	13.296(3)
b/Å	5.8346(10)
c/Å	21.585(4)
α/°	90
β/°	103.096(7)
γ/°	90
Volume/Å^3	1630.9(5)
Z	4
ρ_{calc}g/cm^3	1.398
μ/mm^{-1}	0.365
F(000)	712.0
Crystal size/mm^3	0.25 × 0.2 × 0.05

Radiation	MoKα (λ = 0.71073)
2Θ range for data collection/°	5.518 to 53.224
Index ranges	-16 ≤ h ≤ 16, -7 ≤ k ≤ 7, -26 ≤ l ≤ 27
Reflections collected	18485
Independent reflections	3340 [R_{int} = 0.0983, R_{sigma} = 0.0634]
Data/restraints/parameters	3340/0/211
Goodness-of-fit on F^2	1.054
Final R indexes [I>=2σ (I)]	R_1 = 0.0460, wR_2 = 0.1234
Final R indexes [all data]	R_1 = 0.0808, wR_2 = 0.1513
Largest diff. peak/hole / e $Å^{-3}$	0.48/-0.56

Table 2 Fractional Atomic Coordinates (×10^4) and Equivalent Isotropic Displacement Parameters ($Å^2$×10^3) for final. U_{eq} is defined as 1/3 of of the trace of the orthogonalised U_{IJ} tensor.

Atom	***x***	***y***	***z***	**U(eq)**
K1	4715.2(4)	2107.1(10)	6780.7(3)	20.8(2)
F3	3760.1(13)	952(3)	2660.6(8)	29.3(4)
F1	3671.9(12)	4837(3)	2701.2(8)	28.8(4)
F2	5003.7(12)	2972(3)	3319.9(10)	36.8(5)

O3	1844.7(13)	5399(3)	5311.9(9)	21.9(4)
O2	3086.9(15)	3032(3)	5865.7(9)	25.2(5)
O1	4364.4(15)	-435(3)	4118.4(10)	27.9(5)
N1	2625.8(18)	2917(4)	4793.2(12)	25.8(6)
C4	2407.0(19)	3649(4)	3646.6(13)	15.9(5)
C3	3317.5(19)	2641(4)	3642.8(13)	16.3(6)
C7	1762.4(19)	4950(4)	3105.6(13)	17.8(6)
C2	3730.4(19)	1038(5)	4164.5(13)	19.1(6)
C10	2558.5(19)	3726(5)	5367.7(13)	17.9(6)
C11	1580(2)	6444(5)	5881.2(13)	19.0(6)
C1	3316(2)	1007(5)	4762.4(14)	26.0(7)
C5	1894(2)	3472(5)	4204.2(14)	25.8(7)
C8	1166(2)	3872(6)	2627.1(15)	29.2(7)
C13	2511(2)	7532(5)	6309.8(16)	30.0(7)
C14	801(2)	8243(5)	5576.3(15)	27.2(7)
C12	1086(2)	4638(5)	6218.0(16)	31.4(7)
C9	1804(3)	7505(5)	3147.5(18)	36.4(8)
B1	3932(2)	2856(5)	3073.7(16)	19.6(7)

Table 3 Anisotropic Displacement Parameters ($Å^2 \times 10^3$) for final. The Anisotropic displacement factor exponent takes the form: $-2\pi^2[h^2a^{*2}U_{11}+2hka^*b^*U_{12}+\ldots]$.

Atom	U_{11}	U_{22}	U_{33}	U_{23}	U_{13}	U_{12}
K1	23.0(3)	23.6(3)	17.9(3)	0.1(3)	9.2(2)	5.7(2)
F3	46.5(10)	22.9(9)	25.3(10)	-3.2(8)	22.3(8)	0.4(7)
F1	34.1(9)	23.1(9)	35.6(11)	10.7(8)	20.8(8)	4.6(7)
F2	17.8(8)	45.9(11)	50.2(13)	9.5(10)	14.6(8)	2.6(7)
O3	27.1(10)	26.2(10)	14.0(10)	3.4(8)	8.2(8)	12.2(8)
O2	30.3(11)	30.0(11)	15.5(11)	3.7(9)	5.8(9)	12.2(8)
O1	31.6(11)	32.3(11)	22.4(11)	1.1(9)	11.2(9)	17.3(9)
N1	26.4(12)	39.3(15)	11.9(12)	0.8(11)	4.9(10)	18.0(10)
C4	19.4(12)	15.7(12)	12.6(13)	-3.9(11)	3.6(10)	-0.5(10)
C3	17.4(13)	16.4(13)	15.8(14)	-0.6(11)	5.2(11)	1.4(10)
C7	16.6(12)	19.7(13)	18.2(15)	2.1(12)	6.1(11)	1.6(10)
C2	18.8(13)	25.6(14)	13.1(14)	-1.1(12)	4.0(10)	3.5(11)
C10	20.2(13)	19.6(13)	16.2(15)	1.6(12)	9.0(11)	5.4(11)
C11	24.0(13)	19.7(13)	15.4(14)	-4.4(12)	9.1(11)	5.6(11)
C1	33.1(15)	32.8(17)	15.8(15)	8.3(13)	13.1(12)	18.2(13)
C5	22.5(14)	40.1(17)	16.9(15)	4.0(14)	8.5(12)	12.4(12)
C8	34.6(16)	27.8(17)	21.7(17)	4.9(14)	-0.8(13)	1.5(13)

C13	30.0(16)	28.1(16)	30.5(18)	-7.4(14)	4.0(13)	4.1(12)
C14	30.3(15)	24.9(15)	27.3(18)	2.1(13)	8.3(13)	10.8(12)
C12	39.5(17)	26.1(16)	35.8(19)	1.1(14)	23.7(15)	2.9(13)
C9	41.4(19)	19.4(15)	45(2)	-1.4(15)	3.2(16)	4.8(13)
B1	20.2(15)	18.8(15)	22.0(17)	1.3(14)	9.2(13)	3.0(12)

Table 4 Bond Lengths for final.

Atom	**Atom**	**Length/Å**	**Atom**	**Atom**	**Length/Å**
K1	$F3^{1}$	2.7560(17)	O3	C10	1.348(3)
K1	$F3^{2}$	2.7644(18)	O3	C11	1.484(3)
K1	$F1^{1}$	2.8996(18)	O2	C10	1.213(3)
K1	$F1^{3}$	2.8183(19)	O1	$K1^{2}$	2.700(2)
K1	$F2^{2}$	3.001(2)	O1	C2	1.224(3)
K1	$F2^{1}$	3.257(2)	N1	C10	1.348(3)
K1	$F2^{3}$	2.910(2)	N1	C1	1.455(3)
K1	O2	2.635(2)	N1	C5	1.452(4)
K1	$O1^{2}$	2.700(2)	C4	C3	1.347(3)
K1	$B1^{1}$	3.192(3)	C4	C7	1.490(4)
K1	$B1^{3}$	3.423(3)	C4	C5	1.516(4)
K1	$B1^{2}$	3.386(3)	C3	C2	1.471(4)
F3	$K1^{4}$	2.7559(17)	C3	B1	1.627(4)

F3	K1[2]	2.7644(18)	C7	C8	1.311(4)
F3	B1	1.410(4)	C7	C9	1.494(4)
F1	K1[3]	2.8182(18)	C2	C1	1.514(4)
F1	K1[4]	2.8996(17)	C11	C13	1.507(4)
F1	B1	1.406(4)	C11	C14	1.516(4)
F2	K1[2]	3.001(2)	C11	C12	1.512(4)
F2	K1[4]	3.257(2)	B1	K1[4]	3.192(3)
F2	K1[3]	2.910(2)	B1	K1[3]	3.423(3)
F2	B1	1.405(3)	B1	K1[2]	3.386(3)

[1]+X,1/2-Y,1/2+Z; [2]1-X,-Y,1-Z; [3]1-X,1-Y,1-Z; [4]+X,1/2-Y,-1/2+Z

Table 5 Bond Angles for final.

Atom	**Atom**	**Atom**	**Angle/˚**	**Atom**	**Atom**	**Atom**	**Angle/˚**
F3[1]	K1	F3[2]	111.81(4)	B1[2]	K1	B1[3]	117.96(9)
F3[1]	K1	F1[1]	47.30(5)	B1[1]	K1	B1[2]	101.32(8)
F3[1]	K1	F1[3]	83.95(5)	K1[4]	F3	K1[2]	99.15(5)
F3[2]	K1	F1[3]	79.55(5)	B1	F3	K1[2]	103.58(16)
F3[2]	K1	F1[1]	82.30(5)	B1	F3	K1[4]	94.48(15)
F3[1]	K1	F2[3]	74.52(5)	K1[3]	F1	K1[4]	94.60(5)
F3[2]	K1	F2[3]	125.15(5)	B1	F1	K1[4]	88.65(14)

F3^{2}	K1	F2^{2}	45.81(5)	B1	F1	K1^{3}	103.11(16)
F3^{1}	K1	F2^{2}	122.69(5)	K1^{3}	F2	K1^{4}	85.72(5)
F3^{1}	K1	F2^{1}	43.04(5)	K1^{2}	F2	K1^{4}	84.26(5)
F3^{2}	K1	F2^{1}	68.94(5)	K1^{3}	F2	K1^{2}	161.58(7)
F3^{1}	K1	B1^{2}	127.27(7)	B1	F2	K1^{4}	74.84(16)
F3^{2}	K1	B1^{1}	88.58(7)	B1	F2	K1^{3}	98.98(15)
F3^{2}	K1	B1^{2}	23.89(7)	B1	F2	K1^{2}	93.26(15)
F3^{1}	K1	B1^{3}	84.17(6)	C10	O3	C11	121.2(2)
F3^{1}	K1	B1^{1}	26.13(7)	C10	O2	K1	160.98(18)
F3^{2}	K1	B1^{3}	101.31(7)	C2	O1	K1^{2}	138.16(18)
F1^{3}	K1	F1^{1}	114.50(4)	C10	N1	C1	118.9(2)
F1^{3}	K1	F2^{3}	46.07(5)	C10	N1	C5	123.8(2)
F1^{1}	K1	F2^{2}	75.53(5)	C5	N1	C1	115.8(2)
F1^{1}	K1	F2^{1}	42.23(5)	C3	C4	C7	125.1(2)
F1^{3}	K1	F2^{1}	72.61(5)	C3	C4	C5	122.8(2)
F1^{1}	K1	F2^{3}	121.77(5)	C7	C4	C5	112.0(2)
F1^{3}	K1	F2^{2}	123.88(5)	C4	C3	C2	116.9(2)
F1^{3}	K1	B1^{1}	91.05(7)	C4	C3	B1	125.2(2)
F1^{1}	K1	B1^{3}	126.58(7)	C2	C3	B1	117.6(2)
F1^{3}	K1	B1^{2}	99.43(7)	C4	C7	C9	117.0(3)

F1[1]	K1	B1[2]	85.90(6)	C8	C7	C4	120.7(3)
F1[3]	K1	B1[3]	23.58(6)	C8	C7	C9	122.3(3)
F1[1]	K1	B1[1]	26.12(6)	O1	C2	C3	121.9(2)
F2[3]	K1	F2[2]	161.58(7)	O1	C2	C1	116.8(2)
F2[3]	K1	F2[1]	95.90(6)	C3	C2	C1	121.0(2)
F2[2]	K1	F2[1]	94.12(5)	O3	C10	N1	111.3(2)
F2[3]	K1	B1[1]	97.55(7)	O2	C10	O3	125.2(2)
F2[2]	K1	B1[2]	24.48(6)	O2	C10	N1	123.5(2)
F2[3]	K1	B1[3]	23.92(6)	O3	C11	C13	111.4(2)
F2[2]	K1	B1[3]	141.55(6)	O3	C11	C14	101.1(2)
F2[2]	K1	B1[1]	98.08(7)	O3	C11	C12	108.8(2)
F2[1]	K1	B1[2]	87.47(7)	C13	C11	C14	111.1(2)
F2[1]	K1	B1[3]	88.89(7)	C13	C11	C12	112.6(3)
F2[3]	K1	B1[2]	140.92(7)	C12	C11	C14	111.3(2)
O2	K1	F3[2]	148.88(6)	N1	C1	C2	112.6(2)
O2	K1	F3[1]	90.21(6)	N1	C5	C4	112.2(2)
O2	K1	F1[3]	126.16(6)	K1[4]	B1	K1[2]	79.36(7)
O2	K1	F1[1]	98.88(6)	K1[2]	B1	K1[3]	117.96(9)
O2	K1	F2[1]	130.87(5)	K1[4]	B1	K1[3]	78.80(7)
O2	K1	F2[2]	104.04(6)	F3	B1	K1[4]	59.39(13)

O2	K1	F2[3]	80.77(6)	F3	B1	K1[3]	137.81(18)
O2	K1	O1[2]	87.96(6)	F3	B1	K1[2]	52.53(12)
O2	K1	B1[1]	106.18(7)	F3	B1	C3	112.3(2)
O2	K1	B1[3]	102.62(7)	F1	B1	K1[2]	144.40(18)
O2	K1	B1[2]	125.01(8)	F1	B1	K1[3]	53.31(13)
O1[2]	K1	F3[1]	176.71(6)	F1	B1	K1[4]	65.24(13)
O1[2]	K1	F3[2]	70.93(6)	F1	B1	F3	107.6(2)
O1[2]	K1	F1[1]	135.75(6)	F1	B1	C3	113.2(2)
O1[2]	K1	F1[3]	94.92(6)	F2	B1	K1[3]	57.10(13)
O1[2]	K1	F2[1]	139.47(5)	F2	B1	K1[4]	80.02(15)
O1[2]	K1	F2[2]	60.47(6)	F2	B1	K1[2]	62.26(13)
O1[2]	K1	F2[3]	102.47(6)	F2	B1	F3	106.4(2)
O1[2]	K1	B1[3]	93.55(7)	F2	B1	F1	105.9(2)
O1[2]	K1	B1[1]	157.14(8)	F2	B1	C3	111.0(2)
O1[2]	K1	B1[2]	55.94(7)	C3	B1	K1[4]	168.4(2)
B1[1]	K1	F2[1]	25.14(6)	C3	B1	K1[3]	109.88(17)
B1[1]	K1	B1[3]	100.52(8)	C3	B1	K1[2]	102.20(16)

[1]+X,1/2-Y,1/2+Z; [2]1-X,-Y,1-Z; [3]1-X,1-Y,1-Z; [4]+X,1/2-Y,-1/2+Z

Table 6 Hydrogen Atom Coordinates (Å×10^4) and Isotropic Displacement Parameters (Å^2×10^3) for final.

Atom	*x*	*y*	*z*	U(eq)
H1A	2941	-449	4780	31
H1B	3903	1060	5138	31
H5A	1554	4948	4255	31
H5B	1353	2274	4113	31
H13A	2978	6332	6524	45
H13B	2289	8485	6628	45
H13C	2871	8488	6055	45
H14A	1129	9321	5335	41
H14B	555	9075	5908	41
H14C	216	7497	5289	41
H12A	513	3917	5914	47
H12B	824	5354	6561	47
H12C	1600	3473	6397	47
H9A	1645	7997	3549	55
H9B	1298	8163	2790	55
H9C	2498	8032	3131	55
H8A	710(20)	4800(50)	2285(15)	24(8)

H8B	1210(30)	2170(60)	2642(18)	41(10)

Experimental

Single crystals of $C_{13}H_{18}BF_3KNO_3$ [final] were air stable. A suitable crystal was selected and mounted in parabar oil on a 'Bruker APEX-II CCD' diffractometer. The crystal was kept at 150 K during data collection. Using Olex2,[82] the structure was solved with the ShelXT[83]structure solution program using Intrinsic Phasing and refined with the ShelXL[84]refinement package using Least Squares minimisation. Crystal structure determination of [final]

Crystal Data for $C_{13}H_{18}BF_3KNO_3$ (*M* =343.19 g/mol): monoclinic, space group $P2_1/c$ (no. 14), *a* = 13.296(3) Å, *b* = 5.8346(10) Å, *c* = 21.585(4) Å, *β* = 103.096(7)°, *V* = 1630.9(5) Å^3, *Z* = 4, *T* = 150 K, μ(MoKα) = 0.365 mm^{-1}, *Dcalc* = 1.398 g/cm^3, 18485 reflections measured (5.518° ≤ 2Θ ≤ 53.224°), 3340 unique (R_{int} = 0.0983, R_{sigma} = 0.0634) which were used in all calculations. The final R_1 was 0.0460 (I > 2σ(I)) and wR_2 was 0.1513 (all data).

Refinement model description

Number of restraints - 0, number of constraints - unknown.

Details:

1. Fixed Uiso

At 1.2 times of:

All C(H,H) groups

At 1.5 times of:

All C(H,H,H) groups

2.a Secondary CH_2 refined with riding coordinates:

C1(H1A,H1B), C5(H5A,H5B)

2.b Idealised Me refined as rotating group:

C13(H13A,H13B,H13C), C14(H14A,H14B,H14C), C12(H12A,H12B,H12C), C9(H9A,H9B,H9C)

This report has been created with Olex2, compiled on 2018.05.29 svn.r3508 for OlexSys.

1. References

(1) Aissa, C. *Synthesis* **2011**, *2011*, 3389.

(2) Mundal, D. A.; Lutz, K. E.; Thomson, R. J. *J. Am. Chem. Soc.* **2012**, *134*, 5782.

(3) Fumagalli, G.; Stanton, S.; Bower, J. F. *Chem. Rev.* **2017**, *117*, 9404.

(4) Murakami, M.; Ashida, S.; Matsuda, T. *J. Am. Chem. Soc.* **2005**, *127*, 6932.

(5) Ogoshi, S.; Oka, M.-a.; Kurosawa, H. *J. Am. Chem. Soc.* **2004**, *126*, 11802.

(6) Ogoshi, S.; Arai, T.; Ohashi, M.; Kurosawa, H. *Chem. Commun.* **2008**, 1347.

(7) Huang, W.-S.; Chan, J.; Jamison, T. F. *Org. Lett. 2016,* **2000**, *2*, 4221.

(8) Liu, P.; McCarren, P.; Cheong, P. H.-Y.; Jamison, T. F.; Houk, K. *J. Am. Chem. SOC.* **2010**, *132*, 2050.

(9) Murakami, M.; Ashida, S.; Matsuda, T. *J. Am. Chem. Soc.* **2006**, *128*, 2166.

(10) Huffman, M. A.; Liebeskind, L. S. *J. Am. Chem. Soc.* **1991**, *113*, 2771.

(11) Huffman, M. A.; Liebeskind, L. S. *J. Am. Chem. Soc.* **1990**, *112*, 8617.

(12) Juliá-Hernández, F.; Ziadi, A.; Nishimura, A.; Martin, R. *Angew.Chem. Int.Ed.* **2015**, *54*, 9537.

(13) Ho, K. Y.; Aïssa, C. *Chem. Eur. J.* **2012**, *18*, 3486.

(14) Kumar, P.; Louie, J. *Org. Lett.* **2012**, *14*, 2026.

(15) Ishida, N.; Yuhki, T.; Murakami, M. *Org. Lett.* **2012**, *14*, 3898.

(16) Li, Y.; Lin, Z. *Organometallics* **2013**, *32*, 3003.

(17) Thakur, A.; Evangelista, J. L.; Kumar, P.; Louie, J. *J. Org. Chem.* **2015**, *80*, 9951.

(18) Barday, M.; Janot, C.; Clare, D.; Carr-Knox, C.; Higginson, B.; Ho, K. Y.; Aissa, C. *Synthesis* **2017**, *49*, 3582.

(19) Barday, M.; Ho, K. Y.; Halsall, C. T.; Aissa, C. *Org. Lett. 2016,* **2016**, *18*, 1756.

(20) Kumar, P.; Zhang, K.; Louie, J. *Angew.Chem. Int.Ed.* **2012**, *124*, 8730.

(21) Thakur, A.; Facer, M. E.; Louie, J. *Angew.Chem. Int.Ed.* **2013**, *125*, 12383.

(22) Qiao, J.; Lam, P.; Hall, D. *Medicine and Materials. Wiley* **2011**.

(23) Davies, M. W.; Wybrow, R.; Johnson, C. N.; Harrity, J. *Chem. Commun.* **2001**, 1558.

(24) Helm, M. D.; Moore, J. E.; Plant, A.; Harrity, J. *Angew. Chem. Int. Ed.* **2005**, *44*, 3889.

(25) Helm, M. D.; Plant, A.; Harrity, J. P. *Synlett* **2007**, *2007*, 2885.

(26) Browne, D. L.; Helm, M. D.; Plant, A.; Harrity, J. *Angewandte Chemie International Edition* **2007**, *46*, 8656.

(27) Delaney, P. M.; Huang, J.; Macdonald, S. J.; Harrity, J. P. *Org. Lett.* **2008**, *10*, 781.

(28) Huang, J.; Macdonald, S. J.; Harrity, J. P. *Chem. Commun.* **2009**, 436.

(29) Kirkham, J. D.; Butlin, R. J.; Harrity, J. *Angew. Chem. Int. Ed.* **2012**, *51*, 6402.

(30) Comas-Barcelo, J.; Harrity, J. P. *Synthesis* **2017**, *49*, 1168.

(31) Hilt, G.; Smolko, K. I. *Angew. Chem. Int. Ed.* **2003**, *42*, 2795.

(32) Yamamoto, Y.; Ishii, J.-i.; Nishiyama, H.; Itoh, K. *J. Am. Chem. Soc.* **2004**, *126*, 3712.

(33) Yamamoto, Y.; Ishii, J.-i.; Nishiyama, H.; Itoh, K. *J. Am. Chem. Soc.* **2005**, *127*, 9625.

(34) Iannazzo, L.; Vollhardt, K. P. C.; Malacria, M.; Aubert, C.; Gandon, V. *Eur. J. Org. Chem.* **2011**, *2011*, 3283.

(35) Auvinet, A. L.; Ez-Zoubir, M.; Vitale, M. R.; Brown, J. A.; Michelet, V.; Ratovelomanana-Vidal, V. *ChemSusChem* **2012**, *5*, 1888.

(36) Gomez-Bengoa, E.; Helm, M. D.; Plant, A.; Harrity, J. P. *J. Am. Chem. Soc.* **2007**, *129*, 2691.

(37) Browne, D. L.; Vivat, J. F.; Plant, A.; Gomez-Bengoa, E.; Harrity, J. P. *J. Am. Chem. Soc.* **2009**, *131*, 7762.
(38) Moore, J. E.; Davies, M. W.; Goodenough, K. M.; Wybrow, R. A.; York, M.; Johnson, C. N.; Harrity, J. P. *Tetrahedron* **2005**, *61*, 6707.
(39) Grundmann, C.; Dean, J. M. *J. Org. Chem.* **1965**, *30*, 2809.
(40) Grob, J. E.; Nunez, J.; Dechantsreiter, M. A.; Hamann, L. G. *J. Org. Chem.* **2011**, *76*, 10241.
(41) Lin, B.; Yu, P.; He, C. Q.; Houk, K. *Bioorg. Med. Chem.* **2016**, *24*, 4787.
(42) De Borggraeve, W.; Rombouts, F.; Van der Eycken, E.; Hoornaert, G. J. *Synlett* **2000**, *2000*, 0713.
(43) Gold, B.; Batsomboon, P.; Dudley, G. B.; Alabugin, I. V. *J. Org. Chem.* **2014**, *79*, 6221.
(44) Geny, A.; Lebœuf, D.; Rouquié, G.; Vollhardt, K. P. C.; Malacria, M.; Gandon, V.; Aubert, C. *Chem. Eur. J.* **2007**, *13*, 5408.
(45) Yamamoto, Y.; Hattori, K.; Ishii, J.-i.; Nishiyama, H.; Itoh, K. *Chem. Commun.* **2005**, 4438.
(46) Auvinet, A. L.; Ez-Zoubir, M.; Bompard, S.; Vitale, M. R.; Brown, J. A.; Michelet, V.; Ratovelomanana-Vidal, V. *ChemCatChem* **2013**, *5*, 2389.
(47) Hilt, G.; Janikowski, J. *Org. Lett.* **2009**, *11*, 773.
(48) hwa Jung, S.; Choi, K.; Pae, A. N.; Lee, J. K.; Choo, H.; Keum, G.; Cho, Y. S.; Min, S.-J. *Org. Biomol. Chem.* **2014**, *12*, 9674.
(49) Kim, T.; Song, J. H.; Jeong, K. H.; Lee, S.; Ham, J. *Eur. J. Org. Chem.* **2013**, *2013*, 3992.
(50) Ji, P.; Atherton, J. H.; Page, M. I. *Org. Biomol. Chem.* **2012**, *10*, 7965.
(51) Auvinet, A. L.; Harrity, J. P. *Angew. Chem. Int. Ed.* **2011**, *50*, 2769.
(52) Dreher, S. D.; Lim, S.-E.; Sandrock, D. L.; Molander, G. A. *J. Org. Chem.* **2009**, *74*, 3626.
(53) Molander, G. A.; Canturk, B.; Kennedy, L. E. *J. Org. Chem.* **2008**, *74*, 973.
(54) Molander, G. A. *J. Org. Chem.* **2015**, *80*, 7837.
(55) Dubbaka, S. R.; Nizalapur, S.; Atthunuri, A. R.; Salla, M.; Mathew, T. *Tetrahedron* **2014**, *70*, 2118.
(56) Song, J. H.; Choi, P.; Lee, S. E.; Jeong, K. H.; Kim, T.; Kang, K. S.; Choi, Y. S.; Ham, J. *European Journal of Organic Chemistry* **2013**, *2013*, 6249.
(57) Huang, S.; Omura, K.; Swern, D. *J. Org. Chem.* **1976**, *41*, 3329.
(58) Karlsson, S.; Bergman, R.; Lofberg, C.; Moore, P. R.; Ponten, F.; Tholander, J.; Sorensen, H. *Org. Process Res. Dev.* **2015**, *19*, 2067.
(59) Oliveira, R. A.; Silva, R. O.; Molander, G. A.; Menezes, P. H. *Magn.Reson.Chem.* **2009**, *47*, 873.
(60) Smith, B. D.; Goodenough-Lashua, D. M.; D'Souza, C. J.; Norton, K. J.; Schmidt, L. M.; Tung, J. C. *Tetrahedron letters* **2004**, *45*, 2747.
(61) Cox, C.; Lectka, T. *J. Org. Chem.* **1998**, *63*, 2426.
(62) Frohn, H.-J.; Franke, H.; Fritzen, P.; Bardin, V. *J. Organomet. Chem.* **2000**, *598*, 127.
(63) Ogoshi, S.; Ueta, M.; Arai, T.; Kurosawa, H. *J. Am. Chem. Soc.* **2005**, *127*, 12810.
(64) Ohashi, M.; Saijo, H.; Arai, T.; Ogoshi, S. *Organometallics* **2010**, *29*, 6534.
(65) Iwasaki, K.; Yoshii, K.; Tsuzuki, S.; Matsumoto, H.; Tsuda, T.; Kuwabata, S. *J. Phys. Chem. B,* **2016**, *120*, 9468.
(66) Iramain, M. A.; Davies, L.; Brandán, S. A. *J. Mol. Struct.* **2018**, *1158*, 245.
(67) Gutsulyak, D. V.; Gott, A. L.; Piers, W. E.; Parvez, M. *Organometallics* **2013**, *32*, 3363.
(68) Gómez-Martínez, M.; Buxaderas, E.; Pastor, I. M.; Alonso, D. A. *J. Mol. Catal. A: Chem.* **2015**, *404*, 1.

(69) Yao, M.-L.; Kabalka, G. W.; Blevins, D. W.; Reddy, M. S.; Yong, L. *Tetrahedron* **2012**, *68*, 3738.
(70) Stalling, T.; Harker, W. R.; Auvinet, A. L.; Cornel, E. J.; Harrity, J. P. *Chem. Eur. J.* **2015**, *21*, 2701.
(71) Wang, H.; Grohmann, C.; Nimphius, C.; Glorius, F. *J. Am. Chem. Soc.* **2012**, *134*, 19592.
(72) Souillart, L.; Cramer, N. *Chem. Rev* **2015**, *115*, 9410.
(73) Murakami, M.; Ishida, N. *J. Am. Chem. Soc.* **2016**, *138*, 13759.
(74) Chen, P.; Billett, B.; Tsukamoto, T.; Dong, G. *Chem. Rev* **2017**, *117*, 9404.
(75) Jiao, J.; Nishihara, Y. *J. Organomet. Chem.* **2012**, *721*, 3.
(76) Ishida, N.; Murakami, M. In *Synthesis and Application of Organoboron Compounds*; Springer: 2015, p 93.
(77) Jouvin, K.; Couty, F.; Evano, G. *Org. Lett.* **2010**, *12*, 3272.
(78) Taylor, C.; Bolshan, Y. *Org. Lett.* **2013**, *16*, 488.
(79) Molander, G. A.; Katona, B. W.; Machrouhi, F. *J. Org. Chem.* **2002**, *67*, 8416.
(80) Steves, J. E.; Preger, Y.; Martinelli, J. R.; Welch, C. J.; Root, T. W.; Hawkins, J. M.; Stahl, S. S. *Org.ProcessRes.Dev.* **2015**, *19*, 1548.
(81) Taylor, C.; Bolshan, Y. *Org. Lett.* **2013**, *16*, 488.
(82) Dolomanov, O. V.; Bourhis, L. J.; Gildea, R. J.; Howard, J. A.; Puschmann, H. *J. Appl. Cryst.* **2009**, *42*, 339.
(83) Sheldrick, G. M. *Acta Cryst.* **2015**, *A71*, 3.
(84) Sheldrick, G. M. *Acta Cryst.* **2015**, *C71*, 3.